Dissecting the Developmental Life Cycle and Developing Genetic Tools for Understanding the Biology of *Orientia tsutsugamushi*

Thesis

Dissecting the developmental life cycle and developing genetic tools for understanding the biology of *Orientia tsutsugamushi*

Suparat Giengkam

PI: F5755175

Supervisors:
Assoc. Prof. Jeanne Salje
Prof. Nicholas Day
Prof. Stuart Blacksell

The Open University (OU)

Mahidol-Oxford Tropical Medicine Research Unit (MORU)

Abstract

Orientia tsutsugamushi is an obligate intracellular bacterium that is spread by mites and causes a life-threatening human disease, scrub typhus. This disease affects at least one million people annually with a high risk of mortality if not treated promptly. *Orientia* is poorly understood compared to many other pathogens due to genetic intractability. This bacterium only propagates and replicates within host cells. they are predominantly found in endothelial, dendritic, and monocyte/macrophage cells, and stay inside infected cells for seven days or longer before exiting by a budding mechanism.

The developmental differentiation of the intracellular infection cycle of *Orientia* has not been studied previously. My thesis research initially focused on how *Orientia* differentiates into distinct subpopulations during the infection cycle, how distinct subpopulations of *Orientia* affect the infection in host cells, and different protein profiles of bacteria in distinct stages during the infection cycle. My research demonstrates that *O. tsutsugamushi* differentiates into five distinct subpopulations: early entry, pre-replicative, replicative, maturation, and extracellular, representing a new model for developmental differentiation in the intracellular cycle of *Orientia tsutsugamushi*. Each subpopulation relates to different degrees of metabolic activity, replication, infectivity, including morphology, presence of marker gene, and subcellular localization. The transition between the subpopulations likely results from an integration of signals from the host cell environment and the bacteria which leads to morphological and physiological changes through the regulation of genes and proteins. This work allows us to understand the fundamentals of bacterial development and the regulation mechanism of differentiation of *Orientia tsutsugamushi,* which could be beneficial for the improvement of diagnosis and treatment.

Genetic tools have not been developed previously for *Orientia*, but genetic manipulation in the most closely related bacteria, rickettsial species, has been successfully established in the last decade. My work on genetic manipulation of *Orientia* is described in the second part of this thesis. The transposon mutagenesis vector and nucleotide analog (BNA) were used to manipulate the genome of *Orientia*. Unfortunately, the transposon mutagenesis system failed to integrate

into the *Orientia* genome, whereas BNA was able to down regulate the expression of the targeted protein (TSA56). Using a nucleotide analog to target a specific gene is the first step to manipulate the genome of *Orientia,* and this has led to the study of other targeted genes involving virulence and pathogenicity.

Due to the genetic intractability of *Orientia* that limits the molecular dissection of bacteria pathogenesis, virulence, and host-pathogen interaction, sequencing technologies provide a promising way to understand the molecular processes of the disease. This motivated the third part of this thesis, in which dual RNA-seq was applied to two clinical isolates grown in cultured HUVEC cells. This study revealed the transcriptomic profile of *Orientia* and identified the different immune response networks in response to each strain. Differential activation of the immune response in cultured cells between the two strains was shown to correlate with differences in virulence as measured in a mouse model of infection. These findings will help to understand the mechanism of bacterial pathogenesis in *Orientia tsutsugamushi* and may be used for characterization of other genetically intractable bacterial pathogens.

Contents

Acknowledgements

I would like to express my deep gratitude to my primary supervisor, Assoc. Prof. Jeanne Salje, who guided me through my PhD and shared the excitement of six years of *Orientia* discovery. Jeanne gave me a lot of opportunities for learning and doing research with many collaborators around the world. She is enthusiastic about cell biology, which keeps me constantly engaged with my research. She always supports and helps whenever I have problems, and along with personal kindness and generosity made my PhD journey enjoyable and memorable.

Apart from my main supervisor, I would like to thank my secondary supervisors Prof. Nick Day and Prof. Stuart Blacksell for all their advice and support throughout my whole PhD journey.

I would like to thank all members in the Cell Biology team in both MORU, Bangkok and PHRI, Rutgers, USA. Especially thanks to Dr. Jantana and Dr. Yanin who always helped me with the experiments and stayed until late evening when I have long experiments. Especially, when we hang out together after playing badminton and always had nice scientific chats along with nice wines!

Thank you to all members in microbiology and many friends in other departments including Suwittra, Manusanan, Viriya, Weerawat, Naomi, Angela, and Cherry Lim for all supportive suggestions and nice conversations. Thank you to Gaye Proctor for correcting the language in my thesis.

Thank you to Sharan, who worked closely with me for more than 5 years. She helps me with the imaging at the beginning and many things. We always got along together in the lab with nice conversation, laughter, sorrow, and being a good DJ with Youtube music in the lab.

Special thank you to all collaborators around the world especially Dr Graham Wright (A*STAR, Singapore) for confocal and SIM imaging, Dr. David Liebl and Wah Ing Goh (A*STAR, Singapore) for TEM microscopy, Khun Nusara chormanee (Siriraj Hospital, BKK) for amazing TEM images, Sanghyuk Lee (Rutgers, USA) for STORM imaging, Prof. Lars Barquist, Alexander Westermann (HIRI, Würzburg, Germany) for RNA-seq, and Prof. Sanjay Tyagi (PHRI, USA) for RNA-FISH labeling technique.

Thank you to all best friends who live in Thailand, Singapore, UK, and US for all wonderful treats, support, and guidance. Especially, Gart who I worked closely with during my master degree project and is always a good listener when I have problems.

Lastly, thank you to my beloved family: mom, dad, my brother, husband, and lovely son for all the unconditional love, care, and support.

Attributions

In this thesis, some experiments were carried out by collaborators.

1. Nusara Chormanee, (Pathology department, Siriraj Hospital)
    - Figure 9. Transmission microscopy images
2. Graham Wright and Wah Ing (Institute of Medical Biology, Agency for Science, Technology and Research (A*STAR), Singapore)
    - Figure 11, 14 SIM images
3. Sanghyuk Lee, Taerin Chung, and Hyun Huh (Department of Physics and Astronomy, Rutgers University, Piscataway, New Jersey, USA)
    - Figure 14, 15,16 STORM images
4. Jantana Wongsantichon (Microbiology, MORU, Bangkok)
    - Figure 17 and table 3-4 Proteomic analysis
    - Figure 20 Western blot analysis
5. Lars Barquist, Bozena Mika-Gospodoz and Alexander Westermann (Helmholtz Institute for RNA-based Infection Research (HIRI), Helmholtz Centre for Infection 12 Research (HZI), Würzburg, Germany)
    - Figure. 39-42 RNA-seq analysis
6. Piyanate Sunyakumthorn, Armed Forces Research Institute of Medical Sciences, Bangkok, Thailand
    - Figure 43 a-b
7. Selvakumar Subbian, Public Health Research Institute, Rutgers University, New Jersey, NJ, USA
    - Figure 43 f
8. Suthida Chuenklin, Public Health Research Institute, Rutgers University, New Jersey, NJ, USA
    - Figure 43 d-e

Abbreviations

TSA = type-specific antigen

Sca = surface cell antigen

Eftu = translation elongation factor

gDNA = genomic DNA

(p)ppGpp = guanosine-pentaphosphate

RpoH = RNA polymerase sigma factor

TPRs = tetratricopeptide repeats

Anks = Ankyrin repeat-containing proteins

HPG = L-homopropargylglycine

EdU = 5-ethynyl-2´-deoxyuridine

EU = 5-ethynyl uridine

BSO = Buthionine sulphoximine

GSH = glutathione

Ptk2 = Potoroo kidney cells

L929 = Mouse fibroblast cells

HUVEC = Human Umbilical Vein Endothelial Cells

LAMP1 = Lysosomal-associated membrane protein 1

PNA = Peptide nucleic acid

BNA = Bridged nucleic acid

RNA-seq = RNA sequencing

ncRNA = noncoding RNA

tmRNA = transfer-messenger RNA

ILs = Interlukins

SIM = Structured illumination microscopy

STORM = Stochastic optical reconstruction microscopy

TEM =Transmission electron microscopy

Chapter 1: Literature review

1.1 Overview of scrub typhus

Scrub typhus was first mentioned in Japan in the 1800s to describe vector-associated fevers (1). The term scrub refers to the type of vegetation that retains the vector, and the word "typhus" is derived from the ancient Greek word *typhos* (smoke, mist, fog) which was used by Hippocrates to denote clouding of consciousness (2). Scrub typhus, also known as tsutsugamushi disease, is a neglected infectious disease caused by infection with the gram-negative obligate intracellular bacterium *Orientia tsutsugamushi*, previously called *Rickettsia tsutsugamushi*. Scrub typhus is transmitted to humans by larval stage *Leptotrombidium* mites. The term *tsutsugamushi* is derived from two Japanese words; "tsutsuga" meaning dangerous and "mushi" meaning insect (2). Scrub typhus is considered a serious public health problem in the traditional endemic area, the Asia-Pacific region, and in recently identified endemic regions in Africa, the Middle East, and South America (3). It affects people of all ages including children and pregnant women (4). The disease remains a major underdiagnosed and undifferentiated fever in Asia due to a lack of accurate and accessible laboratory diagnosis. The symptoms present from mild to fatal illnesses. The infection can be life-threatening if patients are left untreated with appropriate antibiotics (5, 6). As a neglected disease, the knowledge of scrub typhus still has wide gaps. Many unknown aspects of the disease are needed to be discovered, including diagnosis, treatment, molecular infection mechanism, and developmental life cycle.

1.1.1 Vector and transmission

Leptotrombidium mites (the larval form of which are commonly known as chiggers), which belong to the family Trombiculidae, are the primary reservoir and vector of *O. tsutsugamushi*. Their life cycle consists of four main stages; eggs, 6-legged larvae, 8-legged nymphs, and 8-legged adults (2). The larval stage is the only stage of the mite that feeds on humans and small mammals, whereas nymphs and adult mites are free-living in soil and feed on the eggs of insects. Infected mites can maintain *Orientia* throughout their life cycle. The adults pass the infection to offspring via a process called transovarial transmission, and transstadial transmission occurs through the

nymph and adult stages (7). Both types of transmission are associated with vertical transmission. The feeding period on rodents is usually 3-6 days and feeding on humans is typically 2-10 days (8).

Once the infected mites attach to the host skin for nutrient uptake, they insert their mouthpart or stylostome into the host's skin at the base of a hair follicle or pores and release *Orientia* from their saliva glands. *Orientia* invades dermal cells and infects the antigen-presenting cells (APC) in the sub-epidermal zone, basal epidermis, and superficial dermis, causing an inflammatory lesion known as eschar. *Orientia* infects several cell types in host cells including professional phagocytic cells (macrophage, dendritic cells, and neutrophils) and non-phagocytic cells (endothelial, epithelial, fibroblast cells) (9, 10). *Orientia* causes disseminated systematic infection in many organs such as lung, brain, heart, and kidney.

There is no strong evidence to support *O. tsutsugamushi* is being maintained in nature via horizontal transmission, which happens when mites receive *Orientia* from the infected host, and their progeny infects a new host (11). Humans are considered to be a dead-end host because bacteria rarely if ever infect a newly attached uninfected mite. However, mite-to-mite transmission can occur during co-feeding in rodents (12). There is still no evidence of transmission of scrub typhus from person to person (13). The transmission of *Orientia* depends on the season which may reflect the local mite ecology, for instance, the increasing outbreaks in Thailand and Lao PDR during the rainy season, a case report during the cold season in the south of India, and two different occurrences in early and late autumn found in the north and south of Japan (14-16).

1.1.2 Epidemiology

The traditionally recognized endemic area of scrub typhus particularly occurs throughout Asia, Australia, and islands in the Indian and Pacific, known as the Tsutsugamushi Triangle (17), however, evidence indicating the presence of the disease has been reported in Africa, South America (Chile and Peru) and the Middle East (UAE). The recent new species *Orientia chuto* was isolated from a patient in Dubai. Another species that was found in Chile is closely related but

not identical to *O. chuto* and other *Orientia* (3, 18-20). This reflects the genetic diversity of scrub typhus across the global geographic distribution. The estimation of newly infected cases per year is about one million in Southeastern Asia, and about one billion people in endemic areas are at risk of infection (2). Given the increase of new cases and reports of scrub typhus in regions not previously thought to be endemic for the disease, scrub typhus is considered a global health problem.

1.1.3 Clinical symptoms

Scrub typhus is characterized as an acute undifferentiated febrile illness with nonspecific clinical manifestations. Symptoms are usually noticeable after 6-21 days of incubation and range from a mild to a severe illness (13). The early clinical signs and symptoms are an eschar, cough, fever, headache, nausea, rash, myalgia, and lymphadenopathy (13, 21). The eschar typically presents as a cigarette-burn-like lesion which is useful for diagnosis; however, it is not present in every infection. The range of eschar detection varies from 7-80% and depends on the host immunity and possibly the infecting serotype (22). If untreated the disease can progress from mild to fatal illness. Severe complications present an acute inflammation that can lead to multiorgan failure, with severe complications including acute renal failure, acute respiratory distress syndrome (ARDS), pneumonitis, meningoencephalitis, and disseminated intravascular coagulation (13, 23).

The non-specific clinical presentation of scrub typhus leads to difficulties of differentiation from other infectious diseases such as dengue, melioidosis, malaria, typhoid, and leptospirosis. The disease mostly occurs in rural areas where access to the hospital, diagnostics, and treatment are limited. These factors contribute to a high number of undiagnosed or untreated cases with a range of mortality rate from 1% to 50%. The severity depends on bacterial strains, patient status, and the endemic area (5, 24, 25).

1.1.4 Diagnosis

Diagnostic methods of scrub typhus are based on serological and molecular assays (26). The indirect immunofluorescence assay (IFA) is the current gold standard test for the diagnosis of

scrub typhus (27). IFA detects the signal from a fluorescent-labeled anti-human antibody that reacts with antibodies from patient serum bound to a smear of scrub typhus antigen from several different serotypes (28). Even though IFA is sensitive, the method can generate a false negative due to the antigenic variation of *O. tsutsugamushi* strains (28, 29). IFA fails to detect early stage infection because the antibody response takes 5-10 days to reach a detectable level (29). IFA is reported as with other serological tests against a cut-off antibody titer. However, the cut-off titers used varies between laboratories and endemic regions and there is a lack of standardization of the antigens used. In addition, IFA is expensive, complicated, and requires technical training, and thus is not suitable for use in resource-poor rural areas (30).

There are other serological assays such as the Weil-Felix test (WF), enzyme-link immunoassays (ELISAs), the indirect immunoperoxidase assay (IIP), and several commercial rapid diagnostic tests (RDTs). The Weil-Felix agglutination assay is based on the cross-reactions between anti-*Orientia* antibodies in the patient's serum and antigens of the *Proteus mirabilis* OX-K strain. This assay is cheap but lacks specificity and sensitivity (31). The IIP is a variant of the IFA which uses peroxidase instead of fluorescein. The results are read under a normal microscope and therefore the IIP can be used in laboratories lacking a fluorescence microscope. The though one study reports that the sensitivity of IIP is higher than IFA with acute sera, at 79.6% and 68.5% respectively (32).

ELISA is a high throughput assay and more standardized compared to IFA and IIP. The principle of ELISA is similar to IFA but the antigen used varies more between assays, ranging from whole-cell lysate from several strains of *Orientia* to recombinant p56 kDa and other outer membrane proteins. ELISA has been used for seroprevalence and surveillance studies with large scale sampling (32). The widely used the InBios Scrub Typhus Detect™ immunoglobulin M (IgM) ELISA kit is easy to use, cost-effective, and provides sufficient accuracy for screening and diagnosis (33). As ELISA provides adequate sensitivity and specificity in several studies, it has the potential to be an alternative gold standard test and may replace the IFA and IIP assays.

Molecular diagnostics for scrub typhus are usually based on the PCR (Polymerase chain reaction). Several assays have been used in rickettsiology including nested PCR (nPCR),

quantitative real-time PCR (qRT-PCR), restriction fragment length polymorphisms (PCR/RFLP), and multilocus sequences typing (MLST). Of these, qRT-PCR is currently used for the diagnosis of scrub typhus, though it is expensive and requires special equipment and training (34, 35).

PCRs usually target the outer membrane proteins genes (*tsa56, tsa47*), *groEL*, or *16S rRNA*. The *tsa56* gene is primarily used for the strain identification because it contains high antigenic variability, however, the sequence variability may affect primer annealing (36). Early in the disease PCR provides better sensitivity and specificity for the detection of rickettsiae compared with serological tests. It can detect bacterial loads of 1-10 genomes per reaction in skin biopsy/eschar, whole blood, and buffy coat (37).

The potential for detecting bacteria by qPCR depends on sample types. PCR is able to detect bacteria in eschar at the early phase before antibody response. Whole blood samples are positive only in the rickettsaemic period (34). Using buffy coat samples could enhance the sensitivity compared with whole blood as bacteria circulate in monocytes or detached endothelial cells (38). In addition, the sensitivity of PCRs reduces during antibiotic treatment (39).

1.1.5 Treatments

Orientia is treatable with specific antibiotics including chloramphenicol, doxycycline, tetracycline, and azithromycin. There is no established evidence of a difference in treatment outcomes between these antibiotics (40). Doxycycline is commonly used for treating scrub typhus, though some studies from northern Thailand have reported a decreased efficacy of doxycycline in both *in vivo* and *in vitro* (41). Azithromycin and other macrolides are considered safe in pregnant women or children and have been shown in several studies to be as effective as doxycycline and chloramphenicol (42, 43).

Orientia is known to be beta-lactam antibiotic resistant due to a minimal level of peptidoglycan in the cell wall (44). Several reports also suggested other antibiotic resistance in scrub typhus (41, 45, 46), (47). However, a recent finding revealed that doxycycline resistance is a misconception. The evidence against doxycycline resistance has been shown in several studies by testing with *O. tsutsugamushi* strains Karp, Gilliam, Kato, UT76, TA763, AFC-3, and AFSC-4 (46,

48). Apparent antibiotic resistance in *Orientia* needs to be investigated with reference to other determinants of slow fever clearance such as bacterial strain, host, and pharmacological factors. Until now, no vaccine is available for rickettsial infection and scrub typhus. There have been considerable efforts to develop a vaccine to prevent scrub typhus infection. In the past 70 years, numerous studies have evaluated several types of vaccines such as formalin-killed, live, attenuated, and subunit vaccines but all tests failed to produce protective heterologous immunity against *Orientia*. Some results showed short-term homologous protection but failed to stimulate cross-protective immunity against other strains. The major barrier to vaccine development is the high antigenic variation of *Orientia* strains in different endemic regions or the difference in bacterial strains in the same endemic area (49, 50).

1.1.6 *Orientia* classification and genetic profiles

Orientia tsutsugamushi is a member of Class α-proteobacteria, Order Rickettsiales, Family Rickettsiaceae, and Genus *Orientia* which is currently shared only with *Orientia chuto* (Fig. 1). Historically, *Orientia* was classified in the genus *Rickettsia* and was named *Rickettsia tsutsugamushi*. In 1995, it was assigned to its own genus *Orientia* based on DNA-DNA hybridization differences (51). *Orientia* is distinct from rickettsia in four major ways. First, the difference in 16S rRNA sequences (52). Second, the genome size of *Orientia* is almost double the size of Rickettsia (53). Third, the cell wall structure of *Orientia* has reduced levels of peptidoglycan (44) and *Orientia* cannot produce LPS due to an absence of genes required for LPS biosynthesis (54, 55). Lastly, *Orientia* exits host cells by a budding mechanism which is not found in other Rickettsia species (56).

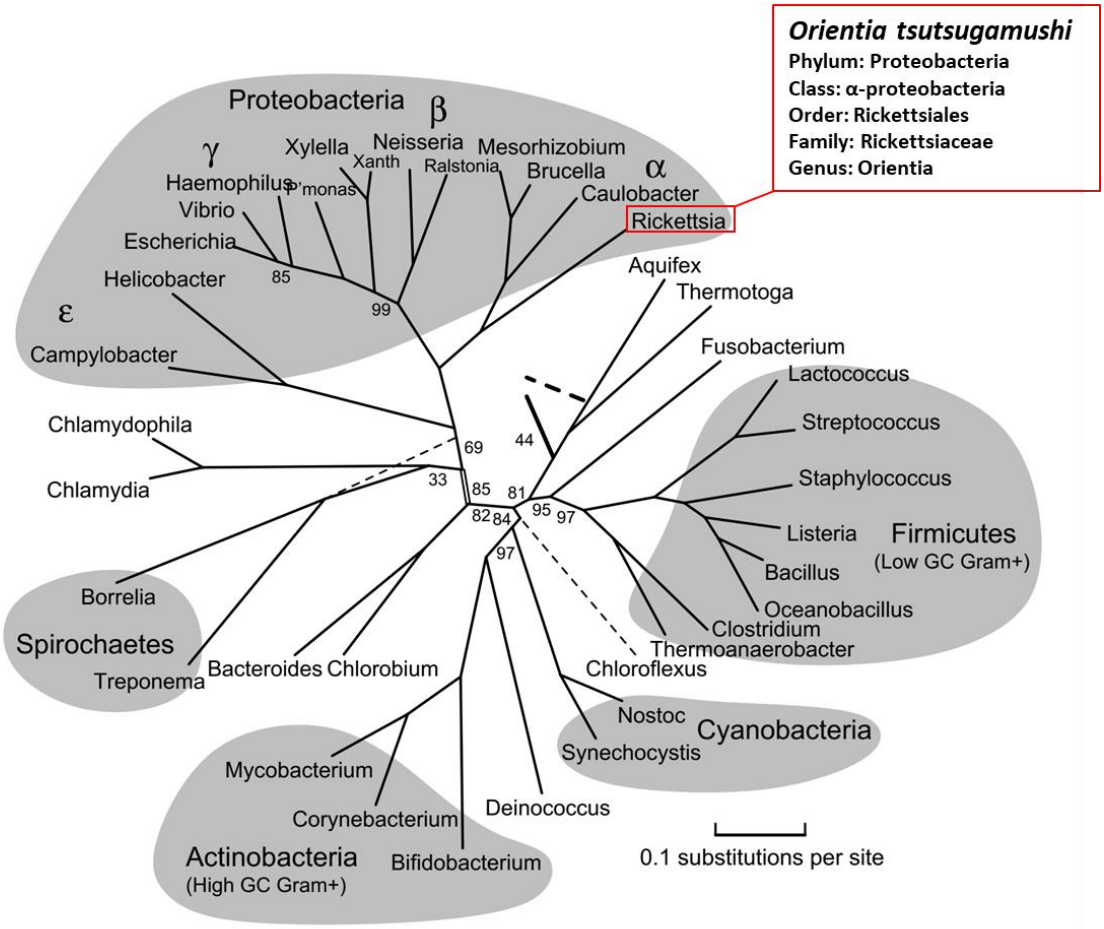

Figure 1. Summary of bacteria phylogenetic tree. The marked red box indicates the Rickettsiales Order to which *Orientia tsutsugamushi* belongs. Image modified from (57)

Most obligate intracellular bacteria tend to have a highly reduced genome of around 1 Mbp which is the result of niche-specific adaptation. Repetitive genes and pseudogenes are a common feature of gene degradation. The reductive genome has been shown in other bacteria such as *Rickettsia prowazekii* and *Chlamydia trachomatis* (58).

The complete genome has been reported in *Orientia* strain Boryong and Ikeda using short-read sequencing technology. However, the highly repetitive genomes make sequencing difficult with short read technology (59). To generate a high quality genome, PacBio single molecule long-read sequencing has been applied in six further strains: Karp, Kato, Gilliam, TA686, UT76, and UT176 (60).

Genome analysis revealed that *O. tsutsugamushi* has an unusual genome compared with the other species in the order Rickettsiales. It has a single circular chromosome consisting of 1.93-2.47 million base pairs (depending on the strain) which is the largest genome size compared with the other obligate intracellular bacterial genomes (Fig.2). The G+C content is 30-31%. *Orientia* contains a unique feature of repeated sequences totaling around 42% of its genome. The repeated sequences consist of the integrative and conjugative element (ICE) named RAGE (Rickettsia amplified genetic element), short repetitive sequences, and transposable elements (including insertion sequence, miniature inverted-repeat, and group II intron). These repetitive sequences can induce genome shuffling, gene duplications, and gene deletion. (55, 61).

The RAGE module has been found in some other rickettsial genomes such as *Rickettsia bellii* and *R. massiliae*. RAGEs are highly divergent and have been found in multiple copies across *Rickettsia* and *Orientia* genomes. Many genes in RAGEs are degraded due to gene insertions or gene deletions (62). RAGE encodes an integrase gene (*int*), transposase genes (*tra* genes) of an F-T4SS (F-type type IV secretion system), and *tra*-associated genes of effectors proteins including ankyrin repeat (AR), tetratricopeptide (TPR) domains, histidine kinase (HK) (55, 63).

Ankyrin repeat-containing proteins (Anks) are predominantly found in eukaryotes and play an important role in several processes such as signal transduction, transcriptional regulation, vesicular trafficking, and cytoskeleton integrity. However, Anks are also found in intracellular pathogens and are thought to be acquired from eukaryotes via horizontal gene transfer. Anks play a role as a virulence factor during intracellular infection by employing several types of secretion proteins to transfer Anks into host cells. *Legionella pneumophila*, *Anaplasma phagocytophilum*, *Coxiella burnetii*, and *Rickettsia spp.* transfer their ANK-containing protein via the Type IV secretion system, T4SS (64-66). It has been reported that Ank is transcriptionally expressed in *O. tsutsugamushi* and is secreted via T1SS during infection in L929 cells (67). Exogenously expressed Ank proteins have been found to localize in the cytoplasm, nucleus, endoplasmic reticulum, and Golgi apparatus (66, 68). T4SS has been reported to be expressed in *Orientia*. The function of this T4SS secretion system is unknown.

Repetitive sequences, transposons, and conjugative elements are likely to be a major factor of numerous homologous recombinations via horizontal gene transfer in *Orientia*. The high level of recombination sequences among bacterial strains could be a potential reason why *Orientia* serotypes have high antigenic diversity (69, 70).

Over the past 10 years, genetic tools have been successfully used in other rickettsial bacteria, for example, the transformation in *R. prowazekii* using Tn mutagenesis (a mariner-based Himar1 Tn system) carrying a green fluorescent protein gene (GFP) to knock down virulence genes and to study host-pathogen interaction (71). However, genetic manipulation in *Orientia* has not yet been achieved. Low transformation efficiency is a major problem for the development of genetic tools in obligate intracellular bacteria. The possible reasons could be host cell restricted growth which requires a long term culture to expand small transformant populations compared with other free-living bacteria, the suboptimal electroporation conditions, the purity of transformants, and restriction/modification systems that degrade integrated DNA (72). Developing a genetic tool in *O. tsutsugamushi* requires technical improvement to increase the efficiency of transformant which is a key challenge to understand the genetic basis of its life cycle.

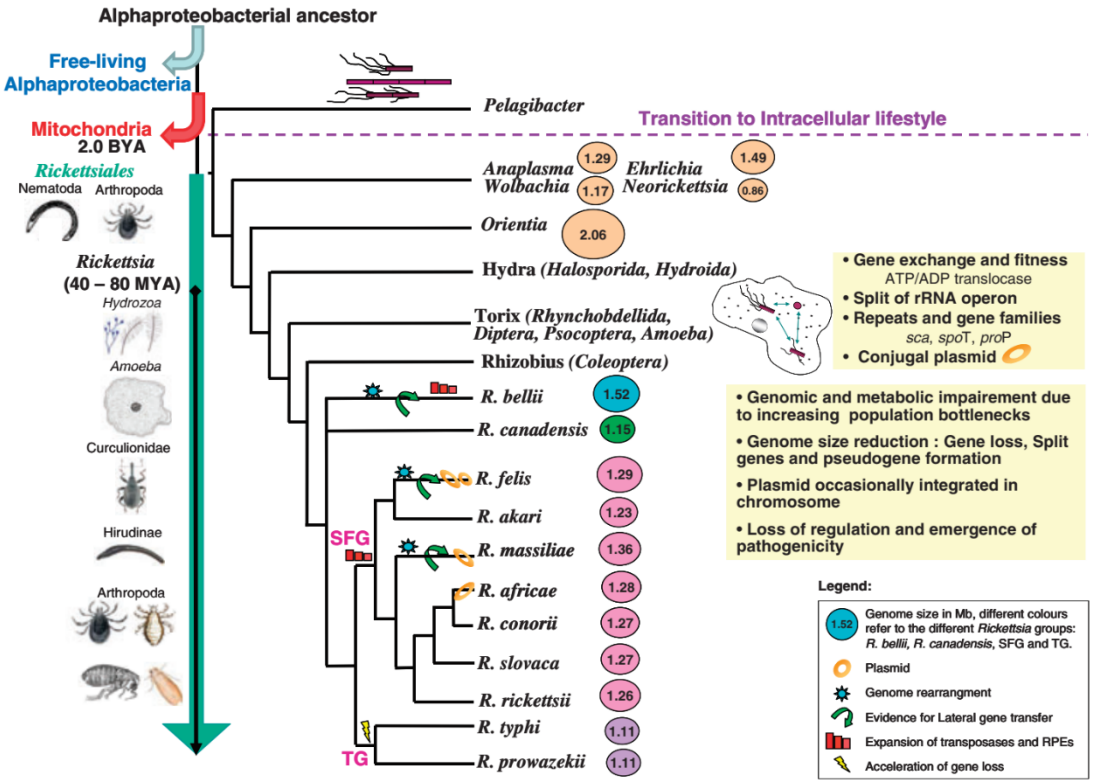

Figure 2. Schematic overview of genomic events in Rickettsial evolution including the different genome sizes and phylogenetic tree of Rickettsial bacteria. Rickettsiaseae and mitochondria presented a close relationship about 200 million years ago. Amoeba-like protozoa are the first hosts of rickettsia ancestors and arthropods appeared to have a symbiotic relationship with a member of Rickettsiales later. The rickettsial genome shows gene loss, gene duplication and genome reduction throughout the obligate intracellular lifestyle within different hosts. SPG: spotted fever group, TG: Typhus group. Yellow boxes illustrate genomic changes. Diagram adapted from ref (53).

1.1.7 Morphology

O. tsutsugamushi is a Gram-negative coccobacillus about 0.3-0.5 µM in width and 0.8-2 µm in length. If cells grow without division, the cells may be considerably longer, up to 3 µm. Flagella or pili are not found in *Orientia* (73, 74). The morphology of *Orientia* is slightly different from *Rickettsia spp*., with *Orientia* more coccobacillus-shaped than the rickettsias. In general,

rickettsias have a rod or bacillus shape, however, they occasionally present long forms during infection which has been found in *R. felis* and *R. prowazikii* (75, 76).

The cell wall structure of *Orientia* is different from other *Rickettsia spp.. Orientia* has been thought to lack peptidoglycan and lipopolysaccharide and to be insensitive to the β-lactam antibiotic penicillin (77, 78). In addition, three important groups of enzymes are absent in the *Orientia* genome; amino acid racemases, glycosyltransferase, and some genes in the meso-diaminopimelic (*meso-DAP*) biosynthesis pathway. However, almost a complete set of genes required for the peptidoglycan synthesis pathway is present in *Orientia* genome (44, 55).

A recent finding from our group revealed that *O. tsutsugamushi* contains a minimal peptidoglycan-like structure. The evidence was strongly confirmed by the detection of peptidoglycan-specific amino acid DAP, and the important peptidoglycan biosynthesis genes (*pbp2*, *murD*, *murF*, and *ddl*) also expressed during the infection cycle. Bioinformatics analysis led to the hypothesis that *Orientia* is intrinsically resistant to β-lactam antibiotics due to a mutation in penicillin-binding proteins (PBP2 and PBP3) (44).

The ultrastructure of budding *Orientia* has been observed by transmission electron microscope (TEM) and found that the budding cells are surrounded by the host cell membrane. In other rickettsia (*R. prowazekii* and *R. rickettsii*), the electron-lucent zone, called a slime layer, surrounds the cells inside and outside of the host cytoplasm. The main composition of the slime layer is polysaccharides. This was proven by positive staining with ruthenium red which is used for staining mucopolysaccharides. Presenting the slime layer may prevent phagocytosis from host immune cells or it may facilitate the attachment to host cells. However, there is no evidence of a slime layer on *Orientia* cells (73, 79).

1.1.8 Surface proteins

The outer membrane proteins of *Orientia* play a key role for bacterial internalization, and have been used as the antigen to activate the humoral immune response for diagnosis or vaccine development (80). Historically, immunoblot analysis of *Orientia* whole-cell lysate with patient serum identified protein antigens with the molecular size. Among these antigens, the type-

specific antigen (TSA)22, TSA47, and TSA56 are the major outer membrane surface proteins of *Orientia* (81). Most of their functions remain uncharacterized.

The TSA56 protein is the most abundant protein on the outer membrane (10-15% of the total cellular protein content) and is the main source of antigenic heterogeneity among different strains. The sequence of TSA56 consists of the signal sequence (SP) in the N-terminal end, transmembrane domains (TMs) in the C-terminal end, four variable domains (VDs), and three extracellular antigen domains (ADs) (81, 82). The variable domain in TSA56 has been used for distinguishing the strains of *Orientia* (83). This supports TSA56 being a strain-specific antigen.

TSA56 protein plays a primary role in bacterial adhesion to host cells which implies that TSA56 is a virulence protein of *Orientia*. Upon attachment, the surface antigen domain (TSA-ADs) directly binds with fibronectin and facilitates the invasion of *Orientia* into host cells. It has been shown that the TSA56-ADI (residue 19-114) had a stronger adhesion ability to host fibronectin and antibody response than TSA56-ADIII (residue 237-366). TSA56 is recognized as a highly immunogenic surface protein. Antibodies to TSA56 are major components of the humoral immune response measurable in scrub typhus patient serum and *Orientia*-inoculated animal serum. Taken together, TSA56 antibodies are important for diagnostic marker and TSA56 antigens are a candidate vaccine antigen against scrub typhus (81, 84).

The TSA47 protein belongs to the HtrA (High-temperature requirement A protein/heat shock protein) family of serine proteases. The sequences of TSA47 are homologous to human HtrA1 protein and contain a trypsin domain. TSA47 is a transmembrane protein highly conserved across strains and is used for species identification (85, 86). This protein also contains a strain-specific B-cell epitope. Immunization with TSA47 antigen induces both long-term cellular and humoral immune responses in mice and cynomolgus macaques (87). One study has reported that TSA47 antigen provided good homologous protection and cross-protection against four heterologous strains in the mouse model. Because of a relatively strong immune protection and cross-reactive epitopes, TSA47 could be a vaccine candidate for broad protection against *Orientia* infection (88). However, cross-reactivity of TSA47 with human serine protease may occur due to the sequence homology.

The TSA47 protein may mediate *Orientia* adhesion to host cells, but the adhesion ability of TSA47 to host fibronectin is lower than that of TSA56 (81). It has been demonstrated that a protein containing a TSA56 antigen fused with a TSA47 was efficient in eliciting humoral and cellular immunity against scrub typhus, suggesting that TSA47 may associate with TSA56 to facilitate the attachment of *Orientia* (89).

The TSA22 protein has no conserved domain and its function remains unknown. It has been reported that TSA22 contains B- and T-cells epitopes (90), and the recombinant TSA22 protein induced antigen-specific proliferation of T-cells that produce IL-2 and IFN-γ. However, this antigen could not induce any immune protection when used as a DNA vaccine in CD1 Swiss mice. TSA22 also inhibited the protective effects of other scrub typhus vaccine candidates (91). The mechanism of inhibition of protective effects is unknown, and further investigation is needed (73).

Another major group of outer membrane proteins (Omp) of *Orientia* are autotransporter proteins, known as surface cell antigen (Sca), which have been identified in Rickettsia genomes including OmpA, OmpB, Sca1, Sca2, and Sca4. The major Sca proteins OmpA, OmpB, and Sca4 have been used for species identification of Rickettsia (92). These proteins are involved in bacterial adhesion and invasion during bacterial entry in nonphagocytic host cells (93, 94). The set of Sca proteins may be different among *Orientia* strains.

Similar to *Rickettsia spp.*, *O. tsutsugamushi* encodes five multiple autotransporter domains (ATD) proteins (ScaA – ScaE) based on the completed genomes of the Boryong and Ikeda strains. Recently, a new Sca protein, ScaF, has been identified based on the partial genomes of the Sido, Karp, and AFSC7 strains (95).

The autotransporter proteins contain a signal sequence at the N-terminal end followed by a surface-localized passenger domain (α domain) and a highly conserved autotransporter domain (β-barrel domain) at the C-terminal end. The signal sequence directs the protein to bacterial periplasm. The autotransporter domain inserts itself into the outer membrane to form a channel. After insertion into the outer membrane, the passenger domain is translocated and

exposed to the bacterial surface (96). The passenger domain is associated with virulence phenotypes, for example, bacterial adhesion, invasion, cytotoxicity, and biofilm formation.

ScaA is the largest protein among *Orientia* Scas and functions as a bacterial adhesion factor. ScaA provides protective immunity against *Orientia* infection in mice, suggesting that ScaA could be a novel vaccine candidate (97). The ScaB gene is present in around one third of *Orientia* isolates. Its function and role in immunity have not been studied (95). The ScaC gene is the smallest *Orientia* Sca and is highly conserved. ScaC plays an essential role in bacterial virulence by facilitating the attachment of bacteria to host fibronectin but not the invasion of nonphagocytic cells. ScaC is a potential candidate antigen either on its own or in combination with ScaA for serological diagnostic assay and vaccine development (98). ScaD has a variable passenger domain. The biological properties and immunogenicity against ScaD are not well characterized (95). The ScaE gene is also well conserved but the size is larger than the ScaC gene so is difficult for cloning and purification for serodiagnostic and vaccines. Like ScaB, ScaF is found in few *Orientia* isolates, and its function is unknown (95).

1.1.9 Virulence and host susceptibility

Virulence factors facilitate bacteria to invade the host, cause disease, and evade host defense mechanisms. *O. tsutsugamushi* isolates can be categorized by their similarity to a number of type strains i.e., Karp, Gilliam, Kato, TA763, and TA716. Karp- and Gilliam-related strains are the most prevalent groups which cause about 50% and 25% of human infections, respectively (21). Each strain was classified into one of three virulence types; high, intermediate, and low virulence based on their relative capacity to kill mice. Karp and Kato have been identified as high virulence strains because only one infected organism can cause death in mice. Gilliam is classified as having an intermediate level of virulence as it causes low mortality in mice. TA716 and TA763 were classified as low virulence strains as they cannot cause death in mice even when infected with high doses of bacteria (99).

The degree of virulence is related to host cell types because each host cell has differences in growth factors, physiology, and immunological defense mechanisms leading to bacterial

replication effect. One study showed that only low doses of Gilliam infection could kill mice strain C3H/He while infection in mice strain BALB/c required higher doses (100). A better understanding of the molecular basis of virulence in each strain could provide a clue to *Orientia*-host relationships.

1.1.10 Metabolic pathways

The general metabolic pathways of *Orientia* are similar to Rickettsia but differ in the carbohydrate metabolism (TCA cycle), the components of cell wall biosynthesis, and transport systems. *Orientia* relies on host nutrients for growth due to reductions in major biosynthetic pathway components. This reflects the presence of numerous transporters for nutrient uptake from host cells (54, 101).

Carbohydrate metabolism

The complete glycolysis pathway, in which glucose is oxidized to pyruvate, is absent in the *Orientia* genome. This suggests that pyruvate cannot be synthesized by the glycolysis pathway. Pyruvate is most likely taken up from the host, or alternatively synthesized from malate which is acquired from the host. The presence of malate permease in the *Orientia* genome may function in transporting malate from the host cell. *Orientia* does not produce acetyl-CoA because it lacks the functional pyruvate dehydrogenase complex and needs to import acetyl-CoA from the host cell (54).

Energy metabolism

Orientia contains almost a complete set of genes for oxidative phosphorylation as a source of energy (ATP) including three proton pumps, ATP synthase complex, and the succinate dehydrogenase complex. However, *Orientia* also uptakes ATP from the host cells through the ATP/ADP translocases. *Orientia* may use the host ATP first and subsequently use its own ATP via aerobic respiration when the host ATP pool is depleted (54).

Nucleotide metabolism

Nucleotide metabolism is divided into two pathways; purine and pyrimidine biosynthesis. Though *Orientia* can produce pyrimidine nucleotides (thymine and cytosine) on its own, *Orientia* imports purine nucleotides (adenine and guanine) from the host via ATP/ADP translocases. The presence of the gene codA (cytosine deaminase) in *Orientia* indicates that cytosine could be converted into uracil (54, 102).

Orientia lacks all enzymes for the pentose phosphate pathway, except for ribose-5-phosphate isomerase (LacA). Phosphorybosyl pyrophosphate (PRPP), a key metabolite for nucleotide synthesis, is probably synthesized therefore by importing ribose-5-phosphate from the host cell (54).

O. tsutsugamushi is the only bacteria in the order Rickettsiales that encodes a fully bifunctional spoT/RelA homolog to produce the guanosine nucleotides (pppGpp and ppGpp). These alarmone nucleotides are essential in the bacterial stringent response during starvation conditions, for example, amino acid starvation, fatty acid depletion, iron depletion, heat shock, and other stress conditions (54, 103).

Amino acid metabolism

Orientia lacks most of the genes for amino acid metabolism. It is likely to import cytoplasmic amino acids from the host cells due to the upregulation of many amino acid transporters in the genome (101). Both *Rickettsia* and *Orientia* lack the alanine racemase (Alr), which functions by converting L-alanine to D-alanine. These amino acids are a key component of peptidoglycan. However, *Orientia* has the enzymes (*ddl*, *murD*, and *murF*) for incorporating D-variants of amino acids into peptidoglycan. This suggests that *Orientia* may uptake D-amino acid from the host cell, or utilize L-variants in murein, the polypeptide chain of peptidoglycan (54, 104).

Lipid metabolism and cell wall components

Most of the enzymes for the fatty acid biosynthesis pathway are present in *Orientia*, with only the β-oxidation system of fatty acid for energy production being absent. Based on the genomic analysis (54, 55), *Orientia* lacks the genes for the LPS biosynthesis such as lipid A.

Even though D-amino acids are not likely to be synthesized in *Orientia* and *Orientia* lacks PBP1, a class A bifunctional enzyme that contains both glycosyltransferase and transpeptidase activity, the genes involved in cell wall biosynthesis are almost completely present in the *Orientia* genome including *murA-G* genes, the *ftsW/RodA* gene from the SEDS (shape, elongation, division, and sporulation) family of proteins, and the penicillin-binding proteins (PBP2 and PBP3). Together with the evidence of a minimal level of meso-DAP in *Orientia*, this indicates that *Orientia* possesses the ability to synthesize peptidoglycan (44, 54).

1.1.11 Immune responses to *Orientia* infection

Innate immune responses

The innate immune system is the first line of defense against bacterial infection. The main functions of the innate immune system are to prevent the spread of pathogens, which include the recruitment of immune cells at the site of infection, the activation of the complement cascade, and co-signaling with the adaptive immune system.

Dermal tissue serves as a niche for *Orientia* replication where the early inflammatory response occurs. The eschar biopsies have shown that *Orientia* presents the cellular tropism for professional phagocytic cells (dendritic cells, macrophage, and monocytes) and vascular endothelium (9). These cells may contribute to local immunity and systematic dissemination from the initial inoculation site toward the bloodstream lymph node and other organs (105).

Generally, professional phagocytic cells sense bacterial infection through pattern recognition receptors (PRRs) i.e., Toll-like receptors (TLR), nucleotide binding domain (NLR), or NOD-like receptor, that recognize pathogen-associated molecular patterns (PAMPs) such as cell wall components, nucleic acids, and lipoproteins of invading pathogen, and contribute immune

activation in response to multiple signaling pathways (106). NOD1 and NOD2 receptors recognize peptidoglycan (PG), a component of the bacterial cell wall. The NOD1 receptor senses PG containing iEDAP (γ-D-glutamylmeso-diaminopimelic acid), M-TetraDAP (MurNAc-L-Ala-D-Glu-mDAP-D-Ala), and M-TriDAP (MurNAc-L-Ala-D-Glu-mDAP). These PG fragments are particularly presented in Gram-negative bacteria and some Gram-positive bacteria, for example, *Listeria monocytogenes* and *Bacillus spp*. NOD 1 receptor also recognizes the small dipeptide iEDAP (D-Glu-mDAP). The NOD2 receptor binds to Muramyl-TriLys (MurNAc-L-Ala-D-Glu-L-Lys) and muramyl dipeptide (MDP), which contains MurNAc, L-alanine, and D-glutamic acid. These structures are found in both Gram-negative and Gram-positive bacteria (107, 108).

The details of the innate immune system recognition of *Orientia* is unclear. *Orientia* seems to be involved in the activation of cytosolic immune receptor NOD-1, an intracellular receptor for bacterial peptidoglycan fragments, based on the supporting evidence as follows: (i) the NLR activation by the γ-D-glutamyl-meso-diaminopimelic acid of peptidoglycan (109, 110); (ii) based on genome analysis, peptidoglycan may be synthesized from UDP N-acetyl-D-glucosamine (54, 105); and (iii) the presence of meso-diaminopimelic acid (*meso*-DAP) and peptidoglycan-like structures in *O. tsutsugamushi* (44). The stimulation of NOD-1 receptors, as well as NF-kB-mediated pathways, leads to massive production of proinflammatory cytokines including IL-6, IL-8, IL-12p70, and tumor necrosis factor (TNF-α), and IL-1β (105, 106). A recent study showed that the secretion of IL-1β is associated with the inflammasome and phagosomal maturation. *Orientia* induces IL-1β production by macrophages through the activation of caspase-1 and the adaptor protein ASC (106). These two proteins are the key components of inflammasome which plays an important role in initiating and maintaining the inflammatory response (111). The IL-1β secretion also requires *Orientia* escape from the phagosome during phagosomal maturation and PAMs of *Orientia* may stimulate one of the NLR/NOD receptors in the host cytosol (106).

Intracellular pathogens or viruses are also recognized by TLRs on phagocytic cells (Antigen-presenting cells, APCs) which present the bacterial peptide antigen to the T-cell receptors (TCR). T-cell activation requires multiple signals that interact with APCs; signal 1 is the interaction between peptide-MHC complex and TCR, signal 2 involves costimulatory molecules

(CDs), and signal 3 is mediated by the various cytokine signaling molecules, i.e. interleukins-1, 6, 12 (IL-1,-6,-12), interferon-α (IFN-α), resulting in the differentiation of naïve $CD4^+$ T-cells (Th0) into mature T-cells (T-helper 1, Th1) that produces IFN-γ (112-114). Some studies have shown that TLR-2 and TLR-4 were related to protective immunity in *Rickettsia akari* and *R. conorii infections*. The role of TLRs in recognizing *Orientia* infection is poorly characterized. TLR-2 seems to increase the susceptibility of *Orientia* infection or enhance pathology in a mouse model. One study showed that the release of TNF-α and IL-6 from infected dendritic cells (DCs) derived from C57BL/6 mice requires TLR-2 (105).

PRRs and TLRs of APCs recognize the pathogen resulting in the activation of APCs. *Orientia*-infected DCs stimulate the DCs' activation by upregulating the expression of major histocompatibility complex (MHC) class II, costimulatory molecules (CD40, CD80, CD86, and CD83) (115, 116), and chemoattractant molecules (CCL3, CCL5, CCL19, CCL21) (105). The antiviral type I interferon pathway of infected DCs is also upregulated via the phosphorylation of p38 mitogen activated protein kinase (MAPK) to produce IFN-β (105). After activation, DCs move toward lymph nodes to present antigen to naïve $CD4^+$ T-cells resulting in the release of type II interferon (IFN-γ) from Th1 cells. The activated T-cells facilitate the elimination of the pathogens. *Orientia* is likely to inhibit the maturation, migration, and T-cell activation of infected DCs, but *Orientia* potentially activates DCs more than other bacteria that reside in the vacuole, including *Coxiella burnetii*, *Brucella abortus* (105, 117).

Orientia-infected macrophages/monocytes induce the upregulation of the expression level of chemokines (CCL2, CCL3, CCL4, CCL5, and CXCL2) through the induction of NF-κB transcription factor (118). The MAPK pathways are involved in the upregulation of IFN-β and TNF-α at the transcriptional level and posttranscriptional levels (119). *Orientia* also activates the immunosuppressive molecule, IL-10, to inhibit TNF-α and increase bacterial survival inside phagocytic cells (120). This strategy is similar to other intracellular pathogens, for example, *Mycobacterium tuberculosis*, *Coxiella burnetii* (121), and *Yersinia enterocolitica* (122). However, the mechanism of anti-inflammatory induction in *Orientia* is not well understood.

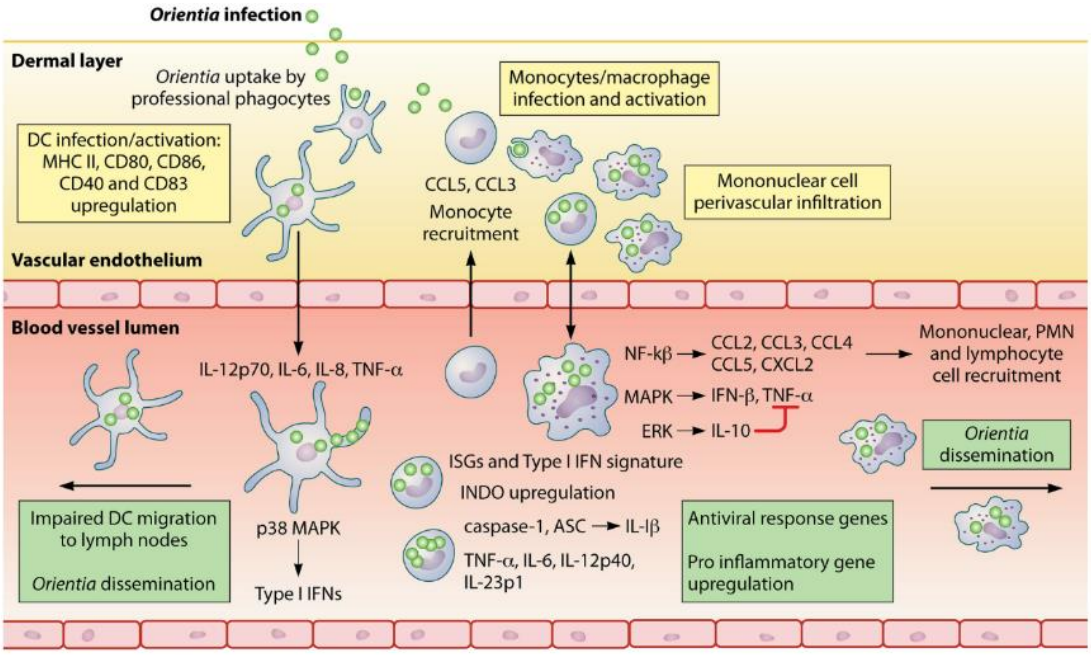

Figure 3. Schematic of early inflammation response following *O. tsutsugamushi* infection. *Orientia* has shown tropism for dendritic cells and monocytes at the inoculation site. Impaired DCs promotes rickettsial dissemination. DCs release proinflammatory cytokines and stimulate a type I IFNs response. Monocytes are recruited to the infection zone, which results in mononuclear cell infiltration and upregulation of proinflammatory genes and the recruitment of other immune cells. Schematic figure from (105).

Endothelial activation plays an essential role in pathogen clearance and immensely influences the activation of cytokine signaling molecules. During infection, the intercellular adhesion molecule (ICAM-1), vascular cell adhesion molecule 1 (VCAM-1), and other adhesion molecules are upregulated to promote the binding of leukocytes and chemokines (105). VCAM-1 and ALCAM (activated leukocyte cell adhesion molecule) have been associated with the severity of scrub typhus and could be a biomarker of clinical prognosis and disease severity (123).

IL-32 plays a role in endothelial activation by inducing several proinflammatory molecules. The binding of *Orientia*-NOD1 may activate the production of IL32 but the mechanism has not yet been elucidated (124). Upregulation of IL-33 during *Orientia* infection may modulate the inflammatory response, and induce the apoptotic response of endothelial cells. The activation

and dysregulation of endothelial is controlled by Ang-1 (vascular stabilizing factor), and Ang-2 (vascular destabilizing factor). Ang-2 is usually stored in the cells but is released in response to inflammatory signals to stimulate endothelial activation (125, 126). High expression of Ang-2 and Ang-2/Ang-1 ratio indicates excessive inflammation and loss of endothelial integrity. This indicates that endothelial cells are a key mediator of the inflammatory response (105, 127). The excessive inflammation, apoptosis, and massive release of pro-inflammatory cytokines can also contribute to acute infection in many organs, for example, hepatitis, meningoencephalitis, and acute respiratory distress syndrome (128).

Adaptive immune responses

The adaptive immune response is the second line of defense against pathogens. The major function of the adaptive immune system is to destroy invading pathogens and the toxic molecules produced by pathogens. The adaptive immune system is divided into two classes; humoral immune responses (HIR, antibody responses) and cell-mediated immune responses (CMIR). HIR and CMIR are carried out by lymphocytes, and B-cells, and T-cells, respectively (129).

HIR plays an important role in providing immune protection against homologous infection (infection by the same pathogen) and heterologous infection (infection of different pathogens) with *O. tsutsugamushi*, mediated by antibodies to TSA56, a strain-specific epitope. TSA56 antibodies targeting TSA56 surface protein can inhibit the entry of *Orientia* into cells and neutralize infectivity, as well as increasing the uptake of *Orientia* by macrophages and neutrophils. However, the concentration of strain-specific antibodies against *Orientia* wanes a few years after infection, and the heterologous immune response is maintained for only a short time (73).

The antibody profiles of animal models challenged with Karp strain have reported that Th1 response is significant for IgG2c/IgG1 subclass switching in acute lethal effect, which suggests that the Th1 cytokine profile (IFN-γ) is important in serious disease development. The high level of IgG1 in response to Th2 indicates a sublethal effect (130). Recently, a study of the antibody response to ScaA and TSA56 in scrub typhus patients showed that anti-TSA56 IgG mainly

consisted of IgG1 and IgG3 subclass and the antibodies were maintained for up to one year after recovery, whereas the anti-ScaA IgG consisted of IgG1 and did not respond to other subclasses (131). Until now, the role of antibody responses remains unclear in human protective immunity and animal infection models.

CMIR has an essential role in T-lymphocyte-dependent cross protection against divergent strains in *O. tsutsugamushi.* Both homologous and heterologous *Orientia* antigens can induce the proliferation of T-cells that produce cytokines and interferon. Immunization of *Orientia* (Gilliam and Karp strains) in mice and cynomolgus macaques produces a high level of IFN-γ from T-cells, indicating that the upregulation of IFN-γ provides protection against *Orientia* infection (105). In human scrub typhus patients, IFN-γ and IFN-γ-inducing cytokines (IL-5 and IL-18) present an early response during the acute phase of infection (105). T-cell recruitment in *Orientia* infection is likely to be enhanced by the inflammatory chemokines, CXCL9, and CXCL10, which are commonly secreted by macrophages, monocytes, and T-cells. These two chemokines are structurally related and share the same receptor (CXCR3) on T-cells. The interaction of CXCL-9,-10, and CXCR3 ligand induces T-cell polarization (132). The cytotoxic activity of $CD8^+$ T cells is an important mechanism for eliminating cytosolic pathogens. Scrub typhus patients show a high level of granzymes A and B that are released from cytotoxic T-cell ($CD8^+$ T cells), possibly due to the cytosolic sensing of *Orientia*. There are few studies of $CD8^+$ T cell response in *Orientia*. A high response of $CD8^+$ T cells in the spleen and lung has been shown in BaLB/c mice infected Karp, which suggests that $CD8^+$ T cells response is required to control infection and protect the mice from fatality (105).

Based on the infection cycle and systematic dissemination of *O. tsutsugamushi*, it is clear that host immunity requires an efficient cross-talk between HIR and CIR, with a tight control of effector cells, in order to eliminate the bacteria. However, the mechanisms of T-cell and cytotoxicity responses against *Orientia* infection are not fully understood and should be considered for future study.

1.2 *Orientia tsutsugamushi* infection cycle

1.2.1 The entry and cell invasion

In the early stage of infection, *Orientia* enters host cells by a clathrin-mediated zipper-like mechanism which requires interaction between bacterial surface proteins, host cell receptors, and extracellular matrix components. This interaction induces a series of signaling cascades that culminate in endocytosis (61).

TSA56, the major outer membrane protein of *Orientia*, directly binds to host fibronectin and facilitates the invasion of *Orientia* into host cells through integrin-mediated signaling. Fibronectin is a large heterodimer glycoprotein that is located on the surfaces of cells, in the extracellular matrix (ECM), and body fluids. A range of cells secretes fibronectin as a disulfide-bonded dimer (133). Fibronectin is involved in several cellular interactions with ECM and plays an essential role in the adherence and entry of several pathogens, such as *R. conorii* (134), *Escherichia coli* (135), *Staphylococcus aureus*(136), and *Neisseria gonorrhoeae*(137). Fibronectin contains multifunctional domains including two major heparin-binding domains that interact with heparan sulfate proteoglycans (HSPGs), a collagen binding domain, two major fibrin-binding sites, a well-known motif for binding with syndecans, and central-cell-binding Arg-Gly-Asp (RGD) motifs which interact with α5β1 integrin receptors, the host's transmembrane receptors (133).

Fibronectin facilitates *Orientia* internalization through the interaction between its RGD motif and β1 subunit of the integrin receptors. This was confirmed using the Arg–Gly–Asp-Ser (RGDS) peptides and a blocking antibody against α5β1 integrin receptors to inhibit *Orientia* infection (138). The antigen domain (AD) corresponding to the extracellular domain of TSA56 serves as the fibronectin-binding region. The ADIII and the adjacent c-terminal region (amino acid residues 243-349) of TSA56 presented the adhesion ability to fibronectin. This was determined by a ligand-binding blot using the TSA56-glutathione S-transferase (GST) fusion proteins (138). It has been reported that the short peptide of TSA56-ADIII (amino acid residues 312-341) interacted with fibronectin and significantly inhibited bacterial invasion in L929 cells, possibly by blocking TSA56-fibronectin interaction (139). Also, the peptides containing TSA56-ADI (amino acid residues 19-114) induced a strong antibody response against the patient's sera and could be a

potential region in adhesion/invasion. However, it is not known whether ADI of TSA56 binds to fibronectin or not (81).

ScaC (surface cell antigen) autotransporter proteins potentially participate in *Orientia* attachment to host cells, through binding with fibronectin, but not in cell invasion. The interaction between fibronectin and ScaC has been confirmed using yeast two-hybrid screening and GST pulldown assays (98). However, the details of the binding mechanism remain unknown. Another *Rickettsia spp*., *R. conorii* internalizes into host cells via the interaction between rOmpB, an autotransporter protein, and its mammalian receptor (K70). This K70 receptor shares sequence homology with integrin A domain, von Willebrand factor A1 and A3 domains that potentially bind to fibronectin (134). *Orientia* may process the internalization via the ScaC-fibronectin-integrin interaction.

Orientia may interact with the heparan sulfate (HS) moiety of HSPGs which are ubiquitously expressed in the ECM and on the cell membrane of host cells. HSPGs consist of HS proteoglycan (GAG) polysaccharide chains and each HS chain contains a polymer of repeating N-acetylglucosamine (GlcNAc)-D-glucuronic acid (GlcA) disaccharide units (140). Bacterial invasion inhibition assays have shown that preincubation of the purified *Orientia* with HS and heparin significantly inhibits *Orientia* attachment in L929 cells in a dose-dependent manner. Other supporting evidence demonstrated the reduction of *Orientia* attachment in mutant Chinese hamster ovarian (CHO) cell lines that were deficient of HS and all GAGs synthesis (141). This suggests that HS is potentially involved in *Orientia* attachment and may mediate endocytosis, however, the specific ligand on the *Orientia* surface membrane involved in the binding of HS is still unknown.

Besides HS, the syndecan-4 may participate in *Orientia* attachment to host cells. Syndecans-4, a transmembrane-HSPG, is numerously expressed on the surface membrane of host cells. It has been shown that the infectivity of *Orientia* depends on the expression level of syndecan-4 on the host cell surface (142). Syndecan-4 also interacts with fibronectin via the α5β1 integrin receptor (143). This could suggest that *Orientia* may utilize Syndecan-4 as a co-receptor to adhere to host cells.

Overall, *Orientia* manipulates its surface proteins to interact with fibronectin, integrin, HS, or syndecan-4 for attachment and internalization/invasion into host cells. However, the in-depth molecular mechanisms of these interactions remain to be elucidated.

1.2.2 The internalization of *Orientia* into host cells

The interaction of TSA56 and fibronectin activates integrin-mediated signal transduction pathways. Activation of the α5β1 integrin receptor induces the activation of the downstream signaling molecules at the inner surface of the plasma membrane, including focal adhesion kinase (FAK), Src tyrosine kinase, and RhoA GTPase. The signaling transduction adaptors talin and paxillin are also recruited to the invasion site, which promotes tyrosine phosphorylation of FAK and Src proteins resulting in the actin cytoskeleton reorganization, and these consequently induce the internalization of *Orientia* into host cells via clathrin-mediated endocytosis (139). The recruitment of actin occurs 10 minutes post infection and *Orientia* is completely internalized by 30 minutes post infection. FAK/Src plays an important role in integrin-mediated signaling, where RhoA GTPase is a key regulator of actin rearrangements by promoting actin stress fiber formation and focal adhesion assembly (139, 144). The exact downstream mechanism of integrin-RhoA GTPase activation remains unknown.

Calcium (Ca^{2+}) plays an essential role in many cellular functions, including cytoskeletal reorganization, vesicular trafficking, and gene expression (145). Other facultative intracellular bacteria such as *Shigella flexneri*, *Listeria monocytogenes*, and *Campylobacter jejuni* induce intracellular Ca^{2+} level during the invasion in non-phagocytic cells (146). Likewise, *Orientia* also induces the release of cytosolic Ca^{2+} in Hela cells and also activates phospholipase C (PLC-γ1), a key enzyme regulating Ca^{2+} that is released from the endoplasmic reticulum. These activations might contribute to the actin cytoskeleton rearrangement during the early phase of *Orientia* infection. However, the specific bacterial proteins and host receptors of Ca^{2+} activation are unidentified (146).

Orientia internalizes host cells via clathrin-mediated, but not caveola-mediated, endocytosis which occurs rapidly. The colocalization of *Orientia* with clathrin and adaptor protein 2 (AP-2) has been found within 30 min post infection. This was confirmed by the inhibition assay.

The results showed that the infectivity of *Orientia* was remarkably decreased by clathrin-mediated endocytosis inhibitors, but not by filipin III, an inhibitor that blocks caveola-mediated endocytosis (147). Upon internalization, *Orientia* enters endosomal compartments and colocalizes with the early endosome markers, EEA1, within 10-30 minutes post infection. The majority of *Orientia* remain inside endosomes for up to two-hour post infection, and this was shown by the colocalization with LAMP2, a late endosomal marker.

1.2.3 Endosomal and autophagic escape

The strategy of *Orientia* to escape from the endosome is not known. In other intracellular pathogens, *L. monocytogenes* use the listeriolysin and phospholipase C protein to escape the early endosome. Based on genome analysis, *Orientia* encodes a hemolysin gene (*tlyC*) and a potential gene encoding phospholipase D (PLD). Presumably, *Orientia* may use hemolysin and phospholipase to disrupt the endosome membrane and subsequently release into host cytosol (147).

The low endosomal pH causes the conformational changes and triggers membrane fusion of bacterial membrane and endosomal membrane (148). The acidification of the endosomal lumen is driven by proton(H^+)-pumping ATPase that is located in the endosomal membrane. It has been demonstrated that *Orientia* requires a low pH condition in the endosomal lumen to escape the endosome. When the acidification of endocytic compartments was inhibited by NH_4Cl or bafilomycin, *Orientia* was not able to escape the endosome, and the infectivity of *Orientia* was significantly reduced. This implies that low pH and H^+ pumps are the key compartments for the endosomal escape of *Orientia* (147).

Once *Orientia* is free in the host cytoplasm, *Orientia* induces and escapes autophagy, which plays a critical role in the innate defense mechanism against invading pathogens. The immunoblot with antibody to LC3-II protein, an autophagosome marker, showed that *Orientia* induced LC3-II during the early infection of *Orientia* in nonphagocytic and phagocytic cells. The LC3-II level was significantly high at 30-60 min post infection, gradually decreasing 2-4 hours post infection. Most of the internalized *Orientia* did not colocalize with LC3-positive autophagosome

throughout the infection, suggesting that *Orientia* can actively escape from the autophagosome and only a few bacteria remain captured. In the presence of tetracycline, it blocks bacterial translation, inhibits *Orientia* invasion, and enhances bacterial entrapment by autophagosomes. This indicates that the active escape of *Orientia* is likely mediated by bacterial gene expression or *Orientia* may use some factors that block autophagic recognition (115, 149).

Unlike many other intracellular pathogens such as *Anaplasma phagocytophilum*, *Chlamydia trachomatis*, and *Francisella tularensis* that reside in vacuoles and survive within autophagy (149), *Orientia* is able to escape autophagy, which is similar to *Rickettsia* (150) and other obligate intracellular pathogens such as *Shigella flexneri* and *Listeria monocytogenes* (149). *Shigella* avoids autophagic recognition by secreting IcsB protein via T3SS, which competitively binds to its surface proteins. *Shigella* also blocks the interaction of the autophagy-related proteins, VIG, to prevent autophagosome maturation (151). *Listeria* also uses its proteins to interact with host cytosolic proteins to prevent autophagic recognition, for example, the binding of Listeria protein ActA with cytosolic actin protein complex, and the linking of Listeria protein InlK with cytoplasmic ribonucleoprotein WVP (152).

1.2.4 Intracellular transportation

Many other obligate intracellular pathogens such as *Listeria monocytogenes*, *Shigella flexneri,* and *Rickettsia conorii* hijack host actin and can polymerize actin into the propulsive actin comet tails for transport within the cell and evasion to neighboring cells (cell-cell spread), whilst *Orientia* is not able to recruit and polymerize host actin but colocalizes with host microtubules instead.

After escaping autophagy, the cytosolic *Orientia* manipulates host microtubules to translocate to the perinuclear region where bacterial replication occurs. It has been proposed that *Orientia* interacts with cytoplasmic dyneins to accumulate near the microtubule organizing center (MTOC), which is typically located at a perinuclear region (153). *Orientia* moves to the MTOC within 90 min post infection, suggesting that *Orientia* requires microtubules for redistribution during the early stage of infection (153). However, it is still unclear how *Orientia*

interacts with dynein, why *Orientia* needs to replicate at the MTOC, which surface proteins on *Orientia* interact with microtubule-binding proteins, and how these proteins are regulated. It has been suggested that *Orientia* employs the host cytoskeleton to move to a glycogen and ATP-rich perinuclear region for a metabolic reason (153). Additionally, *Orientia* is particularly located in the glycogen-packed area which is devoid of lysosomes and other cytoplasmic organelles (154).

Chlamydia trachomatis manipulates host microtubules and dynein to travel to the MTOC and interacts with host cell vesicular transport pathways for promoting its effective growth. Chlamydia hijacks host sphingomyelin and cholesterol from the Golgi complex that localizes near the MTOC, and fragments the Golgi complex into ministacks, which are normally designated for the plasma membrane of chlamydial inclusions. This suggests that the main purpose of the location near the MTOC is to uptake nutrients (155).

Recently, *Orientia* has been demonstrated to colocalize with the Golgi complex and translocate backward to the endoplasmic reticulum (ER) before exiting host cells (105). *Orientia* disturbs Golgi structure by destabilizing the membrane of Golgi and ER through the interaction of the effector protein Ank-9 and COPB2, a host protein that mediates Golgi-to-ER transport. This process occurs during the first 24-48 hours post infection. Destabilization of Golgi also benefits *Orientia* replication (156).

Orientia replicates by binary fission with a doubling time of about 9-10 hours (74). *Orientia* has been found to form a microcolony near the nucleus. It has been proposed that the polysaccharide (N19) which is released from *Orientia*, promotes self-aggregation along with bacterial microcolony (157).

1.2.5 Escape from host cells

After replication is complete, *Orientia* migrates to the periphery of the cells and slowly protrudes from the host cell surface, resulting in extracellular bacteria in which the host cell membrane is still intact (158). Each bud contains a single bacterium. It is thought that the host membrane enclosing budding bacteria remains for a long period, and may protect bacteria from the fluctuating environment outside of host cells (159). The membrane-coated *Orientia* may have

benefits for reinfection by phagocytosis. The host membrane enclosing *Orientia* may be lysed before the infection of new host cells, or alternatively, *Orientia* may be released without host membrane from the heavily infected cells due to host cell membrane damage.

The virus-like budding mechanism of *Orientia* is unique among other bacteria in the Rickettsial family. Similar to *Chlamydia spp*. that extrudes from host cells by pinching off, though the extrusion of a single chlamydial inclusion releases around a hundred bacteria (56). It has been reported that Chlamydia mediates the host actin cytoskeleton by the extrusion(160). Possibly, the budding mechanism of *Orientia* may involve actin (56).

Lipid rafts are sections of the plasma membrane that consists of cholesterol, sphingolipids, glycosylphosphatidylinositol (GPI)-linked molecules, and caveolin-1 (161). Many pathogens utilize lipid rafts to enter into host cells but not to exit from them. For example, *E.coli* binds to CD48 which is associated with GPI-linked lipid rafts and *Chlamydia trachomatis* enters host cells via caveolin and cholesterol (162, 163). *Orientia* also uses lipid rafts from the host membrane during the exit but not entry (164). Two *Orientia* surface proteins, TSA47 (HtrA) and TSA56, were proposed to colocalize with lipid rafts to initiate exit from the cell (164).

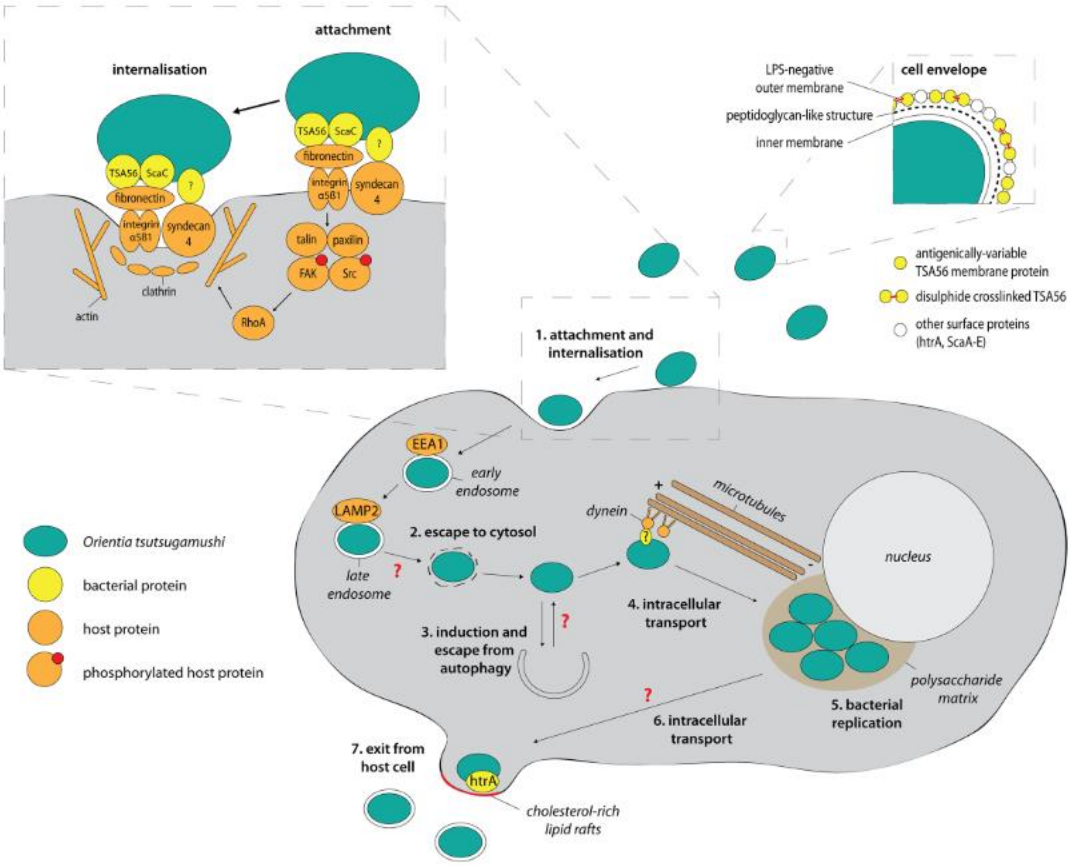

Figure 4. The model of intracellular cycle of *O. tsutsugamushi*. The top right inset shows a schematic view of the cell envelope of *O. tsutsugamushi*. The large inset represents the overview of the attachement and internalisation process. Red arrows indicate unknown pathways. LPS, lipopolysaccharide; ScaC, surface cell antigen C; TSA56, type surface antigen 56. Image from ref (61).

1.3 Bacterial heterogeneity

Generally, bacteria live in fluctuating environments and they have to adapt to a wide range of external conditions for survival. As a result of successful adaptation driven by changes in the environment, bacterial cells undergo a cellular differentiation process by altering cell morphology and/or physiology during the developmental cycle (165).

Caulobacter crescentus is an aquatic gram-negative bacterium that lives in nutrient-poor environments, and it is one of the best models to study the bacterial developmental cycle,

regulatory networks controlling the bacterial cell cycle, and cell differentiation (166). *Caulobacter* exhibits a dimorphic cell cycle (swarmer and stalk cells), and each cell presents a distinctive appearance based on the developmental stage (167, 168). This property allows easy synchronization of populations and follows up gene expression, gene regulation, protein subcellular localization, cell division, and growth over the course of infection (169).

Pathogens exhibit mixed populations (population heterogeneity) to cope with rapidly changing environments. This adaptation can be explained by the fact that bacterial cells require a longer time to initiate recognition of and response to environmental changes by common signal transduction pathways. The response process may be costly because bacteria need to waste energy to produce proteins that would allow them to survive in a restricted condition. These processes may not allow bacterial cells to adapt in time. Bacteria need an alternative strategy by generating subpopulations which rely on genetic and phenotypic variations to ensure that the whole population is not killed by stressors (170).

The heterogeneity within bacterial populations is driven by genetic diversity at the population level and/or phenotypic differences between genetically identical bacterial cells. Two broad strategies have been described for how bacteria undergo heterogeneous adaptation upon the environmental changes. First, the bet-hedging strategy in which some individuals of bacterial populations express genes which facilitate their survival under stress conditions. The variability of bacteria cells occurs within a genetically identical population to ensure that some individual bacteria will adapt and will survive under given conditions, and eventually reproduce more offspring. This process happens before bacteria is exposed to stress environments during infection. On the other hand, heterogeneity results from changing environments. A small population within a bacterial cluster changes the gene expression profile after exposure to environmental stress such as limited nutrient availability and changing pH, temperature, and osmolality (170, 171).

1.3.1 Genetic diversity within bacterial populations

Bacterial gene expression is normally regulated at the transcriptional level through a promoter control mechanism. Bacteria increase several genes for adaptation to more than one environment. This strategy is typically controlled by all-or-none mechanisms and phase variation is an example of this mechanism (172).

Phase variation is a stochastic mechanism for generating heterogeneous populations and involves reversible alteration to the genome. Phase variation describes the switching of protein expression from an ON to an OFF phase in response to rapid environmental changes. This process is caused by reversible mutation where the mutation switches off the expression of a gene and inversely the mutation switches a gene back on again, leading to a variation in the expression level of one or more proteins between individual cells. Phase variation occurs randomly at a high frequency with approximately 10^{-5} per generation (172, 173).

Pathogenic bacteria frequently use phase variation to alter their cell surface structures, such as outer membrane protein, lipopolysaccharide (LPS), flagella, and pili. This helps bacteria evade the host immune recognition due to antigenic specificity changes. Phase variation of *lic1* locus has been demonstrated in *Haemophilus influenza*. The *lic1* locus is required for the addition of phosphorylcholine (ChoP) to LPS. The presence of ChoP on LPS enhances immune resistance by reducing sensitivity to C-reactive protein–mediated complement killing (174). *Neisseria meningitides* can switch Opas, adhesin proteins on bacterial surface membrane, to avoid phagocytosis and complement fixation during the course of infection. The Opas proteins exhibit antigenic variation and have different tissue tropism. Phase variation of Opas could allow bacteria to adapt to different niches during the infection cycle (174).

Obligate intracellular bacteria also employ the phase variation strategy to survive in host environments. It has been demonstrated that phase variation contributes to a rapid adaptation of *Chlamydia trachomatis* by mediating the regulation of lipid A biosynthesis and the functionality of cytotoxin (175). The major surface protein 2 (msp2) in *Anaplasma phagocytophilum* exhibits antigenic variation by recombination of pseudogene into the msp2 operon-linked expression site.

This allows bacteria to escape Th cell recognition and results in life-long persistence in host cells (176). The antigenic variation of major outer membrane protein, TSA56, in *O. tsutsugamushi* might be processed through phase variation to avoid host immune recognition, however, there is no evidence to support phase variation in *Orientia*.

1.3.2 Phenotypic heterogeneity within bacterial populations

The stress in host microenvironments may promote a different growth rate in a subpopulation of pathogenic bacteria. Perhaps the most common form of phenotypic heterogeneity is the presence of slow-growing cells/non-replicating cells within a majority of replicating cells.

Subpopulations of bacteria differentiate into distinct morphological cell types to adapt to the niche environments in which they reside. Many bacteria present two distinct morphotypes in their life cycle which consists of replicating and non-replicating forms. For example, sporulating and vegetative cells in *Bacillus subtilis* (177), stalk and swarmer cells in *Caulobacter crescentus*(168), infectious extracellular (the elementary body-EB) and noninfectious intracellular replicating form (the reticulate body-RB) in *Chlamydia trachomatis* (178), a Large-cell variant (LCV) and Small-cell variant (SCV) in *Coxiella burnetii*, and *Anaplasma* spp. and *Ehrlichia* spp. which both have a large reticulate (RC) and smaller dense-core (DC) form (178-181). However, the *Orientia* life cycle appears not to have a biphasic life cycle because there is no obvious alteration of their morphotype among the subpopulation during the infection cycle. This feature is also found in the closely related bacteria, *Rickettesia* spp. (182). Persister cells have been implicated in chronic infection especially bacteria that produce biofilm formation, such as *E.coli*, *B. subtilis*, and *Pseudomonas putida* (171). Subpopulations of bacteria in macrocolony biofilm differentiate into distinct morphological cell types. Stationary phase-like cells in the surface of the biofilm are small and round while post-exponential-phase cells at the bottom and lower zone present a rod shape (183).

1.4 Detection of bacterial heterogeneity

The most common strategies that have been used to identify distinct bacterial subpopulations are based on utilizing fluorescent probe/reporter of distinct subpopulations such as FISH (Fluorescent in situ hybridization) or detection of fluorescent signals that follow up the expression of specific genes or monitor cell division (171).

The FISH method is used for the detection and quantification of nucleic acid in the cells. This principle is based on the hybridization of nucleotide probes that are complementary to target sites on DNA or RNA. The reaction is directly detected by fluorescently labeled probes or radioactively, or it can be indirectly visualized using antigen binding or biotin-streptavidin interactions (184). FISH was shown to be a useful tool to study the individual cells including the developmental cycle of obligate intracellular bacteria, such as using a set of 16S rRNA-targeted oligonucleotide probes to detect *Chlamydia spp.* in Hela cells (185). The advantage of FISH is that it can be applied with multiple methods such as immunofluorescence, mass, single cell RNA-seq and Mass spectrometry. Also, FISH does not need a strain specific construction and can label several conditions in fixed cells. FISH can be applied with multiple probes labeled with different dyes to reduce the risk of false-positive signals, which are caused by nonspecific binding of host components. Even though the detection of specific 16s rRNA sequences can define the identity of individual cells, FISH cannot distinguish closely related species or cells with identical rRNA sequences (171).

The fluorescent reporter can be used to study the growth rate of individual bacteria by monitoring DNA replication rate, a change in ribosomal protein or RNA content, and fluorescent signal dilution upon cell division (186). Fluorescence reporter can monitor a change in ribosomal RNA content which is a very effective method to observe the individual cell differentiation, especially when the ribosomal proteins significantly change in bacterial cells under different growth phases. For example, the insertion of destabilized GFP at the ribosomal RNA (rRNA) locus has been used to determine ribosome biosynthesis. GFP-tagged single strand binding protein (SSB) can label replication forks of DNA to monitor DNA replication in active dividing bacteria (187). However, the SSB method may not be suitable for fast-growing bacteria because of a poor

fusion of SSB. Fluorescent signal dilution effectively monitors bacterial replication up to 10 generations, however, the fluorescent signal usually reduces below the limit of detection after 10 divisions. Additionally, this method is efficient when the fluorescent proteins are stable with very low turnover rates, which allows a ratio of fluorescence observed/initial fluorescence to be a good readout of the number of cell divisions (171, 188).

In obligate intracellular bacteria, the fluorescent protein-based method has been used to study the life cycle and host-pathogen interaction. However, this approach does not work for genetically intractable bacteria including *Orientia tsutsugamushi* (189). The immunofluorescence approach is currently the main tool for labeling obligate intracellular bacteria by targeting the surface protein on bacterial membrane such as Omps in *Rickettsia spp*., and TSA56 in *Orientia*. Additionally, the surface proteins of each organism always present antigenic diversity, and antibodies against targeted proteins need to be optimized and validated for new strains. The clickable methionine probe is an alternative tool to label the obligate intracellular bacteria. It can be used as a universal probe to label the pathogens and differentiates the metabolic activity within bacterial populations (190).

1.5 Cell growth and bacterial cell cycle

Cell growth depends on the capability of cells that can proceed with successive rounds of the cell cycle. The bacterial cell cycle generally consists of a series of events during cell growth which is divided into three stages: the initiation of DNA replication (B period), genome duplication and chromosome segregation (C period), and completion of replication and cell division (D period). DNA replication and cell division are the two key processes that have to be synchronized with cellular growth, to ensure that the reproduction of progeny occurs along with the maintaining of cell size and shape. Coordination between cell growth and rapid changing environmental conditions are important processes for bacteria to survive. Bacteria must quickly adjust the cell cycle dynamic and growth parameters to accommodate changes in nutrient availability, temperature, and pH, as these factors depend on the host conditions (191).

1.5.1 DNA replication

DNA replication is coordinated with cellular growth and has to be tightly regulated to ensure that the replication occurs only once per division cycle, as well as, both nucleoid segregation and cell division must be completed to facilitate the stability and integrity of the offspring's chromosome. These processes also require sufficient nutrients to drive the cell cycle, suggesting that the replication is coordinated with the nutrient availability and metabolic status (191, 192).

The initiation of replication is activated by a highly conserved initiator protein DnaA which is a member of the AAA+ family of ATPase and probably found in most prokaryotes. DnaA binds to the origin of chromosome replication (*oriC*) at the high-affinity binding sites, Dna-ADP and Dna-ATP, to unwind the double DNA helix and allow the formation of replisome which consists of helicase to unwind DNA strand, polymerases to duplicate the DNA and nuclease and ligase enzymes to process DNA duplication on lagging strand (192, 193).

Nutrient availability has a significant effect on DnaA level during cell growth. Upon amino acid starvation, the DnaA synthesis diminishes and inhibits DNA replication. In *E.coli,* DnaA is regulated by (p)ppGpp. The synthesis of (p)ppGpp is stimulated by amino acid starvation through RelA synthetase enzyme or is triggered by carbon starvation through SpoT synthetase enzyme. It has been demonstrated that the transcription of *dnaA* is inhibited by (p)ppGpp but the mechanism remains unclear (194). Overexpression of RelA induces (p)ppGpp and also blocks the replication initiation(195). This supports that DnaA and initiation of replication are controlled by (p)ppGpp. There are other regulatory mechanisms that work together to regulate DnaA synthesis and activity such as autoregulation of dnaA transcription and positive control by DiaA, an initiator activity of DnaA protein (192). In *Caulobacter*, DNA replication is tightly controlled by the CtrA protein, which is an important response regulator. CtrA binds to the origin of replication and prevents the initiation of new rounds of replication (196, 197). CtrA also controls the expression and cell cycle progression by binding about 55 cell-cycle-controlled operons including flagellum and pili biogenesis (198, 199). The activity of CtrA is essential for the swarmer-to-stalked cell transition, which must be tightly coupled with other pathways involved in polar differentiation,

growth, and cell division. This allows various events to be synchronized during cell cycle progression (169).

1.5.2 Chromosome segregation and cell division

Unlike chromosome segregation in eukaryotic cells, chromosome segregation in prokaryotic cells occurs continuously along with DNA replication. After completion of the replication by binary fission, sister chromosomes in bacterial cells move to opposite ends of the cell before separation. The cells divide into two progeny cells of about similar size. As a consequence, the mid cell region has free space which allows the polymerization of FtsZ, a tubulin homologue protein, into the Z-ring at the future septation region (200).

The cell division process is controlled by divisome, a protein complex that is essential for division and is located at the cytoplasmic membrane. In *E. coli*, the divisome consists of more than 10 proteins such as FtsZ, ZipA, FtsN, FtsK, FtsQ, and FtsI. If cells lack these proteins, cells can continue to grow without dividing and form filamentous cells and may ultimately lyse (201). There are two phases of the divisome assembly which have been demonstrated in *E. coli*, *B. subtilis*, *C. cresentus* and other bacteria (166). The first phase is the formation of proto-ring. The Z-ring is generated along with the accumulation of membrane-associated proteins (ZipA, FtsZ, and FtsA) at the cell envelop. In the second phase, late divisome proteins (FtsK, FtsQ, etc.) that involve peptidoglycan synthesis are recruited to generate septum, as well as other proteins that coordinate between proto-ring and peptidoglycan synthetase such as FtsN, FtsI, etc. (202).

In *E. coli*, the regulation of cell division involves two main systems; the Min complex and nucleoid occlusion. The Min complex consists of the MinC, MinD, and MinE proteins. On the cytoplasmic membrane, MinD binds to MinC (a division inhibitor) and forms a cap-like polymeric layer to prevent the formation of FtsZ ring at the pole of cells. MinE forms as a ring-shape that slowly displaces MinCD from the middle to the polar region of the cell. The second system, nucleoid occlusion, consists of the SlmA protein which binds to the chromosome and directly interacts with FtsZ, maintaining septum formation until chromosome segregation is nearly finished. The integrated function of SlmA and Min complex proteins targets FtsZ ring at midcell

to make sure that the divisome formation is retained to the last phase of the replication cycle (200, 202).

Caulobacter commonly divides into two distinct cell types; swarmer and stalked cells. A swarmer cell lives in the environment searching for nutrients and cannot replicate before it differentiates into a stalked cell. When the conditions are favorable, the stalked cells initiate chromosome replication, and the divisome protein complexes are recruited to mid-cell after chromosome segregation (166). FtsZ ring forms a ring-like structure in the midcell and recruits many other divisome components that are essential for membrane fission, peptidoglycan remodeling, and cell separation (203). Instead of the Min or nucleoid exclusion system, the regulation of cell division in *Caulobacter* is controlled by ATPase MipZ, which belongs to Mrp/MinD family(204). MipZ acts as a checkpoint and coordinates the assembly of divisome. MipZ interacts with the polar ParB-ParS complexes. ParB functions by stimulating the formation of ATP-bound MipZ dimer, which are retained at the pole, and this allows Z-ring formation at the mid cell region (205).

In cell-wall-less obligate intracellular bacteria such as *Chlamydia spp*., *Wolbachia spp*. and *Orientia* there is a lack of FtsZ. The question has been raised as to how these bacteria process the division. It has been reported in *Chlamydia* that MreB actin-like protein and its regulator RodZ of bacterial actin complex partially substitutes for the function FtsZ in the septation process during cell division (206, 207). Evidence of the FtsZ ring in *Orientia* remains to be found.

1.5.3 Growth

Two fundamental types of bacterial growth have been described: growth in biomass in which individual cells increase in mass, and growth in cell number which results from binary fission (208). Bacterial growth rate depends on the environmental conditions especially nutrient availability. Nutrient-rich conditions result in a reduction of mass doubling time and increase in the cell size, whereas starvation conditions diminish the growth and reduce cell size (192).

The typical growth curve of bacteria consists of four main phases; lag, log, stationary, and death. The lag phase is when cells adapt themselves to the growth conditions and cells might

have little or no cell reproduction during this stage. In the exponential phase, cells begin to rapidly multiply by binary fission which leads to an exponential increase in the number of cells. During the stationary phase, the metabolic activity is high and the DNA, RNA, cell wall components, and other important proteins are produced for cell division. This phase can last for several hours or several days, depending on bacterial species. The stationary phase occurs when nutrients are depleted or other conditions such as the accumulation of toxic waste products and stress factors, results in limiting the number of cells or stopping growth. However, metabolism is still active. The rate of cell division is equal to the rate of cell death. Pathogenic bacteria begin to produce substances or virulence factors that help them survive among harsh conditions. Finally, the death phase represents an exponential decline in the number of cells due to cell death (209).

The physical and molecular changes of bacterial cells during the stationary phase have been a recent focus of research due to the importance of adaptation strategies for survival under stress conditions. Major physical changes of the cells during the stationary phase include the reduction of cell size, development of spherical shape, the reduction of membrane fluidity, an increase of cross-links of the cell wall and an increase in the thickness of the peptidoglycan layer (210). Bacterial cells also activate the stringent response mechanism which allows bacteria to reprogram the gene expression pattern to survive in stress conditions. The key regulators of gene expression during the stationary phase are transcriptional factors. Sigma factors are upregulated in several bacteria, for example, σ^{H},σ^{s}, σ^{N} in *E. coli* and σ^{E},σ^{H},σ^{s} in *Pseudomonas aeruginosa* (211, 212). In *C. crescentus*, a large number of alternative sigma factors of the extracytoplasmic function (ECF) have been implicated in stress responses. Three ECFs (σ^{F}, σ^{T}, and σ^{U}) are known to be involved in stationary-phase survival (213), and $\sigma^{T,}$ which is similar to σ^{s} in *E.coli*, has been demonstrated to be the master regulator to stress response (214). The DNA is highly condensed due to a high condensation of cytoplasm. This leads to a reduction in protein synthesis. At the translational level, the ribosome is inactivated to reduce protein synthesis. There is little known about the proteins that are involved in chromosome organization and interaction with DNA during the stationary phase. This needs to be investigated through further research (215).

1.6 Genetic tools in obligate intracellular bacteria.

1.6.1 Transformation

Over the past 20 years, genetic manipulation of obligate intracellular bacteria including *Chlamydia spp*., *Coxiella spp*., *Anaplasma spp*., *Ehrlichia spp*., and *Rickettsia spp*. and *Orientia spp*. has proven immensely difficult due to their genetic intractability. The limitations of genetic manipulation in obligate intracellular bacteria can be described as follows; (i) bacteria must be propagated and manipulated intracellularly (189), (ii) the growth of intracellular bacteria takes longer than other facultative intracellular bacteria and free-living bacteria, for instance, *Rickettsia* and *Orientia* have a replication time of 8-19 hours, which is 2-3 times that of *Legionella pneumophilia* (216), (iii) obligate intracellular bacteria must be purified from host cells before performing the transformation, thus, bacteria could be damaged during the purification process and might become non-infectious (189), (iv) mutating genes that are vital for bacterial invasion and growth may compromise the survival of transformants (189), (vi) selecting appropriate promotors is a key factor in enabling the inserted elements and reporter to function during transformation (189).

A genetic transformation is a common approach in which exogenous DNA is transferred into prokaryote and eukaryote cells, resulting in alteration to the specific targeted-gene in recombinant strains. Transformation methods that have been successfully performed in obligate intracellular bacteria include electroporation, chemical transformation, and PAMAM (polyamidoamine) dendrimers mixed with a plasmid vector (189).

Chemical transformation commonly involves the use of calcium chloride to increase the permeability of bacterial membranes. Calcium ions will bind to both foreign DNA and bacterial cell surface which changes cell membrane permeability. This allows DNA uptake into bacterial cells (217). The advantages of this method are that it is simple, inexpensive, and rapid. However, amongst obligate intracellular pathogens chemical transformation has been used only for *Chlamydia trachomatis* L serovars (218).

PAMAM dendrimers are highly branched polymers that are used for the delivery of small molecules or DNA into mammalian cells. Dendrimers enter targeted cells via endocytosis and can

be modified to enhance the transfection efficiency in different cell types. Dendrimer-plasmid complexes have been used to transform *Chlamydia spp*. (*C. trachomatis* and *C. pneumonia*) and *A. phagocytophilum*. These achievements highlight the potential of dendrimer to penetrate the host membrane and the vacuole-bacteria. In addition, bacterial cells are less damaged by PAMAM dendrimer-mediated transformation than by chemical transformation or electroporation, and this method does not need bacterial isolation and reinfection (219, 220).

Electroporation or electropermeabilization is a method that uses high-intensity electrical field pulses to transiently destabilize cell membranes, leading to temporary pores and allowing cells to uptake exogenous DNA. This technique is rapid and easy but requires bacterial isolation and antibiotic selection. Many obligate intracellular bacteria have been successfully transformed through electroporation such as *C. trachomatis*, *R. prowazekii*, *A. phagocytophilum*, and *E. chaffeensis* (221-224).

Transformation is easy to perform in free-living bacteria. However, proceeding with this approach in obligate intracellular bacteria is challenging due to host cell restricted growth, which causes low transformation efficiency and requires long-term culture to expand small transformant populations. There are several factors that need to be considered in transforming obligate intracellular bacteria, such as plasmid types, bacteria purification, host cell types, host cell confluence, MOI (multiplicity of infection), antibiotic selection markers, promoter selection, and detection of positive transformant population (72).

Plasmids/ shuttle vectors have been used successfully to manipulate the genetics of obligate intracellular bacteria. However, the plasmids are sometimes lost after long periods of passage and cannot mutate essential genes that are important for bacterial growth (189).

Transposon insertion is another molecular tool used for random mutagenesis in the bacterial genome. This approach is effective and widely used for studying bacterial pathogenesis and bacterial virulent factors (225). *Himar1* is a transposon element that was originally isolated from *Haematobia irritans* that has been extensively used to mutagenize large numbers of bacteria including many obligate intracellular bacteria, such as *C. burnetii*, *Anaplasma spp*., *Ehrlichia chaffeensis*, and *Rickettsia spp*.. Generally, the *Himar1* transposase system consists of transposase enzyme and transposon which contains antibiotic resistance cassette and

fluorescent markers flanked by inverted repeat regions. The *Himar1* transposase functions by randomly inserting transposon into AT dinucleotide sites in the bacterial genome via a cut-and-paste mechanism. The fluorescent gene marker in the transposon provides a visual detection and identification of insertion loci in the bacterial genome (189).

Several genetic approaches have been established in many obligate intracellular bacteria, however, genetic manipulation has never been successful in *Orientia* and still needs to be elucidated (Fig. 5).

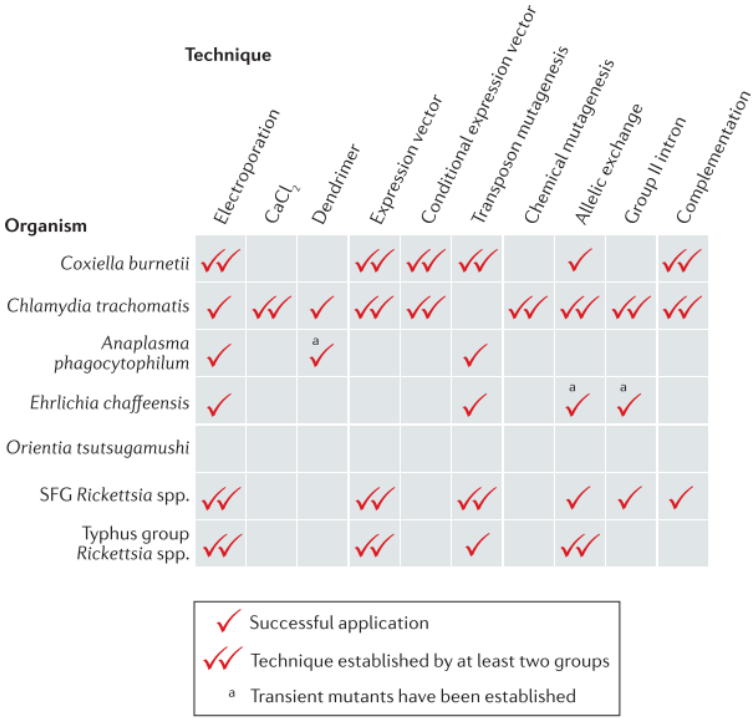

Figure 5. A summary of genetic tools in obligate intracellular bacteria. Successful genetic manipulation is yet to be shown for *O. tsutsugamushi.* Image from ref (189).

1.6.2 Antisense technologies

Synthetic nucleotides are an essential tool for molecular biology, oligonucleotide-based therapies, and clinical diagnostics. Oligonucleotides are widely used in primer-based techniques, such as PCR, library construction, nucleotide polymorphism, and many others. Aside from these methods, oligonucleotides have been extensively used in gene-silencing approaches.

In recent decades, several nucleic acid analogs have been developed that can target cellular DNA/RNA and these include locked nucleic acids (LNAs), peptide nucleic acids (PNAs), 2'-fluoro N3-P5-phosphoramidites, 1', 5'-anhydrohexitol nucleic acids (HNAs), and the latest generation known as Bridged Nucleic Acids (BNA) (226, 227).

LNAs or locked nucleic acids (Fig. 30) are bicyclic nucleotide analogues containing a furanose ring that is modified by adding a methyl group linking 2'-oxygen and 4'-carbon (2'-O, 4'-methylene-β-d-ribofuranosyl nucleotides). LNAs are designed to reduce the flexibility of the ribose residue and remain in a locked N-type conformation, which facilitates the stability of the LNA-DNA/RNA duplex. LNA-containing oligomers have been used in many applications including hybridization of probes/primers, mutagenesis, and SNP genotyping. However, non-specific off-target binding of LNA-containing nucleotides can cause toxic effects, especially in human diseases (228).

Antisense Peptide Nucleic Acids (PNAs) are DNA analogues that consists of a peptide backbone instead of sugar-phosphate and side chains of nucleic acid bases (Fig. 30). The properties of PNAs are high specificity, high sensitivity, chemical stability, thermal stability, and resistance to nucleases degradation when delivered inside cells (229). The use of PNAs is an effective method to inhibit gene expression involved with DNA replication, fatty acid synthesis, and RNA synthesis by binding at specific mRNA sequences in several free-living organisms i.e. *Escherichia coli and Bacillus subtilis* (230). The advantages of PNAs include no antibiotic selection is required, the delivery process can be done by electroporation, protein reduction can be seen within one day, and partial protein reduction could help the further study of essential genes. PNAs have been designed that are complementary to ribosomal binding sites of OmpB and rickA in *R. typhi* and *R. montanensis*, respectively, and they have successfully repressed OmpB and rickA expression as measured by Western blot (231). However, PNAs exhibit poor cellular uptake, low binding efficiency to targeted sequences, and poor solubility in the aqueous phase.

Bridged nucleic acids (BNAs) are the latest modified oligomers which are more effective than earlier generations of synthetic oligomer (PNA and LNA). BNA has high-affinity to DNA and mRNA targets, high RNA selectivity, and high resistance to nuclease degradation. Recently, BNA

has been modified in many derivatives as BNA^{NC} with different substitutions at the N position (Fig. 6). A six-member ring (2',4'-BNA^{NC}) is the most widely used to date and exhibits less toxicity and higher resistance to nuclease than LNA.

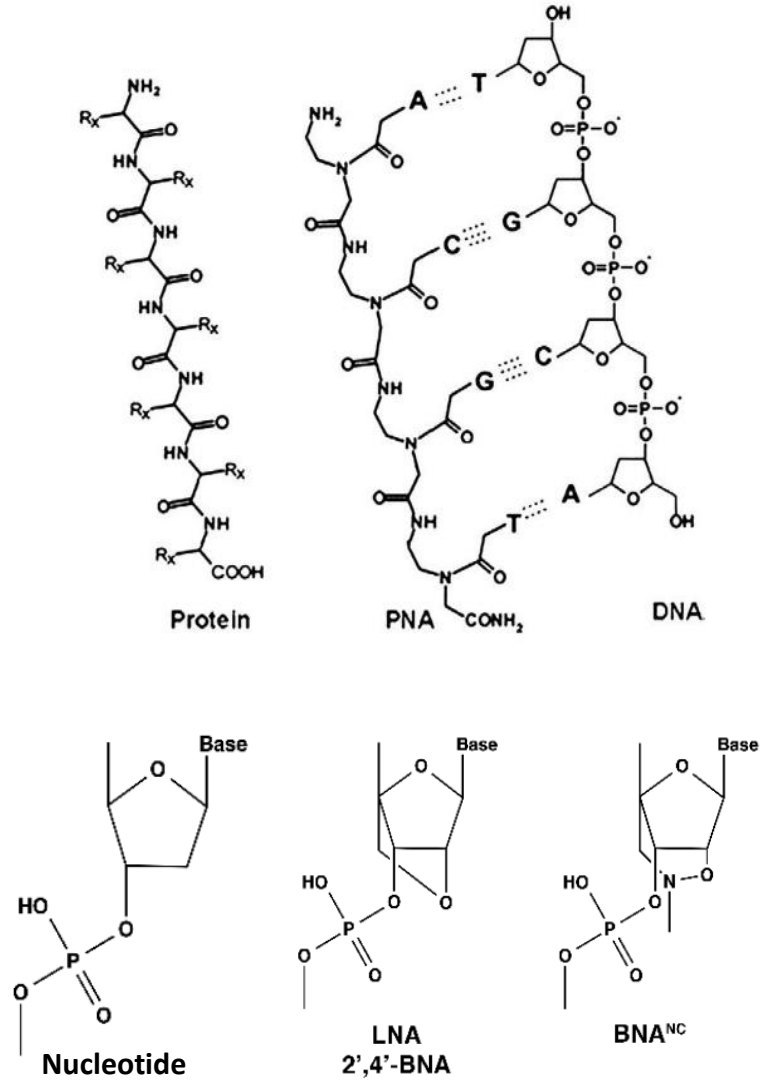

Figure 6. The overall structure of protein, PNA, BNA and DNA. Top panel; A comparison of PNA, DNA and protein structure. PNA consists of an amine-terminus (N-terminus) and a carboxy terminus (C-terminus), corresponding with the 5'- and 3'-ends of the DNA oligonucleotide, respectively. Low panel; 2',4'-BNA^{NC} (BNA^{NC}) is a derivative of the LNA, 2'-O,4'-aminoethylene bridged nucleic acid (BNA), which is the earliest generation of BNA. Images modified from ref (228, 229).

1.7 RNA-seq technology

Pathogens commonly subvert host cellular pathways for survival and growth, and host cells also respond to the invading pathogens through several cascading pathways. These result in changing the transcriptomic profiles and gene expression of two interacting organisms. Understanding the complexity and dynamics of host-pathogen interaction during the infection is very important for improving diagnostic, treatment, and vaccine development (232).

Recently, microarrays have been extensively used for measuring gene expression profiles, studying the mechanism of bacterial infection, and host response to infection (233, 234). However, the profiling of both pathogen and host RNA measured by microarray are inadequate due to cross-hybridization, and high background signal. In addition, the analysis of both pathogen and host cannot be done at the same time (235) and it cannot detect noncoding RNA (ncRNA) classes (234). Tiling arrays are another subtype of microarrays but the probe can be used for interrogation of the genomic region for transcription (236), and alternative splicing (237). This method was developed to solve the detection of ncRNA transcripts, however, this assay is very expensive for studying a large size of the host genome (238). Tag-based sequencing was developed to allow individual transcripts to be digitally counted with a broad range of RNA, but this method cannot discriminate between mRNA isoforms, as well as the inability to annotate ncRNA (239).

RNA-seq or deep sequencing is based on next-generation sequencing (NGS) platforms (240). In principle, total RNA in the sample is reverse transcribed into cDNA, and the cDNA may or may not be amplified before deep sequencing which depends on the platform. After sequencing, the sequencing reads are mapped onto a reference genome. Then, the data are normalized and quantified to obtain the expression of any given transcripts in the sample (240). RNA-seq overcomes many limitations of microarray-based and Tag-based sequencing assays. This approach provides high sensitivity and can define the transcriptome of the targeted organisms with less bias across various experimental conditions and cell types (241, 242). The annotation of RNA-seq is independent and this allows the identification of novel transcripts without relying on preexisting annotation (243). RNA-seq is commonly used to study either pathogen or host after

physical separation (240). In fact, RNA-seq should profile all RNA classes in both pathogen and host, but the approach commonly focuses on messenger RNA (mRNAs) for studying protein expression, resulting in a majority of RNA output from noncoding regions being neglected (244).

Dual RNA-seq is defined as a simultaneous RNA-seq analysis of both pathogen and host (240). This method has proven the ability to capture host and pathogen transcriptomes simultaneously (245). The analysis of dual RNA-seq is a little different from conventional RNA-seq, as follows; sequencing reads are cleaned, normalized, and mapped, differential expression of transcripts identified, and functional analysis performed to aid data interpretation (245, 246). Analysis of multiple genome sequences at the same time is a key challenge of dual RNA-seq design and must be done carefully. It is essential to determine the selectivity of read mapping of both host and bacterial genomes because cross-mapping reads potentially affect transcript quantification (245). After finishing mapping, the data must be normalized and quantified, for example, using a within-sample normalization approach to obtain an overview of the transcriptional dynamic (TPM-transcription per million) (247, 248), and using a scaling normalization method to solve “batch effects” between RNA-seq experiments (249).

The differential expression analysis is the core of RNA-seq analysis and can be performed using packages from the Bioconductor framework for the *R* statistical programming language (250). The common analysis packages are edgeR (251), DESeq (252), and limma/voom (253). Differential expression analysis provides a long list of genes of both host and bacteria. These genes need to be interpreted for identifying gene function using the Gene Ontology (GO) (254) and the Kyoto Encyclopedia of Genes and Genomes (KEGG)(255). To determine which gene sets are differentially expressed during infection, the gene analysis must rely on a proper statistical analysis (245) and should follow the benchmark of gene set enrichment methods (256).

Dual RNA-seq data can be used to link genes through a network interference (NI) assay which helps to create the global regulatory network from the expression data in several conditions (257). Dual-RNA-seq can be integrated with proteomics. Even though the pairwise integration of RNA-seq and proteomic is controversial, this integrative approach can be used to identify novel mRNA isoforms or detect unreported peptides (246). Moreover, data integration between

transcriptomics with metabolomics has been demonstrated to identify pathways that regulate both gene expression and metabolite level (258).

Dual RNA-seq has been successfully performed on several intracellular pathogens such as a study of small noncoding regulatory RNA (sRNA) during *Salmonella* infection of host cells (244) and the investigation of transcriptional adaptation of *Mycobacterium bovis* in the THP1 human macrophage cell line (259). The use of Dual RNA-seq in obligate intracellular bacteria was first demonstrated in *Chlamydia trachomatis* to study the transcriptional dynamics of metabolic metabolism during early infection in (232). This opens an avenue for applying Dual RNA-seq in other obligate intracellular bacteria, including genetically intractable bacteria such as *Orientia tsutsugamushi*.

1.8 Thesis outline and objectives

Developmental differentiation of *Orientia tsutsugamushi* (chapter 3-5)

O. tsutsugamushi has an obligate intracellular lifecycle that requires host cells for replication and growth. The model of the intracellular infection cycle of *O. tsutsugamushi* is described in the literature review and includes attachment and entry of bacteria into host cells, the downstream signaling upon entry, the mechanisms of escaping the host immune response, and the exit of infective bacteria from host cells. However, some mechanisms during the infection cycle are unknown, lack details, or are poorly characterized, including a precise understanding of the developmental differentiation of *Orientia* which has never been described in detail. Thus, this study will focus on how *O. tsutsugamushi* differentiates during the course of the intracellular infection cycle.

To observe the developmental differentiation in *O. tsutsugamushi* over the course of its infection cycle (5-7 days), several techniques have been performed in this study including immunofluorescence labeling, confocal microscopy, SIM (Structured illumination microscopy), STORM (Stochastic optical reconstruction microscopy), TEM (Transmission electron microscopy) and mass spectrometry.

The key findings in this study correspond to the following four objectives:

1. To characterize *O. tsutsugamushi* subpopulations of both intracellular and extracellular populations.
2. To study how *O. tsutsugamushi* differentiates into a specific maturation stage (extracellular stage).
3. To investigate how *O. tsutsugamushi* senses the entry into the host cytoplasm.
4. To distinguish the stages of growth in intracellular bacteria.

The outcomes of this study show that *O. tsutsugamushi* differentiates into five distinct subpopulations which have different degrees of metabolic activity, replication, and infectivity. The extracellular population is distinct from the intracellular population. Intracellular bacteria present a marker protein (ScaC) at the maturation stage prior to exiting to the extracellular stage. In addition, the intracellular bacteria senses the host reducing environment after entry into host cells.

Developing genetic tools for *O. tsutsugamushi* (chapter 7)

Until now, the molecular mechanisms of host-pathogen interaction in *Orientia tsutsugamushi* has been understudied due to the lack of genetic manipulation tools and its unique lifestyle, as bacteria normally grow in host cells only. In addition, the transformation efficiency of obligate intracellular bacteria is normally low compared with free-living bacteria and requires long term culture (72). Developing genetic tools for *O. tsutsugamushi* is an important research need which has now been successfully achieved in other intracellular bacteria. For instance *Rickettsia spp.* and *Anaplasma spp*. have been randomly mutated using a transposon system (Tn mutagenesis) carrying a fluorescent gene. This has been used to provide novel information on virulence mechanisms and host-rickettsia interactions (260, 261).

This study aims to develop genetic tools for *O. tsutsugamushi* using Transposon base system and an alternative new tool, Bridged Nucleic Acid (BNA) technology, and these two methods rely on genetic transformation systems to introduce the foreign DNA into bacteria. This step is not easy to conduct in obligate intracellular bacteria compared with free-living bacteria, and needs

to be carefully optimized including electroporation conditions, voltages, antibiotic selection markers, and confirmed PCR of fluorescent protein being expressed in bacteria. The development of a novel genetic tool of *Orientia* will be crucial for research into the intracellular cycle and disease pathogenesis, and this could benefit the development of future treatment options and vaccines.

The findings in this study correspond to the following two objectives:

1. To manipulate *O. tsutsugamushi* genome using transposon-based vector (pCis-mRuby2-MurA-HimarI) via electrotransformation.
2. To down regulate specific genes in *O. tsutsugamushi* using BNA technology.

The outcomes of this study illustrate that the transposon-based vector is unable to manipulate the *Orientia* genome successfully. BNA is able to reduce the expression of the targeted protein (TSA56).

Dual RNA-seq provides insight into the biology of the neglected intracellular human pathogen *Orientia tsutsugamushi* (chapter 8)

Given the lack of genetic tools to manipulate the *Orientia* genome, RNA sequencing is a potential approach to study the transcriptome of an organism, which helps to understand the bacterial infection cycle and pathogenicity. Dual RNAseq is a novel approach to study host and pathogen transcriptomes which are both analyzed in parallel. The advantages of this approach include detection of transcripts with low abundances, higher sensitivity than microarray and Northern blot assays, and no requirement for predesigned species-specific probes (240, 245). Dual RNAseq allows monitoring of specific transcripts and gene expression of both host and pathogen in mixed samples at different time points throughout the infection processes.

In this study, the differences in clinical isolate strains (Karp and UT-176), were used to compare the transcriptome structure and gene expression profiles between infected cells and uninfected cells using dual RNAseq combined with proteomics and bioinformatics. Both strains were propagated in a human endothelial cell line (HUVEC) which is the most closely related to the pathology of *Orientia* infection in humans.

The findings in this study correspond to the three objectives:

1. To measure the growth and observe the infection *in vitro* of two clinical isolates of *O. tsutsugamushi* strain Karp and UT176.
2. To investigate the transcriptional profile of *O. tsutsugamushi* grown in cultured cells.
3. To compare the host cell response to infection two clinical isolates (Karp and UT176) in cultured cells.

The outcomes of this study demonstrate that dual RNA-seq can provide the transcriptomic profile of *Orientia* during the infection cycle, identifying bacterial non-coding RNAs, and discovering distinct host immune responses to each bacterial strain. This was related to differences in virulence as measured in a mouse model of infection.

Chapter 2: Materials and methods

2.1 Cell culture

Mouse fibroblast L929 cells (ATCC CCL-1), a gift from Prof. Stuart Blacksell at the Mahidol Oxford Tropical Medicine Research Unit, Bangkok, Thailand and HeLa cells, which were provided by Mitchison Laboratory Harvard were maintained in Dulbecco's modified Eagle medium (DMEM; Thermo Fisher Scientific, 21013024, USA) supplemented with 10% heat-inactivated bovine serum (FBS; Thermo Fisher Scientific, 16140071, USA) in 25 or 75 cm^2 flasks at 37 °C and 5% CO_2. Potoroo kidney Ptk2 cells (Sigma Aldridge, 88031601) were cultured in Minimum Essential Medium (EMEM; Sigma M0325, USA) with 10% heat-inactivated FBS in 25 cm^2 flasks at 37 °C and 5% CO_2.

2.2 Bacterial propagation

The Karp-like clinical isolate *Orientia tsutsugamushi* strain UT76 was routinely propagated in L929 cells in 25 or 75 cm^2 culture flasks at 37°C and 5% CO_2 using DMEM medium supplemented with 10% FBS. The intracellular fraction of infected cells were taken 5-6 days post infection. Bacteria purification was performed as follows; scraping infected host cells from the flask, lysing them by bullet blender tissue homogenizer (NextAdvance, USA) at power 8 for one minute or lysing with 0.1 mm glass bead with vortex for one minute, removing host debris by low speed spin at 300 rcf for five minutes, and collecting bacteria in the supernatant fraction. Bacteria were resuspended into fresh media or buffers. The resuspension volume depends on the bacteria concentrations which are measured by qPCR of the 47 kDa gene (Table 2). The details of the protocol are described here (262). Propagation of bacteria from the extracellular fraction (supernatant) proceeded the same as the intracellular fraction.

2.3 Microscopy

2.3.1 Immunofluorescence labelling

Bacteria were grown on 4-well or 8-well chambered coverslip/µ-Slides (ibidi, 80426:4-well, 80826: 8-well, USA) containing L929 cells or Ptk2 cells. Cells were fixed with 4% formaldehyde (Thermo Fisher Scientific, 28906, USA) for 10 minutes at room temperature. After

fixation, cells were washed with 1X PBS (pH 7.4) three times and permeabilized in 0.5% Triton-X for 15-20 min on ice. Then samples were incubated in blocking buffer (1X PBS + 1 mg/ml BSA or 1XPBS with serum from host species of the labeled antibody diluted to 1:20) for 15-20 mins at room temperature. Primary antibodies were added and incubated at 37°C for one hour. The in-house antibodies, rat monoclonal antibody against TSA56, and rabbit polyclonal antibody against *Orientia* ScaC were diluted 1:200. The commercial antibodies, LAMP1 (Thermo Scientific monoclonal mouse MA1-164) were diluted 1:200. After washing excess primary antibody with 1XPBS twice, appropriated fluorescent secondary antibodies (goat anti-mouse IgG superclonal Alexa Fluor 647 conjugate, Thermo Fisher A28180; goat anti-rat Alexa Fluor 488, Thermo Fisher, A11006; goat anti-rabbit, Alexa Fluor 594, Thermo Fisher A11012) were diluted 1:1000 and incubated with samples at 37°C in the dark for 30 mins. The nuclear stained Hoechst (Thermo Fisher Scientific, H1399) was diluted to 1:1000 and added with secondary antibody incubation. Then, samples were washed with 1X PBS twice to remove the excess secondary antibody. Before adding mounting media (20mM Tris, pH 8.0, 0.5% N-propyl-gallate, 90% glycerol), samples were washed twice with 1XPBS. Labeling samples were imaged using Zeiss Observer Z1 LSM700 confocal microscope with HBO 100 illuminating system, equipped with a 63x/1.4 Plan-APOCHROMAT objective lens (Carl Zeiss, Germany) and 405 nm, 488 nm and 555 nm laser lines, and a Leica TCS SP8 confocal microscope (Leica Microsystems, Germany) equipped with a 63x/1.4 Plan-APOCHROMAT oil objective lens with 1.4 mm working distance, and 405 nm, 488 nm, 552 nm, and 638 nm laser lines.

The measurements of fluorescence intensity were performed manually using Fiji Image-J software. Each single bacterium was quantified by determining the brightest pixel intensity within the area of bacteria. All images within each experiment were obtained under the same laser intensity and image acquisition conditions. Bacterial length was measured manually using Fiji Image J software (263).

2.3.2 STORM imaging and analysis

The 3D-STORM data was obtained using a homebuilt multi-color T that is based on an inverted microscope (Nikon, Ti-E), a high NA objective (Nikon, CFI-Apo 100X, NA 1.49), a 405 nm

photoactivation laser (Coherent, OBIS 405 LX 100mW), a 488 nm excitation laser (MPB, 2RU-VFL-P-20000642-B1R), and an EMCCD camera (Andor, iXon Ultra-888). The immunolabelled samples with Alexa 488 were mounted on the microscope, transferred to STORM buffer (OxyFluor/Oxyrase, 50mM BME (Sigma), 2.5mM COT (Sigma)), and illuminated with a strong 488 nm laser to record single-molecule fluorescence blinking events at 25Hz frame rate. The illumination at 405nm was intercalated with pulsed 488nm excitation to enhance photoactivation of Alexa 488 without exacerbating background signal. A cylindrical lens (Thorlabs, LJ1516RM-A) was placed in front of the camera in order to determine the z-coordinates of fluorescent molecules through the elongated point spread function (PSF) method. Each STORM image was reconstructed from single-molecule localization data obtained by the analysis of 30,000 frames with custom Matlab code. Briefly, bright single fluorescence spots were identified by thresholding methods, and their 3-D coordinates were determined by 2-D elliptical Gaussian fitting along with a pre-calibrated conversion table between eccentricity and z-coordinate. Focus drift was actively stabilized with Perfect Focus System (Nikon) while acquiring the data, whereas xy-drift was post-corrected using redundant cross-correlation algorithm. Each localization event was represented as a 2-D Gaussian of 20 nm standard deviation in STORM images. For the analysis of bacteria morphology, we picked cells that showed clear cell boundary, manually adjusted the z-coordinate to find the cell midplane, and measured the length of long and short axes.

2.3.3 SIM imaging and analysis

L929 cells were grown on coverslips (High precision Deckglaser No. 1.5H, 18x18 mm) coated with fibronectin 50 µg/ml in 6-well plate for one day before infection with *O. tsutsugamushi* at MOI 10:1 and 100:1. Infected cells were fixed with 4% formaldehyde and permeabilized in 0.5% triton on ice for 15-20 min and washed twice with 1XPBS + 1mg/ml BSA prior to immunofluorescence labeling. After labeling, coverslips were transferred from each well and placed on cleaned standard microscope slides (75mm x 25mm). Residual PBS on coverslips was removed before mounting using pipette tips and slides were sealed with nail polish. Imaging was performed using SIM microscope (DeltaVision OMX™). ImageJ software was used to analyze

the lengths and widths of bacterial cells. Due to poor resolution in the z axis using these approaches we only measured the dimensions in the x-y plane. This results in an underestimation of cell length because the dimensions of any cells that are not positioned exactly in the horizontal plane will appear reduced in length. Therefore, these numbers do not represent the exact dimensions of *O. tsutsugamushi* but indicate relative changes in dimensions over time.

2.3.4 iclick labeling

The methionine click-labeling assay is based on the Click-iT HPG Alexa Fluor Protein Synthesis Assay Kits (Molecular Probe by Life technologies). The alkyne-containing amino acid, L-homopropargylglycine HPG was added to infected cells at a specific time point. Infected cells were grown in a specific medium without L-methionine (Dulbecco's Modified Eagle Medium, DMEM, Cat. no. 21013) containing 25µM HPG for 30 min at 37°C. After incubation, labeled bacteria were washed twice with PBS+ 1mg/ml BSA to remove excess HPG probe. Cells were fixed with 4% formaldehyde and permeabilized with 0.5% Triton-X for 20 min on ice. Cells were washed again with PBS+1 mg/ml BSA and Click-iT reaction cocktail added for 30 min at room temperature protected from light. The details of Click-iT reaction cocktail is based on Click-iT HPG Alexa Fluor Protein Synthesis Assay Kits cat. C10428. The conjugated-Azide dye (Alexa Fluor 488) was used at the final concentration of 5µM. After washing twice with PBS + 1mg/ml BSA, cells were ready for immunofluorescent labeling and imaging.

2.3.5 Electron microscopy

Cell culture medium was aspirated from infected cells grown in T75 cm^2 flask. The cells were directly incubated with pre-warmed (37°C) fixative buffer (2% Glutaraldehyde, 4% formaldehyde in 0.1M Sorensen's Phosphate Buffer; pH 7.4) for one hour on ice. The fixed cells were gently scraped in long continual stripes using the scraper to get sheaths or rolls of cell monolayer as compact as possible. Cell sheaths were transferred into a 15ml tube using plastic Pasteur pipette or cut P1000 tips to avoid sheer forces, and briefly spun cells down at 100g. Cells were kept in fixative buffer at 4°C overnight. The cells were then washed three times in 0.1M Sodium Cacodylate buffer (pH 7.4) at room temperature to remove phosphate and further

incubated with post-fixative buffer (1% OsO4 + 0.1% Ruthenium red) for one hour at room temperature. After post-fixation, cells were dehydrated with cold graded series of ethanol solutions (30%, 50% and 70%) each for 15 min, and incubated with 4% Uranyl Acetate in 75% EtOH overnight in the dark at 4°C. Cells were dehydrated with 80, 90, 95, 98% ETOH, each for 15min and 100% EtOH 3 X 20mins. Samples were embedded in a low-viscosity Epon mixture and polymerized at 60°C for 48 hrs. Ultrathin sections (60 to 90 nm thick) were cut on ultramicrotome (UC7 Leica) and imaged in FEI TECnai 20 electron microscope operated at 100kV.

2.3.6 RNA FISH

The RNA FISH protocol was modified from the protocol described in ref (264). Cells were grown in chamber coverslips for two days before infection with bacteria at MOI 100:1. These infected cells were washed twice with 1X PBS before fixing with 4% formaldehyde for 10 mins at room temperature and subsequently incubated with 70% ethanol for one hour on ice. Cells were further permeabilized with 0.5% triton for 15-20 mins, incubated with 1 mg/ml lysozyme for one hour at room temperature, and washed with 1X PBS in between. These samples were labeled using immunofluorescence and further performed RNA FISH labeling. After complete immunofluorescence, cells were fixed with 4% formaldehyde again to stabilize the immunofluorescence signal. Then samples were equilibrated in washing buffer containing 2X SSC and 10% formamide at room temperature for 5-10 min before hybridization. An in-house RNA-FISH probe containing 33 oligos was designed to target *O. tsutsugamushi 16s* gene strain UT76 and labeled with TexaRed (Table 1). The probe was resuspended in hybridization buffer containing 10% Dextran sulfate (w/v) (Sigma, D8906), 1mg/ml Escherichia coli tRNA (Sigma, R8759), 2mM Vanadyl ribonucleoside complex (New England Biolab, Ipswich, MA, Catalogue Number, S142, 0.02% RNase free BSA (Ambion, AM2618), 10% formamide and used at a final concentration of 2ng/µl. Samples were pre-incubated with the probe at 50°C for 3-4 hours and further incubated at 37°C for 18-24 hours in the dark. Cells were then washed with washing buffer twice for 10 min at room temperature in the dark prior to adding mounting media. The labeled samples were ready for imaging under the confocal microscope.

Table 1: Details 16s RNA FISH probe containing 33 oligos.

Oligo numbers	Probes sequences (5’ to 3’)
1	TGAGCCAGGATCAAACTCTT
2	ACTTGCATGTGTTAGGCATG
3	GCAAGCTCAGCATTAATTCG
4	GTTTGCCACTAATTAATGCT
5	AGATTCCCACGTGTTACTCA
6	ATGTTATTCCGTACTGATGG
7	GTAGAGGGCATACGGTATTA
8	CAGCGATAAATCTTTCCTCC
9	TACCAACTACCTAATCTGCC
10	CAGGCTTGGTAAGCCATTAC
11	CTCTCAGACCAGCTACAGAT
12	TTCGCCCATTGTCCAATATT
13	TAAGGCCTTCATCACTCACG
14	CTTTTTCTGTAGGTACTGTC
15	CCAGTAATTCCGAACAACGC
16	CCTAACTTATTAAACCGCCT

17	TTTTAGAAGCAGTTCCAGGG
18	CTACCATACTCTAGCCTAAC
19	AGTAATGGCCCAGATGACAG
20	TATCTAATCCTGTTTGCTCC
21	TTTACAGCGTGGACTACCAG
22	CCCCAATATCTAGCACTCAT
23	AGTGCTTAATGCGTTAGCTA
24	ACCCGCTGGCAAATAAGAAT
25	CGGCAGTTTTCCTATAGTTC
26	ATGATGACTTGACCTCATCC
27	CGTGTAGCCCAACTCATAAG
28	CTCTGTAGGTACCATTGTAG
29	AATGATTAGCTCCACGTCAC
30	GAGTGCAATCCGAACTGAGA
31	ACTTCAGGTACCACTGACTC
32	TGCCTCTTACGTTAGCTCAC
33	GCTGCCCCCCGTAGGAGT

2.4 Gene expression analysis by RT-qPCR

Infected cells were collected at each time point and were stored in RNAProtect Bacteria Reagent (Qiagen, catalog number 76506) at -80°C before extraction. Total RNA was extracted using the Qiagen RNeasy Plus kit (Qiagen, catalog number 74136) following the manufacturer's instruction. To remove the DNA contamination, total RNA sample (10 µg) was treated with DNaseI (Thermo Fisher Scientific, catalog number AM2238) at 37°C for 30–60 min. The purified RNA was then taken for cDNA synthesis using the iScript reverse transcription supermix (Biorad, catalog number 170-8841) with random primers. cDNA was verified to confirm no DNA contamination by using a reverse transcriptase-free control reaction. No amplification of PCR products was an indication of an absence of DNA contamination in RNA samples. cDNA was kept at -20°C until used. A certain cDNA amount of each sample was taken to amplify targeted genes using gene-specific primers for *TSA22, TSA47, tsa56, ScaA, ScaE, ScaD, murA, murD, murF, ddl*, and *pbp2*. qPCR was performed using SYBR green qPCR mix (Biotools, Houston, USA, catalog number 10.609). All the expression levels were relatively normalized to the housekeeping gene *mipZ*.

Table 2: A summary of primers that used for RT-qPCR analysis.

Primer name	Primer sequences (5’ to 3’)
TSA22_FW	TGGGTGTAGCTGCAGGCATAC
TSA22_RV	GTTGATACACTAGCTGAAGATGATG
TSA47 forward	TCCAGAATTAAATGAGAATTTAGGAC
TSA47 reverse	TTAGTAATTACATCTCCAGGAGCAA
TSA56 forward	TGCCCAACAAGAAGAAGATG
TSA56 reverse	TTTAACTTGGCCGACAATCA
ScaA forward	ACCGCATTCAAACAGTGATCT
ScaA reverse	CAGTTTTTCCGCCATGAGTTG
ScaC forward	AAGTGTAAATATCCTCAGGCAGAGG
ScaC reverse	CAGTATTTCTTGCTAGTGCTTGCTC
ScaD forward	GAGCGACTACGAATGCATCA
ScaD reverse	CAGTTGCATCGTTGTTTTGG
ScaE forward	AGACCACGCAGTAACATGCTT
ScaE reverse	ACTGCGCGCCATTGTTGATT
50S_Ribosome/L25 FW	CCAAGGTAAGGTTCCAGGAG
50S_Ribosome/L25 RV	CACGCTTAATTCCCAACGAC
murA forward	AACGCATGCATCACTTAGACC

murA reverse	CAGGAATTCTTTGGACTCTTGC
murD forward	GCTGGAGGAGTTGCTAAAGAAG
murD reverse	CCCACTTTGATCAGATTCAGC
murF forward	GCCGGTTGATCAGTTGTTG
murF reverse	TTCGATGACTTGCCAAAGC
ddl forward	GGAGAGGATGGATGTATTCCTG
ddl reverse	TATCAAATGCAGCAGCAGAAGT
pbpA2 forward	CGCCTACCCAACATAAACAAG
pbpA2 reverse	TCCTGCTAAACCACGCATATC
mipZ forward	GTGGTGCAGGTAAGACTACTGTTG
mipZ reverse	GTGAATGCTGACGTGAATCAG

2.5 Western blot analysis

Both infected and uninfected cells were mechanically lysed in a Bullet Blender at power 8 for one min and pelleted, washed with PBS 1–2 times, and resuspended in 1X PBS. The protein concentration was measured by nanodrop analysis and the sample volume was adjusted to ensure equivalent loading. Samples were resuspended with SDS-PAGE buffer with or without 20% ß-mercaptoethanol and samples were then loaded on 12% Mini-PROTEANVR TGXTM Precast Protein Gels (Bio-Rad, USA, 4561043). Western blots were probed using a rat monoclonal antibody against the major surface protein TSA56 and then probed with a secondary antibody conjugated with alkaline phosphatase (Promega, USA, catalog number S3831) and developed using an alkaline phosphatase detection kit (Promega, USA, catalog number S3841).

2.6 Proteomics sample preparation and analysis

2.6.1 Sample preparation

O. tsutsugamushi strain UT76 was propagated in L929 cells at MOI 10:1 and 50:1. Infected cells were maintained in 75 cm^2 flasks at 37°C and 5% CO_2, using DMEM media supplemented with 10% FBS. Isolation of intracellular bacteria (Int) was taken at 3, 5 and 7 days post infection and purified as described previously. Extracellular bacteria (Ext) were harvested from the supernatant by centrifugation at the same time points. Purified bacteria were then washed with 0.3 M sucrose three times, resuspended in PBS, and subsequently lysed with 1% Triton X-100 at 4°C for 30 mins. Precipitation of bacterial proteins was performed by resuspending in 80% ice-cold acetone at 4°C for 30 mins and followed by centrifugation at 13,000g for 10 min. Protein pellets were collected and dissolved in 50% trifluoroethanol in 100 mM TEAB buffer. Proteins were dissolved in reducing agent, 20mM TCEP, and alkylating agent, 55 mM CAA. Then, proteins were digested with LysC (1:50 of LysC:protein) at 37°C for four hours and further digested with trypsin (1:100 of trypsin:protein) at 37°C overnight. Samples were acidified in 1% TFA. After centrifugation to get rid of any precipitant, samples were desalted using Water HLB in 96 well plate format as follows; activation with 500 µl of 100% acetonitrile and equilibration with 500 µl of 0.5% acetic acid, loading samples on the plate, washing sample on selected well with 500 µl of MS grade water, and elution of peptide mixtures using 800 µl of 80% acetonitrile in 100 mM TEAB buffer.

In preliminary runs, 2.5% total volume (20 µl) of each peptide mixture was dried in a speedvac and pellets dissolved in 15 µl of 100 mM TEAB. Two sets of samples were from bacterial culture at MOI 10:1 and MOI 50:1. Each set consists of six samples including ExtD3, IntD3, ExtD5, IntD5, ExtD7, and IntD7, and each sample was labeled with 10 µl selected isobaric TMT tags (Thermo Fisher Scientific, USA) of TMT10-126, TMT10-127N, TMT10-128C, TMT10-129N, TMT10-130C, and TMT10-131, respectively. All reactions were incubated at room temperature for one hr. For each MOI set, 2µl of each labeled sample was taken and added into 50µl of 10mM ammonium formate (pH 10) to a total volume of 62µl per set. Each pooled sample set was desalted through high pH C18 reverse-phase material stage tips (C-18 ReproSil-Pur Basic, Dr.

Maisch, 10µm). In brief, C18 desalting tips were equilibrated with 50 µl of 100% acetonitrile and subsequently dissolved in 50µl of 10mM ammonium formate pH 10 (Solution A). The pooled samples in solution A were loaded onto equilibrated C18 tips, the tips were then washed with 80µl of solution A, and eluted with 50µl of 10mM ammonium formate in 50% acetonitrile (Solution B.) Lastly, both sample elutions were completely vacuum dried and pellets were resuspended with 5µl of [0.5% acetic acid, 0.06% trifluoroacetic acid, 1% acetonitrile] for LC-MS/MS. Protein frequency distributions from preliminary runs were used to normalize sample loadings in actual experiments thereafter.

Intracellular and extracellular bacterial samples harvested at 4 d.p.i were harvested from three independent replicates of UT76 infecting L929 cells at MOI 50:1 with the same growth conditions as those previously described for samples of 3, 5, and 7 d.p.i.. Lysis condition and sample preparation were also performed in the same way but with label-free quantitative mass spectrometry.

2.6.2 LC-MS/MS and data analysis

Protein samples were separated in 120 min gradient (0.1% formic acid in water and 99.9% acetonitrile with 0.1% Formic Acid) on 50 cm x 75 um id Easy-Spray RP column (C-18, 2 µm particles, Thermo) using Easy nLC1000 (Thermo) chromatography system coupled online with Orbitrap Fusion mass spectrometer (Thermo). Data dependent mode was used in a time loop mode -3 s cycle using the Orbitrap analyzer for both scans with the following ion targets and resolutions (OT-MS 4xE5 ions, resolution 60K, OT-MS/MS 8E4 ions, resolution 15k). Peak lists were generated using Proteome Discoverer 2.2 software (Thermo). Searches were done with Mascot 2.6.1 (Matrix Science) against forward/decoy Mouse Uniprot and *Orientia* UT76 database with the following parameters: precursor mass tolerance (MS) 20ppm, OT-MS/MS 0.06 Da, 3 miscleavages; Static modifications: carboamidomethyl (C), TMT6plex. Variable modifications: Acetyl N-terminal, oxidation (M), deamidation (NQ). Forward/decoy searches were used for false discovery rate estimation on peptide and PSM level (FDR 1% high confidence FDR 5% medium confidence).

2.7 Transposon mutagenesis.

To make competent cells, purified *O. tsutsugamushi* was resuspended in sterile sucrose (200 – 500mM) and kept on ice. *Orientia* cells were transformed using a mariner-based Himar1 transposon system (Fig. 7) via electroporation. The plasmid was modified from the original plasmid (pCis-Cherry SS-himar), a gift from Ulrike G. Munderloh at the department of entomology, University of Minnesota, USA. Competent cells were pre-incubated with 0.1µg of transposon plasmid in electroporation 0.2cm gap sterile cuvette for 15 min on ice, and cells were electroporated with 1.2-2kV using the BioRad Gene Pulser II. After electroporation, bacterial cells were recovered with 100µl of culture medium and centrifuged at 500g for five mins. Cells were then left at room temperature for 15 mins and directly incubated onto L929 cells in a 6-well plate containing DMEM + 10%FBS. After 24 hrs of incubation at 35°C, fresh media containing fosfomycin 250 – 500µg/ml was added, and the infection was further incubated for seven days at 35°C. Each week cells were collected to check the bacterial level and the presence of a fluorescent gene (mRuby) by qPCR, and cells in each well were continued passaging and expanded by inoculation on fresh L929 cells in the presence of fosfomycin. The culture was examined microscopically to see the fluorescent signal of mRuby gene in the transformants. Images were acquired with Zeiss Observer Z1 LSM700 confocal microscope with HBO 100 illuminating system.

2.8 BNA synthesis and electroporation

BNA synthesis was carried out by Bio Synthesis (Lewisville, TX). The BNA oligomers were designed to be complementary to the *tsa56* gene (Fig. 8). Purified *Orientia* (1x 10^7 copies) was mixed with 2-8µM BNA in total volume 100µl of 250mM sucrose in pre-chilled 0.2cm gap sterile cuvette. Cells were incubated for 15 min on ice before electroporation with 4-5ms pulse. The BNA-*Orientia* suspension was transferred to a microcentrifuge tube and resuspended in 400µl of culture media (DMEM + 10% FBS) for recovery at room temperature for one hour. After incubation, BNA-*Orientia* was transferred to a 12-well plate containing L929 cells and incubated at 35°C for four days. Bacterial cells were then harvested to measure gene expression level and protein expression level by western blot.

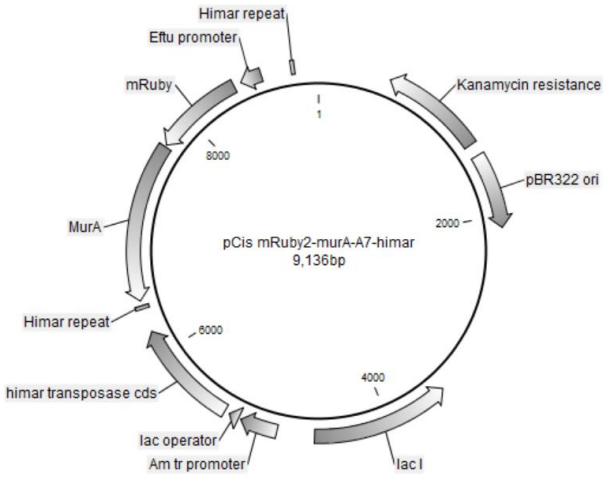

Figure 7. Plasmid pCis mRuby-murA-A7-himar used for transformation of *O. tsutsugamushi*. The transposon consists of mRuby2 gene and fosfomycin resistance gene, both driven by *Orientia*-Eftu promoter. The transposon is flanked by the left and right Himar repeats which are recognized by transposase.

A

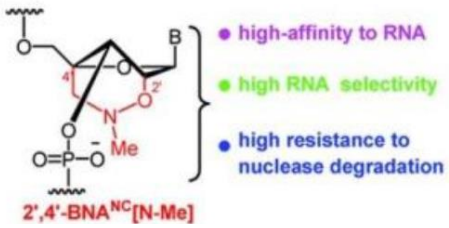

B

Target gene	Description	BNA sequences (N-terminal to C-terminal-DNA: 5'-3')
TSA56	Outer membrane protein	NH2-KFFKFFKFFK-Linker-5'+C+T+TAACTTTACCTTC+T+T+C-3'

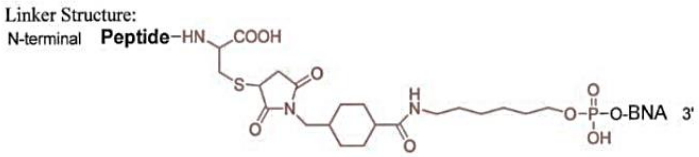

Name/Item: Peptide-BNA/DNA ASO-2
Lot Number: SP2176-1

Figure 8. (A) The design scheme of nucleotide 2'4'-BNA that contains a six member bridged structure with a unique N-O bond in the ribose sugar moiety at C3, which is important in DNA binding as a conjugation site (B) BNA/DNA structure in this study which contains peptide conjugate (H-$(KFF)_3$, linker, targeted DNA region and BNA.

2.9 RNA-seq sample preparation and RNA isolation

The clinical isolate strains (Karp and UT176) of *Orientia tsutsugamushi* were cultured in a confluent monolayer of host cells (HUVEC, Human Umbilical Vein Endothelial Cells; ATCC PCS-100-010) for five days at MOI 100:1. Cells were cultured in Media200 (Thermo Fisher, Catalog no. M200-500) supplemented with LVES media (Thermo Fisher, Catalog no. A14608-01) at 35°C and 5% CO_2. The infectivity was determined by qPCR of the single-copy Orientia gene 47kDa at day 5-7.

Bacterial propagation for RNA isolation was prepared using bacteria from frozen stocks and were pregrown in HUVEC cells in a T25 cm^2 culture flask. At five days post infection, bacteria were harvested and immediately propagated onto HUVEC cells for a second round of growth. Each condition in this experiment was done in 2 x 6-well plates (12 wells). The MOI of infections was estimated by measuring the number of bacteria in the pre-growth supernatant one day before bacteria were harvested. The exact inoculum was subsequently confirmed by using qPCR, and it was determined that the MOI for infection was 35:1 bacteria: host (Karp) and 32:1 bacteria: host (UT176). Note that the actual number of bacteria that entered into host cells is likely to be less than this because not all bacteria are viable for infection. At three hours post infection, bacteria that did not enter host cells were washed away with fresh media. Both uninfected cells and infected cells were harvested and quickly resuspended in RNAprotect Bacteria Reagent (Qiagen, catalog no. 76506). Samples were stored at -80°C until use. RNA extraction was performed using the Qiagen RNeasy Plus kit (Qiagen, catalog number 74136) according to the manufacturer's instructions and as described previously (44).

The procedure of bacterial propagation for growth curve measurements was carried out in the same way by using bacteria five days pregrowth in HUVEC cells, but bacteria in the second round of growth were propagated in 24-well plates. The MOI was subsequently measured to be 8:1 (UT176) and 25:1 (Karp). At each time point bacteria were isolated and the bacterial genome copy number determined by qPCR as described previously (262).

2.10 RNA processing and sequencing

The DNase-treated RNA samples were measured for the integrity using Bioanalyzer (Agilent). All RNA samples had RIN (RNA integrity number) values ≥8.0. Ribosomal RNA was removed using the Ribo-Zero Gold (epidemiology) kit (Illumina). 500ng of total DNase-treated RNA was used as an input to the ribo-depletion procedure. rRNA-depleted RNA was subsequently precipitated in ethanol for 3 h at -20°C.

cDNA libraries for Illumina sequencing were produced by Vertis Biotechnologie AG, Freising-Weihenstephan, Germany. To generate a range of 200- to 400 nucleotide (nt) RNA fragments, rRNA-free RNA samples were first sheared via ultrasound sonication (four 30s pulses at 4°C). The short fragments of 20 nt were eliminated using the Agencourt RNAClean XP kit (Beckman Coulter Genomics), followed by ligation of the Illumina TruSeq adapter at the 3' ends of the remaining fragments. First-strand cDNA was synthesized using M-MLV reverse transcriptase (NEB) wherein the 3' adapter served as a primer. The first-strand cDNA was purified, and the 5' Illumina TruSeq sequencing adapter was ligated to the 3' end of the antisense cDNA. The resulting cDNA was PCR-amplified to about 10 to 20ng/µl using a high fidelity DNA polymerase. The TruSeq barcode sequences were part of the 5' and 3' TruSeq sequencing adapters. The cDNA library was purified using the Agencourt AMPure XP kit (Beckman Coulter Genomics) and analyzed by capillary electrophoresis (Shimadzu MultiNA microchip).

For sequencing, cDNA libraries were pooled in approximately equimolar amounts. The cDNA pool was size fractionated in the size range of 200 to 600 bp using a differential cleanup with the Agencourt AMPure kit (Beckman Coulter Genomics). Aliquots of the cDNA pools were analyzed by capillary electrophoresis (Shimadzu MultiNA microchip). Sequencing was performed on a NextSeq 500 platform (Illumina) at Vertis Biotechnologie AG, Freising-Weihenstephan, Germany (single-end mode; 75 cycles).

2.11 Non-coding RNA prediction

Noncoding RNAs were annotated using Rockhopper, ANNOgesic (v0.7.17), and Infernal (v1.1.2) searching sequences against the Rfam database. These provided inconsistent predictions of intergenic sRNAs. Intergenic sRNAs were manually curated by visual comparison of the predicted sRNA coordinates with the read coverage in the Integrative Genomics Viewer (v2.5.2). Infernal predicted the core housekeeping ncRNAs tmRNA, RNaseP, SRP, and 5S rRNA. The quantification of the bacterial transcriptomes complemented with predicted ncRNAs was performed using Salmon.

2.12 Differential gene expression

For the bacteria, differential gene expression analysis was performed between orthologous genes identified by Poff. Genes that were predicted as an orthologous group (more than two genes) were removed from the analysis. Additionally, duplicates (transcripts with perfectly identical sequence), that were identified by Salmon in either strain, were removed. For both human and bacterial RNA-seq data, differential gene expression analysis was performed with the edgeR package (v3.20.9) using robust quasi-likelihood estimation, including genes with CPM (Counts Per Million) > 10 (for Ot) or CPM > 1 (for HUVEC) in at least three libraries. To identify biological processes that differ between two *Orientia* strains, gene set analysis was determined using KEGG and GO terms that contain at least four expressed genes using the fry test in the edgeR package.

2.13 Host Network/Pathway analysis

To identify pathways that are affected in Karp and/or UT176 infected host cells, genes differentially expressed with an adjusted p-value of < 0.05 were analyzed using Ingenuity Pathway Analysis (IPA) software (Ingenuity® Systems, Inc. Redwood City, CA) as described previously(265). Selected pathways were chosen based on enrichment p-values and activation Z-scores.

2.14 Mice and ethics statement.

All animal research was performed strictly under protocol approved by the Armed Forces Research Institute of Medical Sciences (AFRIMS) Animal Care and Use Committee and carried out in accordance with the Thai laws, the Animal Welfare Act, and all applicable U.S. Department of Agriculture, Office of Laboratory Animal Welfare and U.S. Department of Defense guidelines. The protocol number was PN16-05. The animal research was conducted in compliance with All animal research adhered to the Guide for the Care and Use of Laboratory Animals, NRC Publication (8th Edition). AFRIMS is an AAALAC International-accredited facility located in Bangkok, Thailand. Mice were cohoused (4 mice/case, 2 cases/group) in standard polycarbonate microisolator cages with filter tops and natural ventilation and stainless steel metal feeding hoppers and water bottle holders at 21 °C, and relative humidity was maintained within the range of 30–70%. The acceptable range is 21 °C ± 1 °C or 20–22 °C.

Female C57BL/6NJcl mice (Inbred) at age of 6–8 weeks (lot numbers 2-37, 2-41,and 2-45) were purchased from Nomura Siam International, Bangkok, Thailand. Mice were housed under specific pathogen-free (SPF) in an animal biosafety level 2 facility, AFRIMS and moved to an animal biosafety level 3 containment, AFRIMS 2 days before the inoculation. Female mice at 6–8 weeks of age were used in these experiments. Two group offemale mice (n=8 per group) were intravenously injected in the tail vein with 1.25 × 106 genome copies of *O. tsutsugamushi* of either Karp strain or UT176 strain. The *O. tsutsugamushi* inoculum was derived from *O. tsutsugamushi*-infected L929 cells (kind gift from Stuart Blacksell, Mahidol Oxford Tropical Medicine Research Unit, Bangkok, Thailand). Clinical signs and body weight were evaluated daily. After 12 days post inoculation, all mice were killed. Blood and tissue samples including lungs, liver, spleen, and kidneys were collected for bacteria quantification and histopathology. Adult mice were humanely euthanized with CO2 inhalation. Gas flow at 2 l/min (at 15 psi CO2) were maintained in the euthanasia chamber at least 5 min after the animals stop breathing. Death were confirmed by physical examination (the absence of a heartbeat) and ensured by an adjunctive physical method such as cervical dislocation or exsanguination.

Chapter 3: Characterization of *O. tsutsugamushi* subpopulations (extracellular and intracellular populations)

This research has been preprinted on bioRxiv under the title of Developmental differentiation in a cytoplasm-dwelling obligate intracellular bacterium: Giengkam S, Wongsantichon J, Atwal S, Jaiyen Y, Goh WI, Wright G, Chung T, Huh H, Lee S, Sobota R, Salje J. Developmental differentiation in a cytoplasm-dwelling obligate intracellular bacterium. bioRxiv. 2020 Jan 1.

Orientia can be classified into two subpopulations (extracellular and intracellular bacteria) based on their location. Extracellular populations are the bacteria that exit from infected cells by a budding mechanism and become metabolically inactive. Intracellular populations are the bacteria that enter into host cells, live in intracellular compartments of the host, and become metabolically active. These can be observed by transmission electron microscopy (TEM) (Fig. 9). The definition of metabolically inactive/active bacteria in this work is based on the detection of nascent protein synthesis by a clickable methionine-alkyne (HPG) probe. The extracellular populations that exhibit a low metabolic activity may not be detected by this method. The goal of this section was to characterize these different populations of *Orientia.*

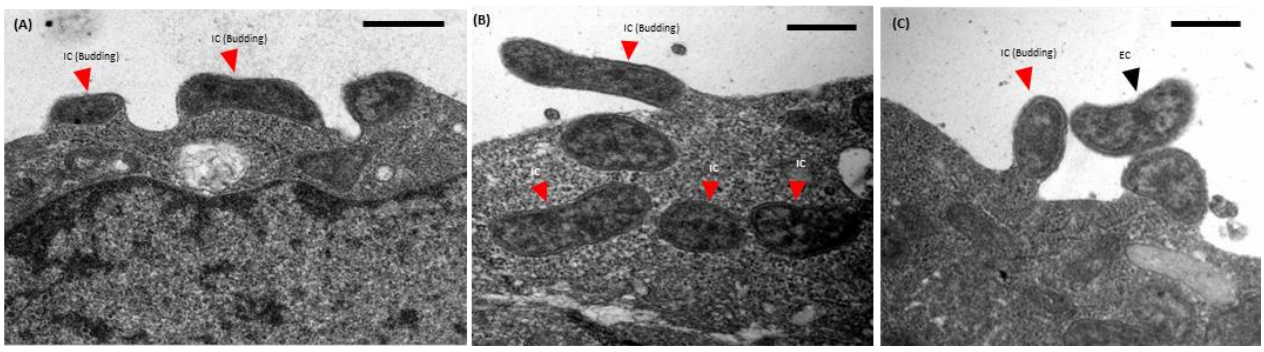

Figure 9. Transmission microscopy images (A, B,C) of *O. tsutsugamushi* after 5 days post infection in Hela cells. Black arrowhead and red arrowhead point to the extracellular bacteria (EC) and intracellular bacteria (IC), respectively. Scale bar 500 nm.

3.1 Extracellular bacteria and intracellular bacteria have a different shape.

In the current model of the intracellular infection cycle, the morphology of *Orientia* does not change throughout the course of infection but this may be because the shape and size of *Orientia* among subpopulations have never been measured and analyzed in detail. Characterization of the shape and size of *Orientia* will help to understand a cellular infection pattern that might correspond to different subpopulations and will help to distinguish bacterial stages in the life cycle.

Due to the small size of *Orientia* (1-2 µm), structured illumination microscopy (SIM) was used to observe the morphology of *Orientia* together with confocal microscopy because SIM provides a high-resolution image and gives greater image contrast of small structures than confocal microscopy. SIM does not need a special fluorescence probe to improve the resolution, it only requires an optical approach to reconstruct fluorescence images (266).

In this study, *O. tsutsugamushi* strain UT76 in L929 cells was labeled with the surface protein TSA56 or a protein synthesis probe, HPG, (described later) throughout the infection cycle (Fig. 10). The primary antibody against TSA56 protein, which is detected by fluorescent conjugated secondary antibody, can label both extracellular and intracellular bacteria while HPG only labels the active dividing intracellular bacteria as shown in figure 6 (190). The confocal and SIM images show that intracellular bacteria are small and round at the early stage of infection, and start elongation over time through the process of replication after 1-2 days post infection, while the extracellular bacteria remain small and round over the course of infection. A quantitative analysis of confocal images showed that the average length of extracellular cells was 1.2-1.3 µm and the elongated cells were not found in extracellular populations. The average length of intracellular cells during early post infection (3-24 hrs) was 1.3 µm and the average length of cells during elongation (day1-day7) was 1.6 µm. Also, some elongated cells were 4-5 µm in length (Fig. 11).

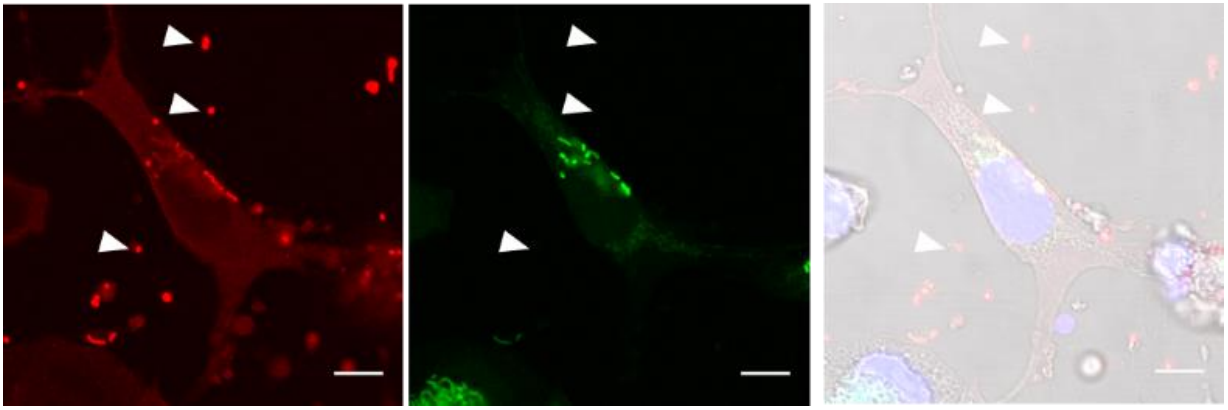

Figure 10. Confocal microscopy images of metabolically active and inactive bacteria by clickable methionine-alkyne (HPG) probe. HPG can be used as an indicator of metabolically active bacteria. *O. tsutsugamushi* in L929 cells 7 days post infection were labeled with HPG probe which reacted with an azide-conjugated fluorophore (green). Bacteria were counter stained with TSA56 antibody (red). Host cell nuclei are shown in blue (DAPI). The arrowhead indicates that extracellular bacteria are metabolically inactive. Scale bar = 10 µm.

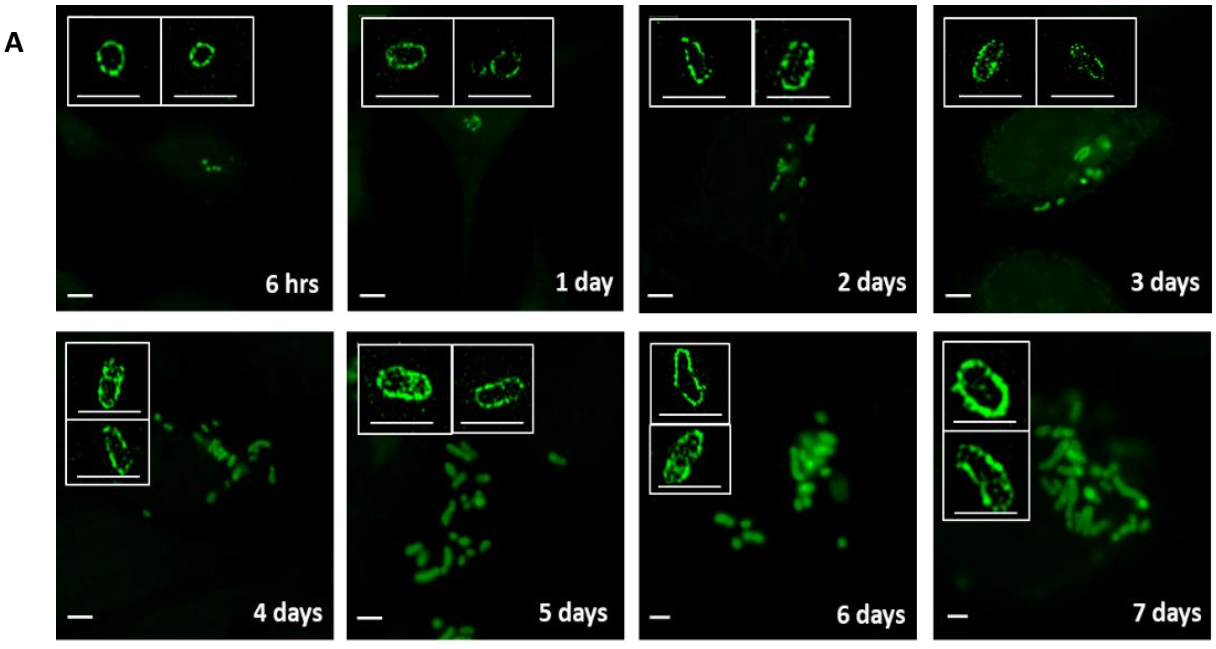

B

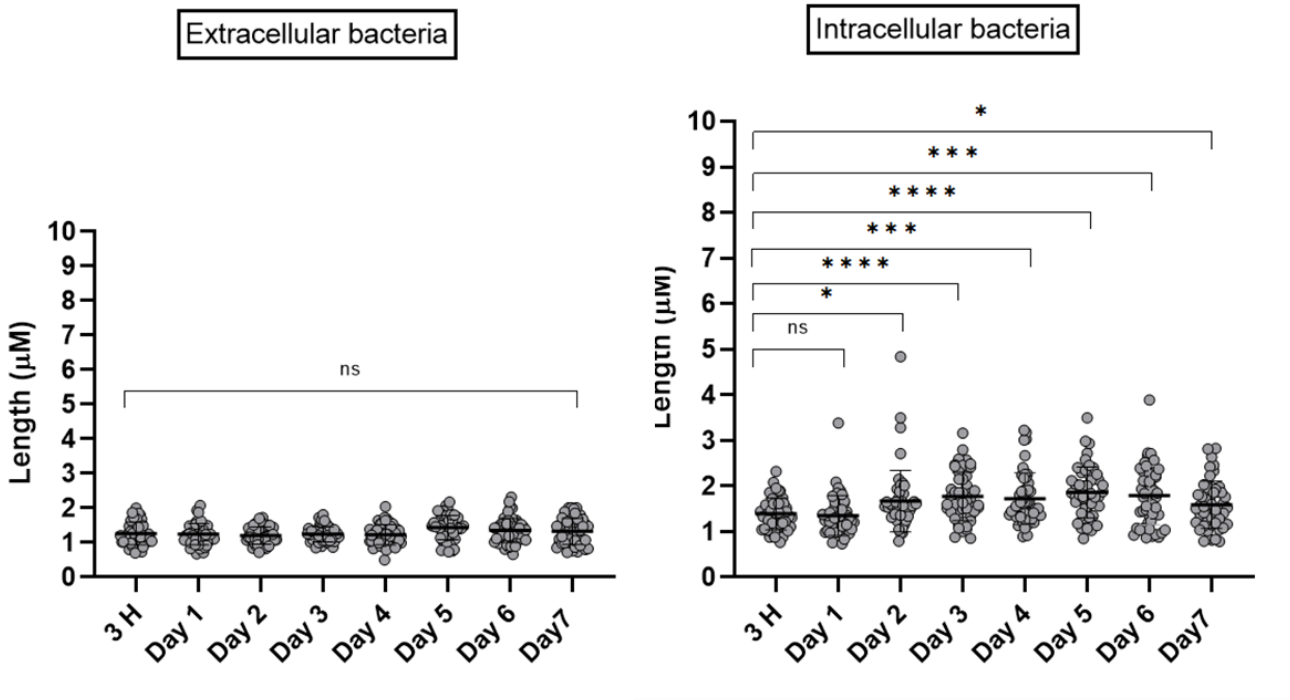

Figure 11. The shape of *O. tsutsugamushi* in L929 cells during the infection cycle. A. Large images are confocal images of intracellular bacteria labeled with the protein synthesis probe (HPG). HPG reacted with an azide-conjugated fluorophore to reveal cells actively undergoing protein synthesis (green). Scale bar (6 hrs and 1-5 days post infection) = 5 µm and scale bar (6-7 days post infection) = 2 µm. The inset images are structured illumination images of bacteria labelled with TSA56 antibody (green). Scale bar of in set images = 2 µm . B. Graph shows cell length of extracellular and intracellular populations labeled with TSA56 antibody at different time after infection from confocal images. Quantification involved measuring the length of 100 bacteria of from each single time point. Statistical significance was determined using an unpaired t test analysis. P values are represented as follows: ns ($P>0.05$); * ($P\leq0.05$); *** ($P\leq0.001$); **** ($P\leq0.0001$).

To observe the morphological pattern of *Orientia* in other cell lines, the length of *Orientia* during the infection cycle was observed in Potoroo epithelial cells (Ptk2) which are derived from the kangaroo kidney. *Orientia* has never been inoculated in Ptk2 before, therefore, the growth of *Orientia* was monitored to see whether *Orientia* can grow in Ptk2 cells or not. Intracellular *Orientia* taken from day 6 post infection was used to infect Ptk2 cells, and the growth curve was monitored by qPCR throughout the 7-day infection cycle. The results showed that the growth of *Orientia* in Ptk2 is similar to L929 (Fig. 12).

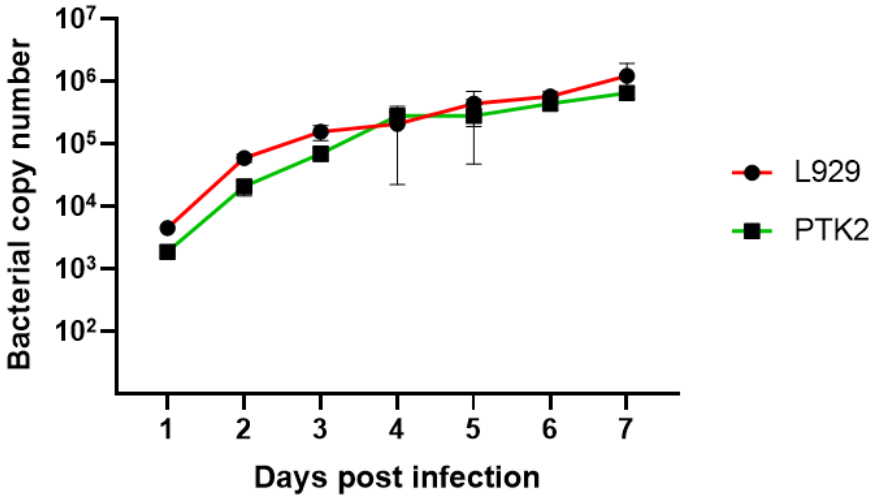

Figure 12. Growth curves showing the growth of *O. tsutsugamushi* in L929 and Ptk2 cells by measuring bacterial copy number in one well of a 6 well plate over time. Bacteria were taken from the intracellular fraction after 6 day post infection pregrowth in L929 or Ptk2 cells. The intracellular bacterial cells were measured.

Next, *Orientia* strain UT76 in Ptk2 cells was labeled with TSA56 during the 7 day infection cycle. The results revealed that the morphology of *Orientia* in Ptk2 cells is similar to that in L929 cells (Fig. 13A). Amongst the extracellular bacteria, no elongated cells were found and cells were small and round over the time course, while the intracellular bacteria were small and round at the early time point of infection (3 hours) and became elongated bacteria after 24 hours post infection. The average lengths of *Orientia* cells were 1.2-1.4 µm in the extracellular fraction, 1.5µm in the intracellular fraction at 3H post infection, and 1.7-2 µm at later time points (1-7 days)(Fig. 13B).

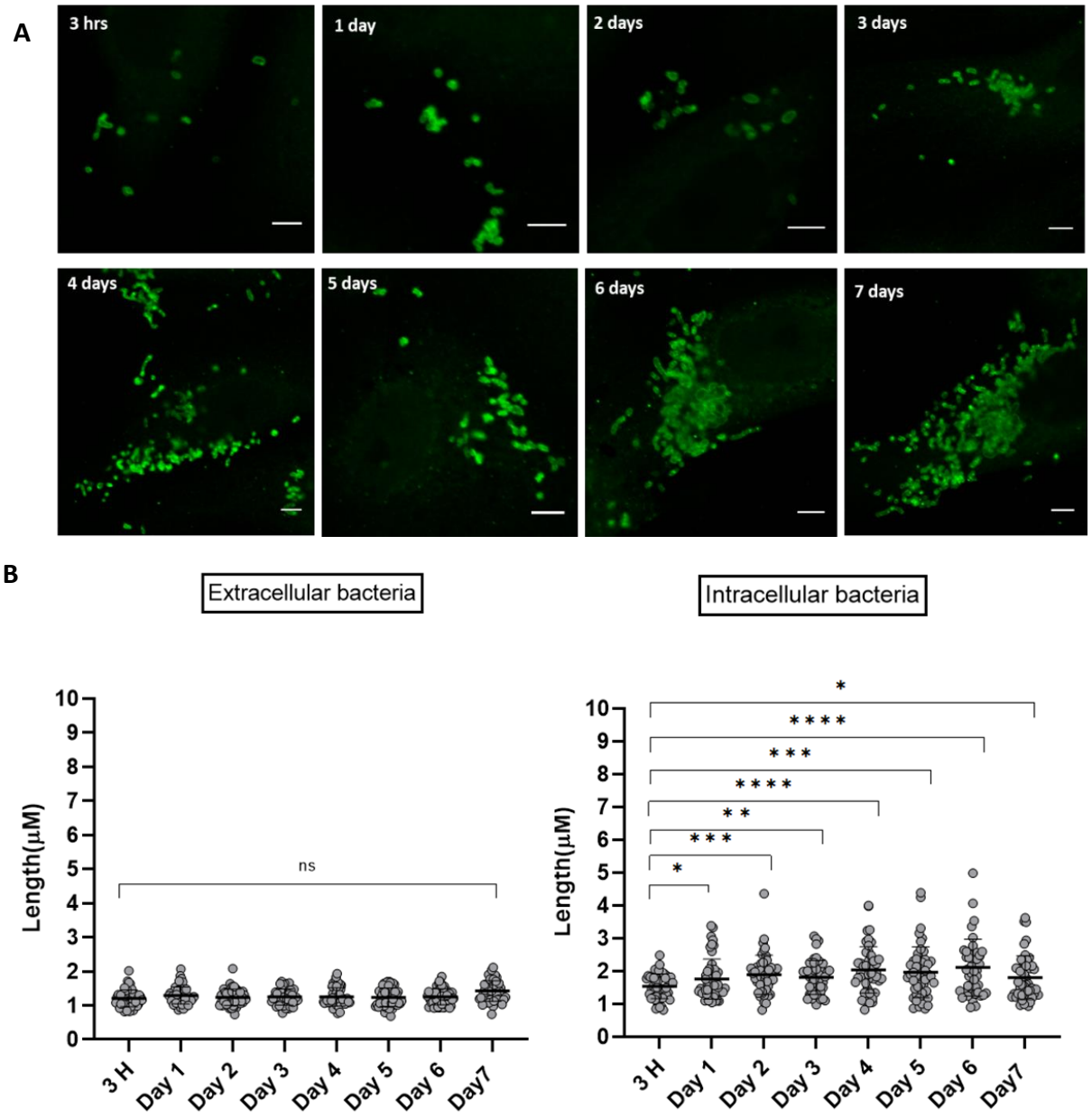

Figure 13. The shape of *O. tsutsugamushi* in Ptk2 cells during the infection cycle. A. confocal images of extracellular and intracellular bacteria labelled with *Orientia* surface protein TSA56 (green). Scale bar = 5 µm. B. Graph shows cell length of extracellular and intracellular populations labeled with TSA56 antibody and measured from confocal images. Quantification involved measuring the length of 100 bacteria of each single time point. Statistical significance was determined using an unpaired t test analysis. P values are represented as follows: ns (P>0.05); * (P≤0.05); ** (P≤0.01); *** (P≤0.001); **** (P≤0.0001).

Even though SIM microscopy provides a high-resolution image, it also has a limitation when imaging aggregated bacteria. Figure 14 shows that an individual bacterium in a tightly packed microcolony near the nucleus cannot be distinguished by SIM. To solve this problem, the localization-based super-resolution technique, stochastic Optical Reconstruction Microscopy (STORM), was used to distinguish *Orientia* morphology over the time course. Based on the localization approach, a single fluorescence probe switches between on and off states onto target molecules (267). This process is repeated many times until most fluorescence probes have been imaged. STORM can resolve the localization of a single-molecule with high precision even in dense populations (268, 269). Therefore, STORM was chosen to provide a precise localization of ultra-fine structures in a cell.

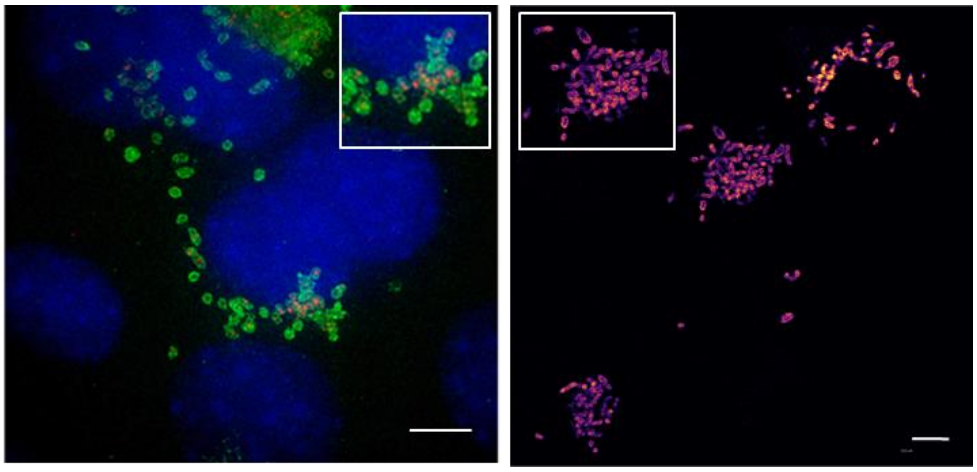

Figure 14. Comparison of SIM (left) and STORM (right) images of aggregated *O. tsutsugamushi* after 5 days post infection in L929 cells. (Left) Bacteria are labelled with anti-*O. tsutsugamushi* human serum (green) and anti TSA56. (Right) Bacteria are labelled using an antibody against surface protein TSA56. Scale bar = 5µM. The inserts show a zoomed in of aggregated bacteria.

STORM imaging (Fig. 15) of the *Orientia* infection life cycle (3 hours to 7 days post infection) provides a better image resolution which allows quantification of bacterial size in a tightly packed microcolony. Quantitative analysis of *Orientia* cell length showed that intracellular bacteria are round at three hours post infection and become elongated at day 1 to day 7 post

infection. The length measurement of bacteria in a crowded area was not significantly different from the length measurement of single isolated bacteria (Fig. 16).

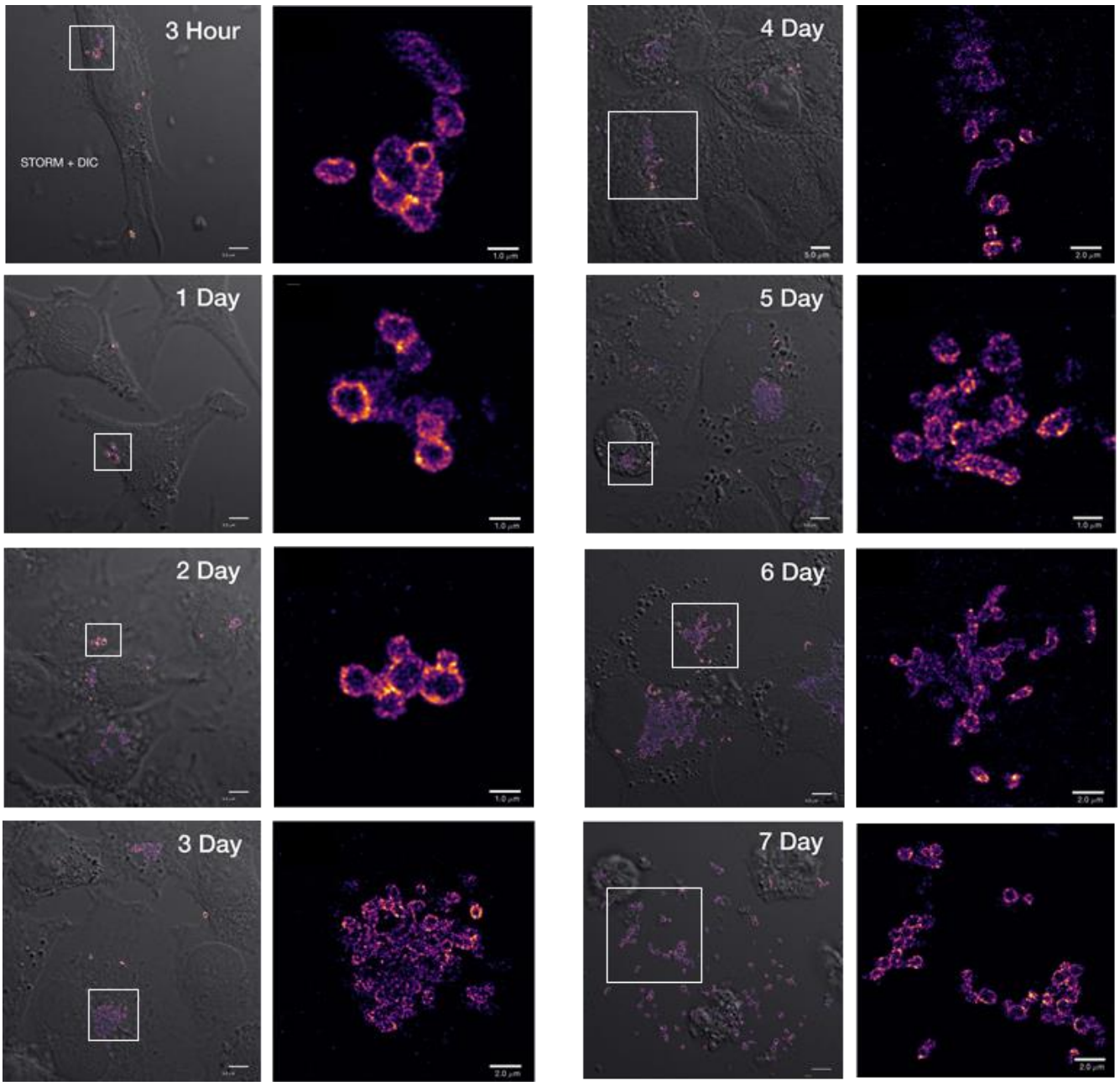

Figure 15. STORM images of *O. tsutsugamushi* infection cycle (3 hrs– 7 days post infection) in L929 cells showing the round and elongated morphology of bacteria during the infection. Intracellular bacteria were labelled using an antibody against surface protein TSA56. White square boxes indicate the location of the enlarged areas.

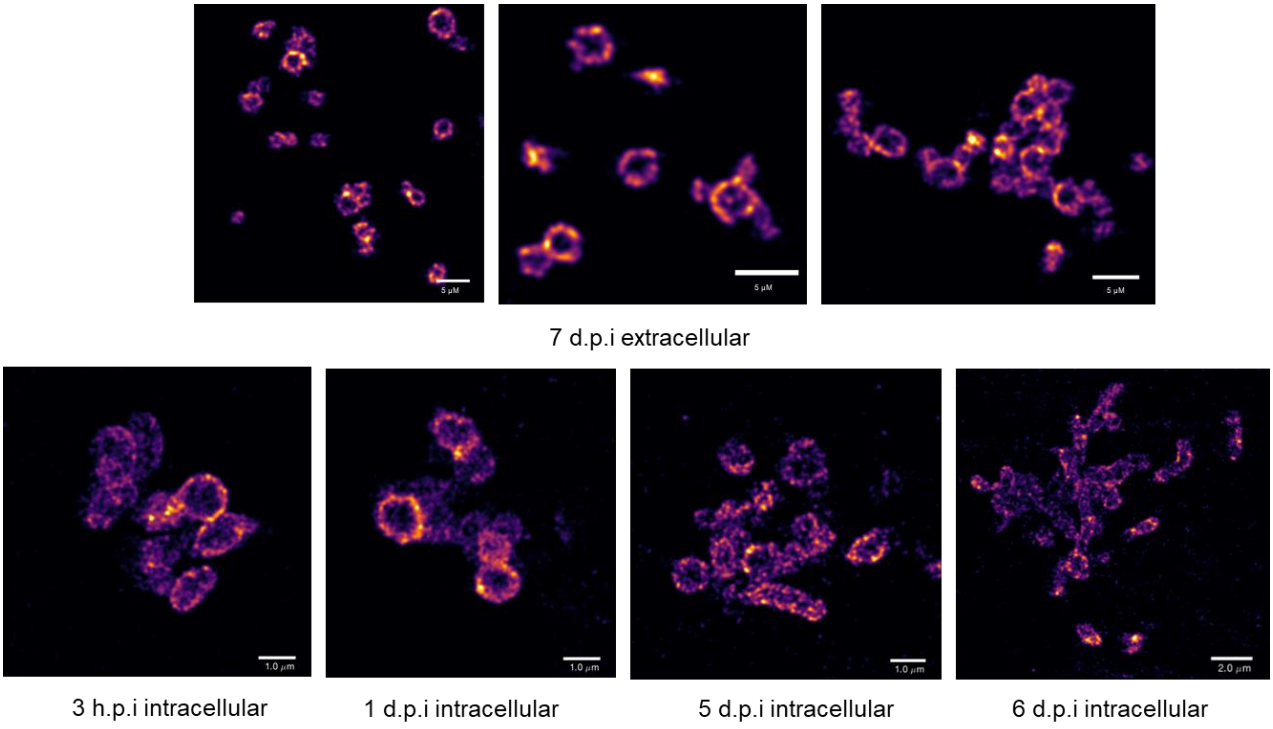

Figure 16. STORM images of intracellular and extracellular populations showing the round and elongated morphology during the infection. *O. tsutsugamushi* was infected in L929 cells and was labelled using an antibody against surface protein TSA56.

The morphology of the extracellular population (day 7 post infection) was compared with the intracellular population (3 hours – 6 days post infection) by STORM imaging (Fig. 16). It is a feature of *Orientia* infection that host cell density is always high during the mid stage of infection (day 3-day5). This makes it difficult to observe the morphology of extracellular bacteria. During the later time points (day 6-7 post infection), more bacteria are budding out of host cells and host cells become damaged, leading to easy observation of the extracellular population. The results showed that extracellular bacteria after budding out from host cells are small and almost spherical whilst intracellular bacteria are round during first 24 hours post infection and become elongated over time (day 1-day 7 post infection). This suggests that the morphology of extracellular and intracellular populations is slightly different.

The reason why some intracellular populations are elongated and others become round or coccoid is that bacteria change their shape in response to the hostile environment in which they reside in order to survive (270). The small size allows for a better escape from host immune cells and allows bacteria to form a pack colony in a restricted host cell volume such as *S. pneumonia* reduces the size to avoid the complement-mediated killing by the host (271, 272). Unlike biofilm-forming in other bacteria, such as *Pseudomonas aeruginosa*, *E.coli*, and *Staphylococcus aureus*, *Orientia* releases a polysaccharide molecule, NT19, and forms self-aggregates (157, 273). The function of this protein is unknown but it might be involved in forming a biofilm-like structure within host cells. Extracellular bacteria also form aggregation after exiting host cells. TSA56 is a major outer membrane protein in *Orientia* and was previously reported to form higher order intermolecular aggregation in the presence of a reducing agent (44, 274). TSA56 might be involved in forming aggregated extracellular bacteria via highly cross-linked disulfide bond on the bacterial surface membrane.

3.2 Extracellular bacteria and intracellular bacteria have distinct protein profiles.

The protein profiles demonstrated differences in metabolic status between the extracellular and intracellular populations. Shotgun proteomics analysis was used to compare the protein profiles of isolated bacteria at different times after infection (3, 5 and 7 days post infection). To achieve bacterial isolation in this experiment, extracellular bacteria were collected from the supernatant of infected cells and intracellular bacteria were collected by lysis of infected cells. After the lysis step, host debris and intracellular bacteria were separated by a low-speed centrifugation. The limitation of the bacterial purification method is that we cannot completely separate the intracellular populations from the extracellular population. Furthermore, a subpopulation may be pelleted with host cell debris especially the bacteria at the surface of the host cells and those attached to membranes.

The relative abundance of protein in both fractions was compared at each time point. The results revealed that on day 3 and day 5 post infection, extracellular and intracellular bacteria show a difference in protein profiles (Fig. 17), suggesting that extracellular and intracellular bacteria have distinct developmental stages. In addition, the protein profiles were similar to each

other at day 7 post infection. This revealed that the intracellular stage becomes the extracellular stage before exiting host cells.

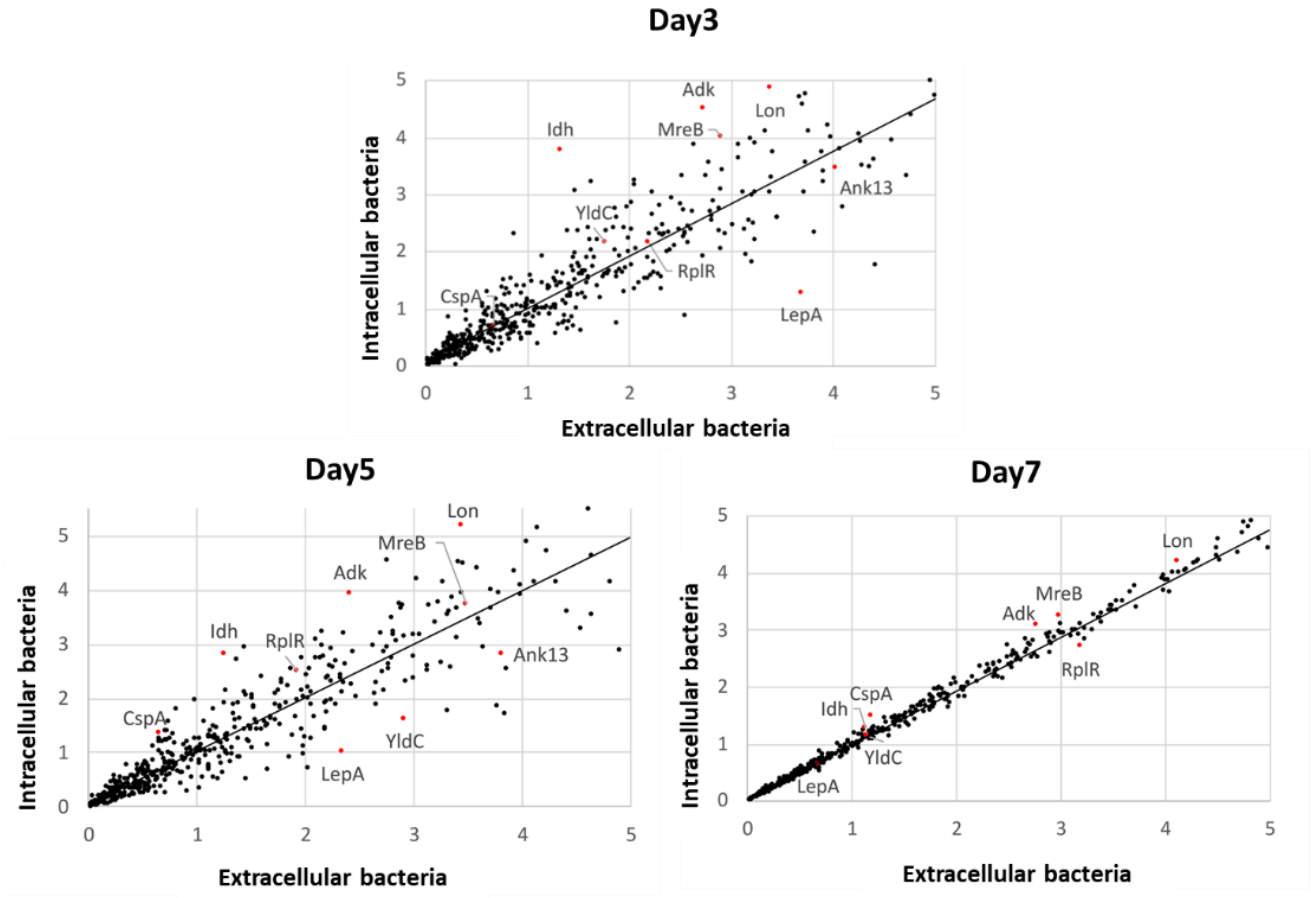

Figure 17. A comparison of protein expression levels in extracellular and intracellular populations at 3 d.p.i, 5 d.p.i. and 7 d.p.i. (d.p.i = days post infection). Relative protein levels, as determined by peptide counts in a normalised proteomic dataset, are compared between extracellular (X-axis) and intracellular (Y-axis) bacterial fractions. Selected proteins are highlighted in red.

3.3 Both extracellular and Intracellular populations are infectious.

The differences in protein profiles between extracellular and intracellular bacteria leads to the next question; whether extracellular and intracellular populations have different infectivity or not. The isolated intracellular bacteria taken from day 5 and day 6 post infection were used to infect host cells. The growth of intracellular and extracellular populations at each single time

point (day 1- day 7) was measured by qPCR. Bacteria were selected from day 5 and day 6 post infection because the protein profiles of extracellular and intracellular populations at day 5 and day 7 are different. This could also reflect a difference of infectivity between mid and late stages of infection (5-7 day post infection). The results showed that even though they have different protein profiles, both extracellular and intracellular populations were able to infect host cells and replicate over time during the 7 day infection cycle (Fig. 18), suggesting that both extracellular and intracellular populations are infectious.

In addition, the growth pattern of bacteria taken from day 5 post infection was slightly different among intracellular and extracellular populations, whilst there was no difference in the growth from bacteria taken from day 6 post infection. This result supports the hypothesis that extracellular and intracellular bacteria are similar at the late stage of infection (day 6 - day 7).

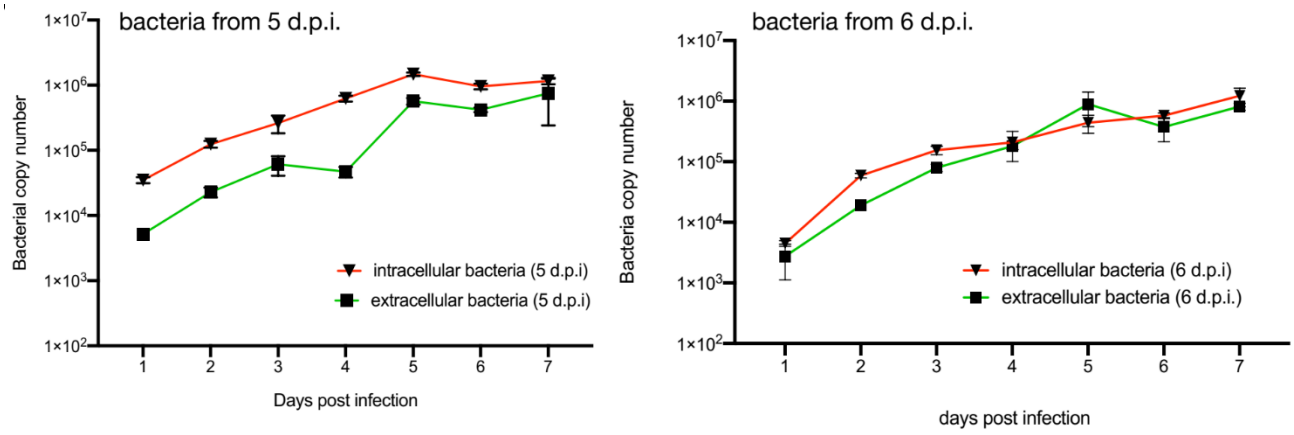

Figure 18. Growth curves showing the growth of *O. tsutsugamushi* in L929 cells by measuring bacterial copy number in one well of a 6 well plate over time. All time points were performed in triplicates. Bacteria were taken from the intracellular fraction after 5 day and 6 day post infection pregrowth in L929 cells. The extracellular supernatant and intracellular bacterial cells were measured.

3.4 Distinct bacterial gene expression profiles during intracellular stage of infection

Orientia exhibits distinct subpopulations which show a difference of cell shapes, protein profiles. This leads to the next hypothesis that *Orientia* might present heterogeneity in the expression of the other genes and it might also be controlled at an appropriate time and place in response to a fluctuating host environment during the infection cycle. To determine whether other genes were differentially regulated throughout the intracellular cycle, qRT-PCR was used to measure the RNA level of specific genes. In this study, two sets of genes were selected: genes that encode for bacterial surface proteins (*ScaA, ScaC, ScaD, ScaE, TSA22, TSA47*, *TSA56*); and genes encoding proteins involved in peptidoglycan synthesis (*pbp2, pal, ddl, murA, murD, murF*). RNA was isolated from infected L929 cells at 1, 3, 5 and 7 days post infection to measure the gene copy number relative to the housekeeping gene *MipZ*. Each gene expression had a different pattern (Fig. 19A). The expression of *ScaA, TSA47,* and *TSA56* were increased whilst the expression of *pbp2, ddl, murA, murD, ScaC, TSA22*, and *pal* were decreased. A group of *murF, ScaD, ScaE*, expressed constantly throughout the time-course. To check the consistency of the expression between RNA and protein level, the relative protein levels of ScaC and TSA56 were measured by western blot assay. The protein levels were normalized to the bacterial DNA copy number. The immunoblot results (Fig.19B) showed that the ScaC level decreased while TSA56 increased over time. These trends were similar to the RNA levels, suggesting that the expression among RNA and proteins in ScaC and TSA56 were consistent. Even though the RNA and proteins were measured in different subpopulations within a single time point, the expression patterns were shown to be different throughout the infection cycle.

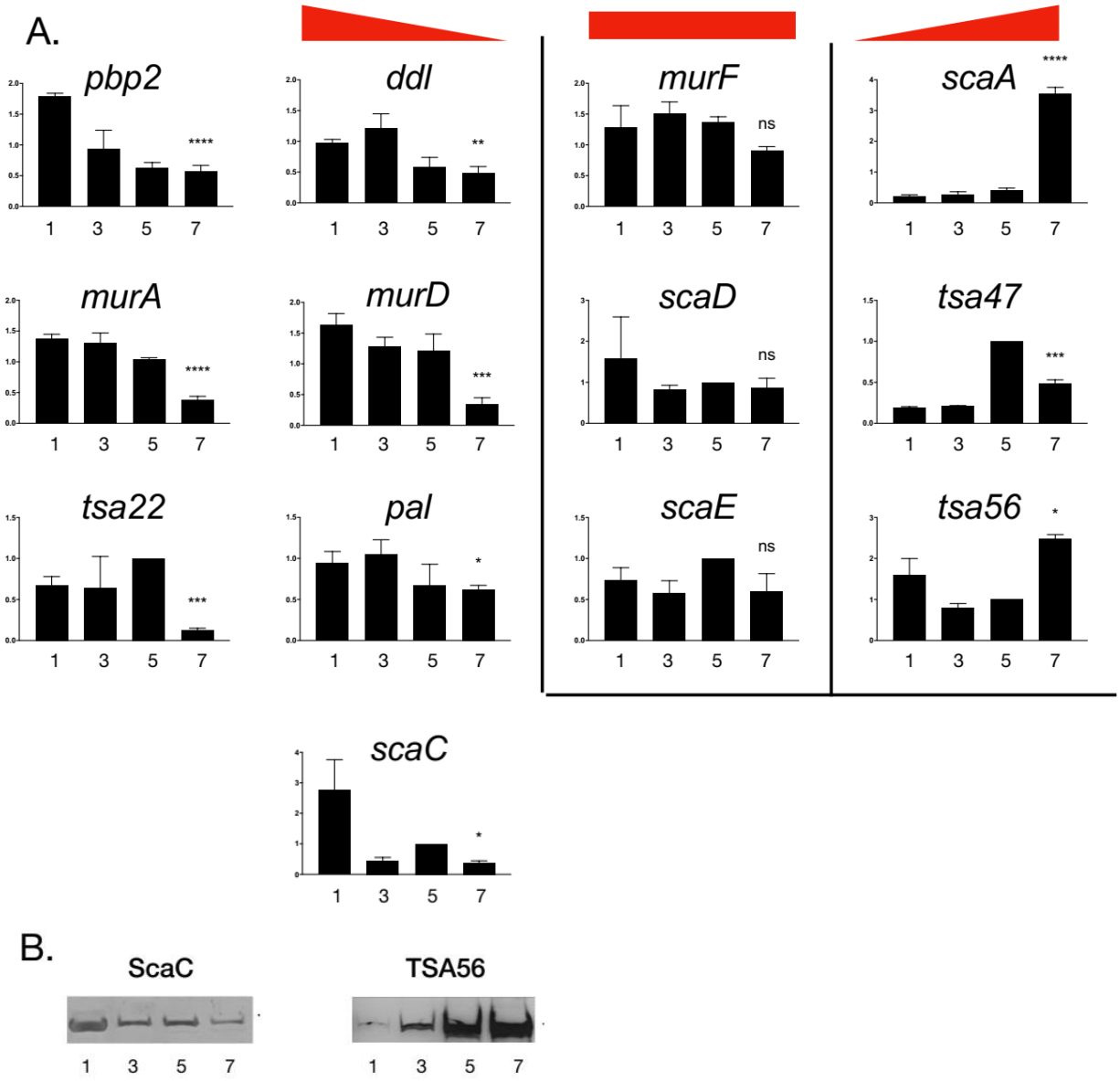

Figure 19. The intracellular stages of growth by *O. tsutsugamushi* are associated with changes in bacterial gene expression. A. The relative expression of several genes at different times after infection by qRT-PCR. Y-axis = relative copy number compared with housekeeping gene mipZ, X-axis = days post infection (d.p.i). All experiments performed in triplicate. Statistical significance when compared with 1 d.p.i is calculated using a parametric unpaired t test. **** p≤0.0001 ***p≤0.001 **p≤0.01 *p≤0.05, ns p>0.05. B. Western blot presenting the relative levels of ScaC and TSA56 at 1, 3, 5 and 7 d.p.i. Sample loading was normalized by bacterial copy number as measured by qPCR.

Chapter 4: *O. tsutsugamushi* differentiates into a specific maturation stage (extracellular stage)

This research has been preprinted on bioRxiv under the title of Developmental differentiation in a cytoplasm-dwelling obligate intracellular bacterium: Giengkam S, Wongsantichon J, Atwal S, Jaiyen Y, Goh WI, Wright G, Chung T, Huh H, Lee S, Sobota R, Salje J. Developmental differentiation in a cytoplasm-dwelling obligate intracellular bacterium. bioRxiv. 2020 Jan 1

4.1 *ScaC* is a marker gene for identification of the maturation stage

Based on the evidence above, extracellular bacteria and intracellular bacteria have different protein profiles and infectivity at the early stage of infection (day1-day5), but are similar at later stages (day6 - day7). This leads to the next question; how do mature intracellular bacteria become extracellular? The transition event in which mature intracellular bacteria become extracellular is exit via a budding process. To monitor the transition-maturation stage of *Orientia* subpopulations, a polyclonal antibody against ScaC protein was generated to perform immunofluorescence labeling throughout the infection time-course for 7 days (Fig. 20). ScaC was selected because ScaC is one of the major surface proteins of *Orientia* and plays a role in bacterial adhesion and invasion. *Orientia* might utilize ScaC, which is the autotransporter outer membrane protein, during the maturation stage prior to exit.

Immunofluorescence microscopy showed that ScaC labeling is only present on subpopulations located at the plasma membrane of infected cells. This suggests that ScaC is differentially expressed amongst *Orientia* subpopulations and can be used to identify bacteria in the “maturation” stage of development. In addition, bacteria were labelled by the scac antibody at the early time point and the labeling disappeared when bacteria localized into the host cytoplasm, and this labeling re-presents when bacteria are located at the host cell surface at day 3-4 post infection. The involvement if any of ScaC in the budding mechanism is unknown, but ScaC might help bacteria prepare for re- infection by helping the entry into new cells.

The reason why ScaC labeling is lost from the bacteria surface shortly after entry might be explained as follows; firstly, the transcription level of the *ScaC* gene decreased during the

infection, and this might reflect the depletion of ScaC protein over time (Fig. 21). Thus, the ScaC protein level might be too low and undetectable by IFM. Secondly, the autotransporter protein may be degraded through a cleavage process. The ScaC antibody in this study targets the epitope on the extracellular autotransporter domain which might undergo cleavage, leading to a loss of ScaC labeling during infection. Lastly, ScaC might be secreted to the cytoplasm. *Orientia* has been shown to form outer membrane vesicles (275). Thus, ScaC might be secreted through this process.

A

Name	**Type Antigen**	**sequence**	**Species**
TSA56	monoclonal	KLTPPQPTIMPISIADRDF	rat
ScaC_p	polyclonal	KIQLQQLQVTLQNSLFLQNKNNNPA + IAEVSKLLCMLE	rabbit

B

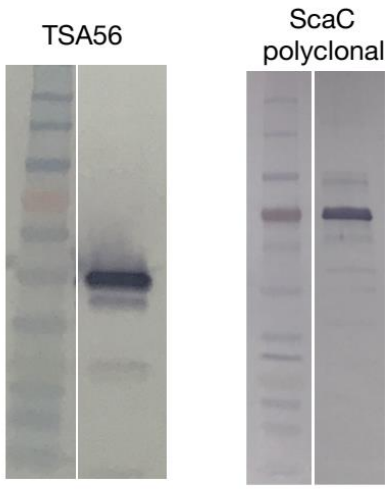

Figure 20. Antibodies used in this study. A. Overview of antibodies details. B. Immunoblot blot showing specificity of antibodies generated and used in this study. MBP-fusion proteins containing the peptide used for generation of anti-TSA56 and anti-ScaC. These two antibodies were constructed and purified in this work. MBP = pure MBP (maltose binding protein).

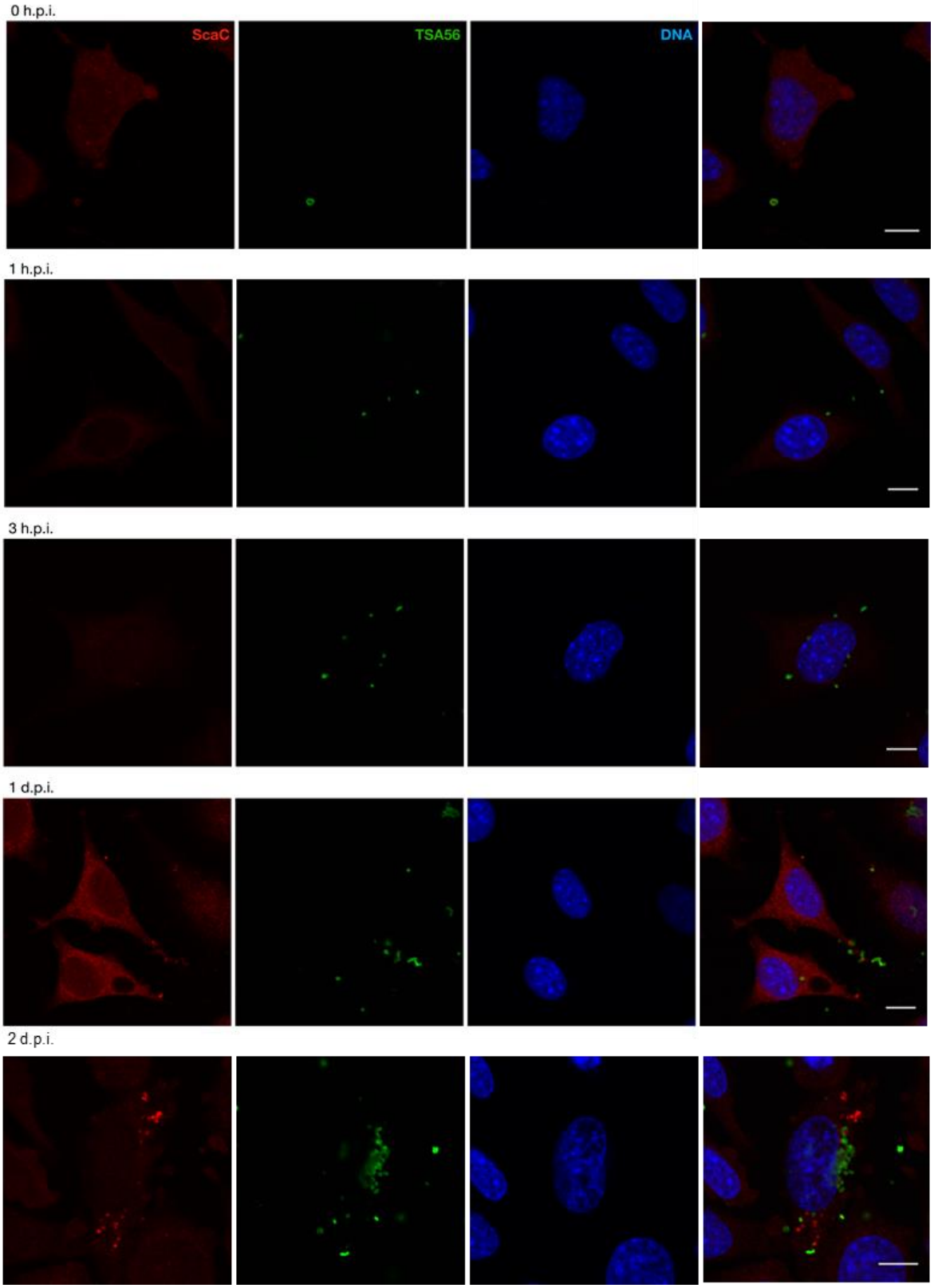
0 h.p.i.
ScaC
TSA56
DNA
1 h.p.i.
3 h.p.i.
1 d.p.i.
2 d.p.i.

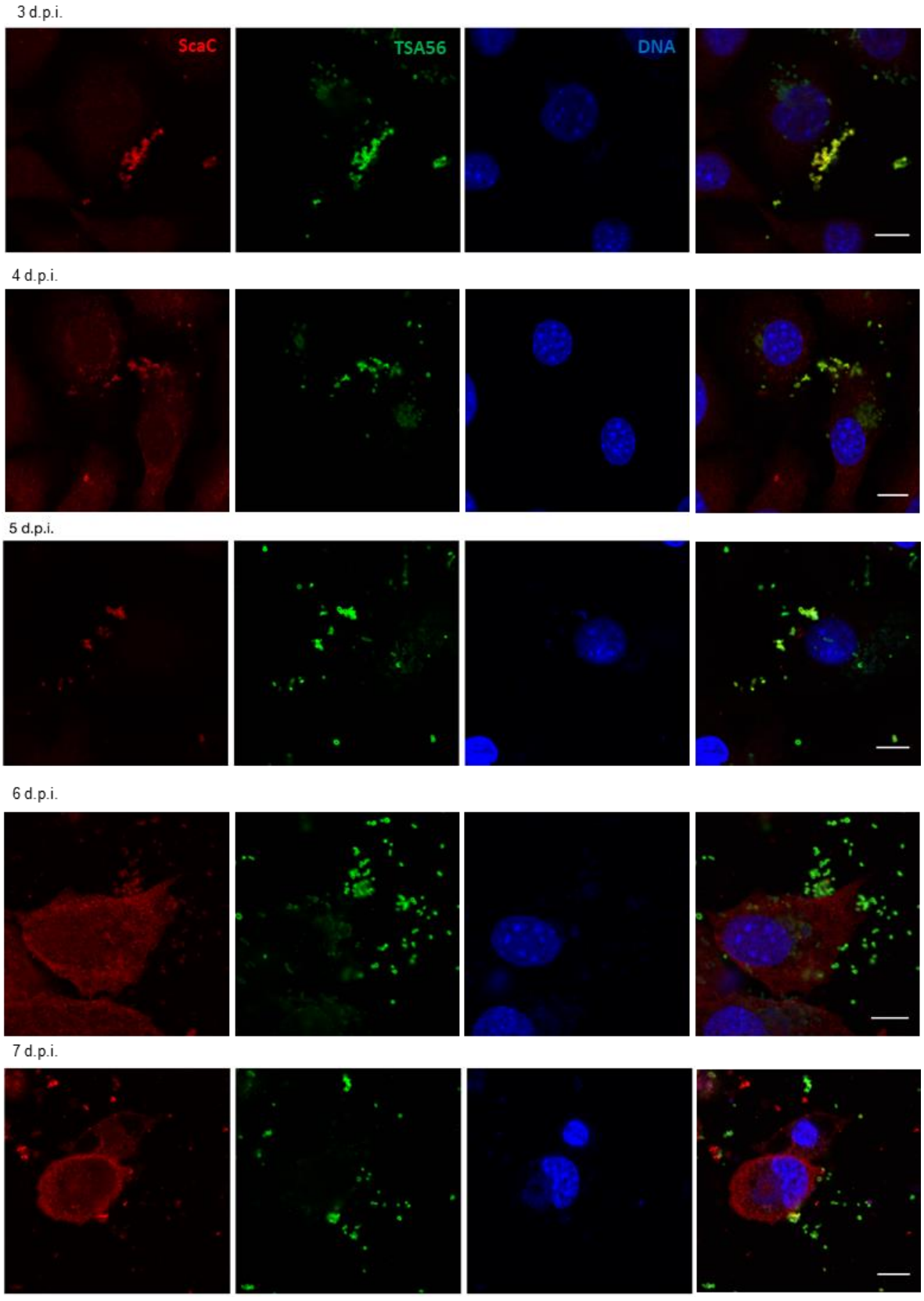
3 d.p.i.
ScaC
TSA56
DNA
4 d.p.i.
5 d.p.i.
6 d.p.i.
7 d.p.i.

Figure 21. The surface protein ScaC is differentially expressed in *Orientia* cells grown in L929 cells. Confocal microscopy images of *Orientia* grown in L929 cells at different times after infection. h.p.i = hours post infection and d.p.i = days post infection. Red = ScaC antibody labelled cells, green = TSA56 labelled cells, blue = hoescht-labelled DNA. Scale bar= 10µM

In order to observethe ScaC expression pattern, ScaC labeling was further observed in Ptk2 cells. This cell line was selected because Ptk2 remains flat throughout the cell cycle when grown in monolayer culture (276), whilst many other cell lines become rounded up during cell division. The flat dimensions of Ptk2 allow easy visualization of the cellular compartment under a microscope.

Orientia in Ptk2 cells were labeled with ScaC antibody during a 7-day time course (Fig. 22). The immunofluorescence results illustrated that the ScaC antibody can label all extracellular bacteria but only a subpopulation of intracellular bacteria. The ScaC antibody also labels the mature intracellular bacteria before budding out. However, the labeling pattern of ScaC in Ptk2 is different from that seen in L929. Intracellular bacteria located near the perinuclear region were able to be labeled with ScaC antibody from day 3 to day 7 post infection, whilst intracellular bacteria in L929 cells were never labelled. This suggests that *ScaC* is switched on earlier after entry which implies that the maturation stage of *Orientia* in Ptk2 cells begins earlier than in L929 cells. Therefore, the host cell type affects the stage progression of the intracellular infection cycle of *Orientia*.

Based on the ScaC labelling (Fig. 21-22), the host cytoplasm is also labelled with ScaC antibody. This could suggest that ScaC is secreted into the host cytoplasm. Additionally, the ScaC labelling of some populations at the surface of host cells was not clear enough to distinguish between the host membrane and bacteria. To solve this labelling issue, CellMask, which is the host plasma membrane dye, can be used for co-labelling with ScaC antibody.

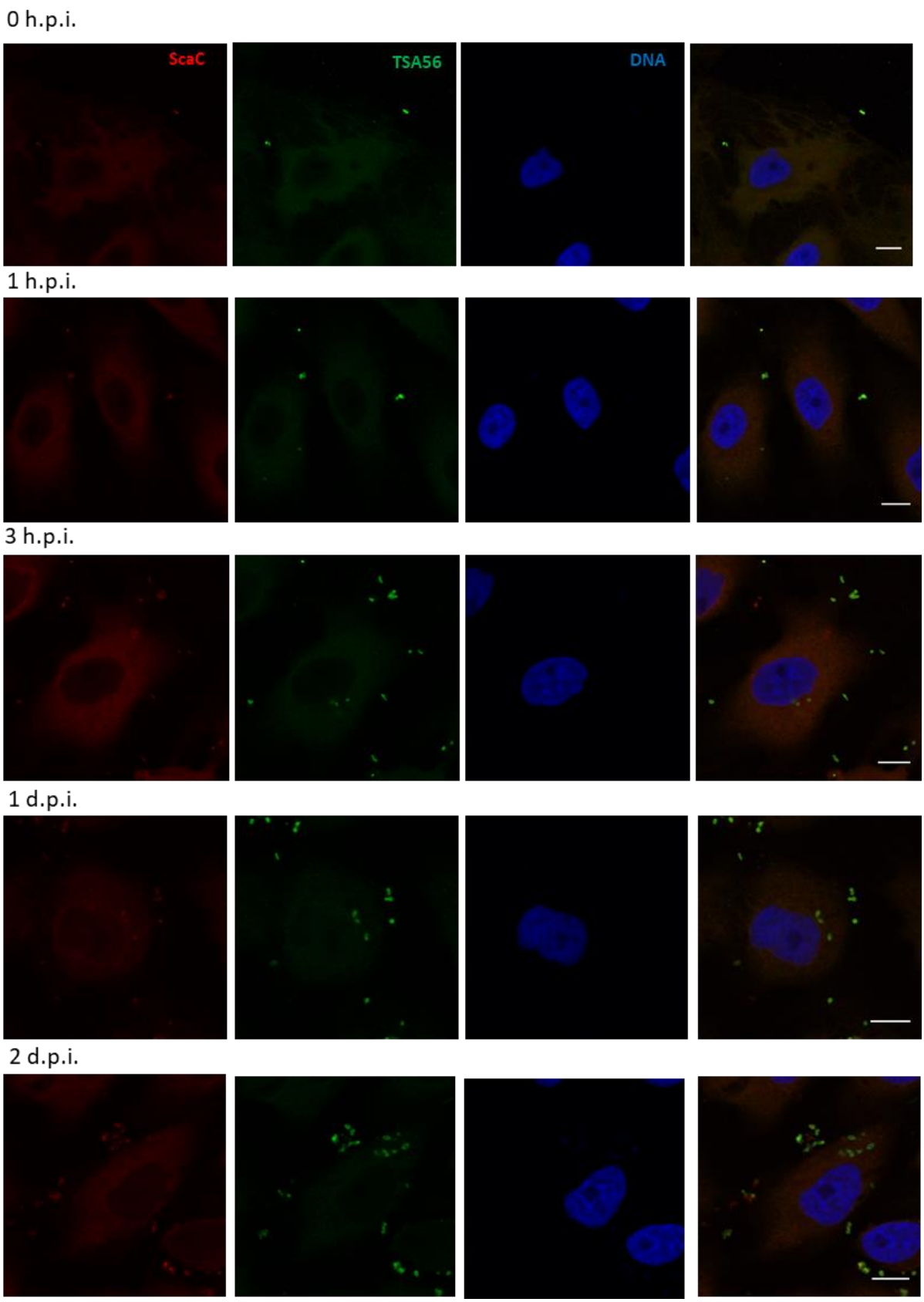
0 h.p.i.
ScaC
TSA56
DNA
1 h.p.i.
3 h.p.i.
1 d.p.i.
2 d.p.i.

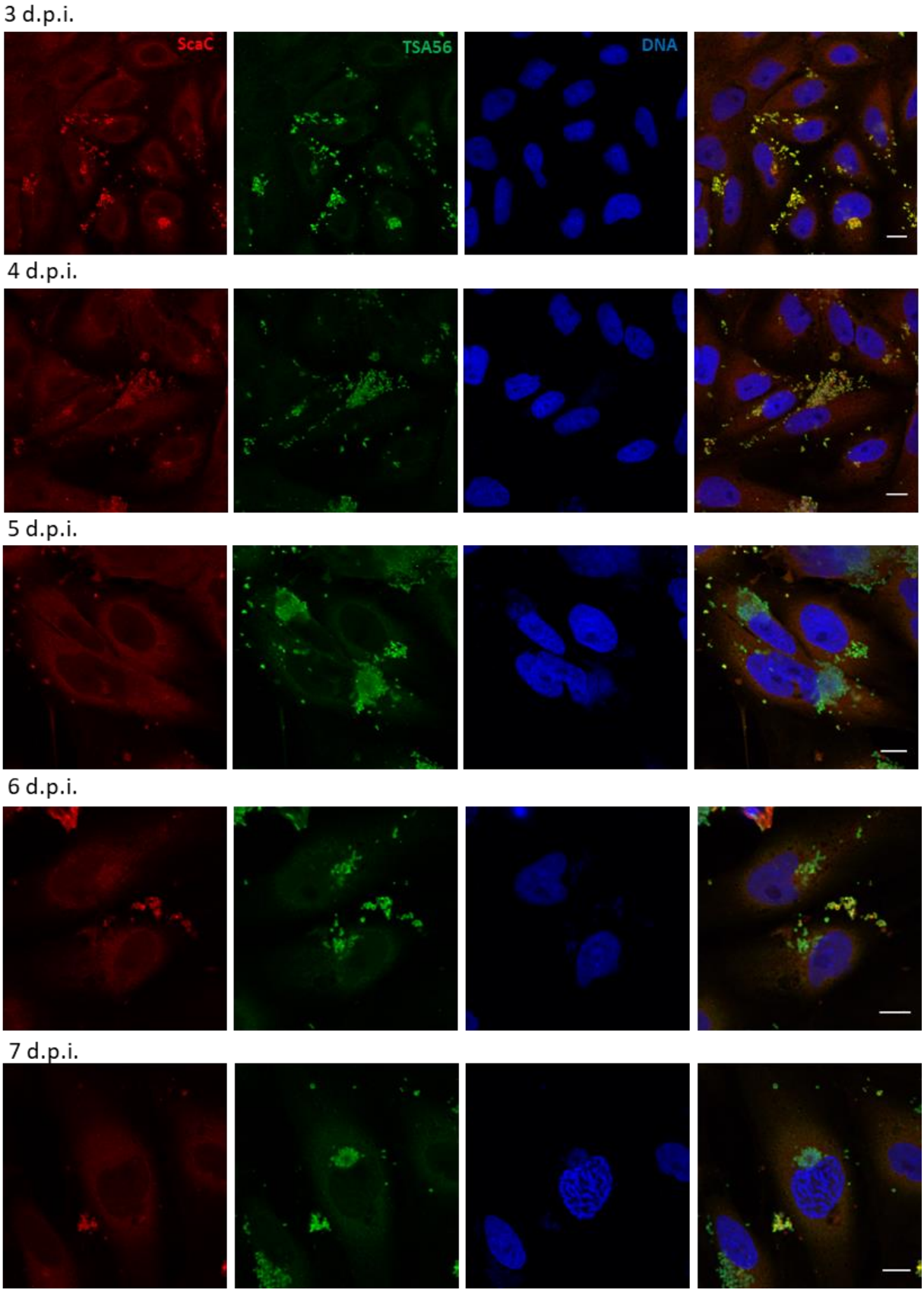
3 d.p.i.
ScaC
TSA56
DNA
4 d.p.i.
5 d.p.i.
6 d.p.i.
7 d.p.i.

Figure 22. The surface protein ScaC is differentially expressed in *Orientia* cells grown in Ptk2 cells. Confocal microscopy images of *Orientia* grown in Ptk2 cells at different times after infection. h.p.i = hours post infection and d.p.i = days post infection. Red = ScaC antibody labelled cells, green = TSA56 labelled cells, blue = hoescht-labelled DNA. Scale bar= 10µM

4.2 The maturation stage is involved in dormancy and other mechanisms

Bacteria contain dedicated mechanisms to respond to a fluctuating environment for survival (277). Several extracellular factors such as limited nutrients, antibiotic stress, accumulation of toxic by-products, changes in pH, osmolarity, and temperature activate bacteria to reprogram the gene expression pattern and metabolic activities. Examples include reduction of phosphate metabolism in *E. coli* (278) and depletion of catabolic proteins in *P. aeruginosa* (279). In many bacterial species, some populations enter a dormant stage or non-growth condition in which cells are metabolically inactive, and these dormant bacteria usually constitute about 1% of the whole population in the non-growing stationary phase (277, 280). Reduction or cessation of metabolic activity alters bacterial protein levels resulting in a change in their protein profiles. Since *Orientia* enters an extracellular stage and becomes metabolically inactive, *Orientia* might need to use similar mechanisms to survive.

The proteomic profile of extracellular and intracellular populations was analyzed in detail to observe whether or not the subpopulations have a different protein profile. Any differences suggest a mechanism of gene regulation, and changes in profiles provide insight into the functions of individual proteins during a cell-cycle stage. Protein fractions from both populations during the mid-stage of infection (day 4) were compared with one another to see the pattern of protein profiles (Table 3-4.). The total number of single-hit proteins from the host, and bacteria was 4,190 and 531, respectively. To reduce variation between replicates, the data was normalized by median normalization (281). We found a significant (>2 fold) upregulation of 60 and 47 proteins in the intracellular and extracellular populations, respectively. The summary of the proteomic analysis revealed that the proteins upregulated in extracellular populations were involved in protein synthesis (20), metabolism (13), effectors and secretion system (13), oxidation-reaction processes (11), RNA binding and processing (4) including dormancy and the

stringent response (3). This finding supported the hypothesis that *Orientia* might differentiate into a dormant, extracellular stage.

There are three proteins involved in dormancy and stringent response that were upregulated in the extracellular population: SpoT ((p)ppGpp synthetase), RpoH (the alternative heat response sigma factor), and the GTPase ObgE. SpoT is a bifunctional enzyme that synthesizes and hydrolyses (p)ppGpp or alarmone guanosine tetraphosphate, an unusual nucleotide typically produced during starvation or stress that controls the regulation of stress-response related genes (282). RpoH is a starvation sigma factor which has been found to upregulate during the stationary phase in *E. coli* and *Salmonella typhimurium* (215, 283). ObgE is in the highly conserved Obg GTPase family (spo0B-associated GTP-binding protein) and acts as an anti-association factor, which binds to the 50s ribosome and blocks the formation of the 70s ribosome resulting in inhibition of the initiation of translation (284). ObgE has been shown to be regulated by (p)ppGpp during the stress response (285).

The DNA binding protein YbaB/EbfC was highly expressed in the extracellular state. This protein has been reported to be a nucleoid-associated protein or DNA-binding protein and plays a role in gene regulation during stationary and exponential stages *in Borrelia burdorferei* (286, 287).

Several effector proteins and secretion system proteins were expressed differently in extracellular and intracellular states, for example, tetratricopeptide repeats (TPR3, TPR8) are highly expressed in the extracellular state, and Ank1, Ank13 are highly expressed in the intracellular state (Table 2-3). TPR mediates protein-protein interaction and is associated with the specific interactions of multiple proteins (34). Previous evidence showed that TPR-containing proteins play an important role in cell cycle control, transcription, and protein transportation in *Saccharomyces cerevisiae* (288-291). The ankyrin repeats are common protein-protein interaction motifs associated with the plasma membrane and promote the interaction between the cytoskeleton and integral membrane proteins (292). A large number of ankyrin repeats have been found in eukaryotes but there is little evidence in prokaryotes. Ankyrin has been shown to be transferred into host cells by type IV secretion system (TFSS) in intracellular pathogens such

as *Legionella pneumophila* and *Coxiella burnetii*, *Anaplasma phagocytophilum* and *Wolbachia* (293-296), suggesting that *Orientia* might use TPR and Ank proteins for interaction with host cells at different stages of infection.

Several proteins which are involved in protein synthesis such as ribosomes associated proteins, are upregulated in the extracellular populations. This evidence suggests that the metabolic activity of extracellular bacteria may be active. The transcription and translation levels of the extracellular bacteria might be too low under the detectable level, and this could be a reason why the metabolic probe (HPG) cannot detect the metabolic activity of extracellular populations. In *Chlamydia*, the EB lacks metabolic activity but the transcription is active during the primary differentiation (178). Chlamydial EB may have a specific mechanism to differentiate newly transcribes mRNA from the carryover mRNA. This process involves RNA binding proteins that transport the carryover mRNA from ribosomes. Carryover mRNA have a short life and normally are below the detectable level by 6 hours post-infection (297). *Orientia* may present carryover mRNA but the mechanism is needed to investigate further.

	Locus Tag	Gene ID	Gene name	Ratio (E/I)	Function
p value < 0.0001	UT76-HP_02266	nuoA	NADH-quinone oxidoreductase subunit I	12.4	energy metabolism
	UT76-HP_00279	tpr3	TPR repeat-containing protein 03	10.0	effectors and secretion systems
	UT76-HP_01586		aplha/beta hydrolase	8.9	enzyme
	UT76-HP_02172		nucleoid-associated protein, YbaB/EbfC family	8.2	DNA binding
	UT76-HP_01102	spoT	(p)ppGpp synthetase	8.1	dormany/stringent response/heat/ stress
	UT76-HP_01915	tpr8	TPR repeat-containing protein 08	8.0	effectors and secretion systems
	UT76-HP_01867	murC	UDP-N-acetylmuramate--L-alanine ligase	7.9	peptidoglycan
	UT76-HP_00409	nusB	transcription antitermination factor NusB	7.4	RNA binding and processing
	UT76-HP_00905		histidine phosphotransferase	7.1	signalling
p value < 0.01	UT76-HP_01844		intradiol ring-cleavage dioxygenase	6.0	oxidation-reduction processes
	UT76-HP_01355		potassium transporter	5.6	transport
	UT76-HP_01080		type IV secretion protein	5.3	effectors and secretion systems
	UT76-HP_01602	nuoD	NADH-quinone oxidoreductase subunit D	5.3	energy metabolism
	UT76-HP_00613	rpoH	RNA polymerase factor sigma-32	5.3	dormany/stringent response/heat/ stress
	UT76-HP_01946	xerD	site-specific tyrosine recombinase XerD	5.3	DNA binding
	UT76-HP_01601	nuoc	NADH-quinone oxidoreductase subunit C	5.0	energy metabolism
	UT76-HP_01945	virB6/	conjugal transfer protein	5.0	effectors and secretion systems
	UT76-HP_02056	tpr8	TPR repeat-containing protein 08	5.0	effectors and secretion systems
p value < 0.05	UT76-HP_01121		cytochrome b	4.8	energy metabolism
	UT76-HP_00794		hypothetical protein	4.6	hypothetical protein
	UT76-HP_01543		hybrid sensor histidine kinase/response regulator	4.6	signalling
	UT76-HP_01097	obgE	GTPase ObgE	4.5	dormany/stringent response/heat/ stress
	UT76-HP_02239	idh	isocitrate dehydrogenase, Idh	4.5	energy metabolism
	UT76-HP_01254		hypothetical protein	4.5	hypothetical protein
	UT76-HP_01589	atpC	ATP synthase subunit epsilon	4.2	energy metabolism
	UT76-HP_00497	dsbB	disulfide bond formation protein B	4.1	oxidation-reduction processes
	UT76-HP_01634	parB	chromosome partitioning protein	4.0	DNA binding
	UT76-HP_02164	rpmA	50S ribosomal protein L27	4.0	protein synthesis
	UT76-HP_00841	rplX	50S ribosomal protein L24	3.9	protein synthesis
	UT76-HP_01490	rbfA	ribosome-binding factor A	3.9	protein synthesis
	UT76-HP_01010	fabI	enoyl-ACP reductase	3.8	lipid metabolism
	UT76-HP_01866		hypothetical protein	3.8	hypothetical protein
	UT76-HP_00570	aat	aspartate aminotransferase	3.7	protein catabolic process
	UT76-HP_01003	murE	UDP-N-acetylmuramoyl-L-alanyl-D-glutamate--2, 6-diaminopimelate ligase	3.7	peptidoglycan
	UT76-HP_00817	virB9	P-type conjugative transfer protein VirB9	3.7	effectors and secretion systems
	UT76-HP_00815	ftsY	signal recognition particle-docking protein FtsY	3.7	protein synthesis

Table 3. Summary of proteins abundant in extracellular bacteria. *O. tsutsugamushi* was infected in L929 cells in independent triplicates. The intracellular and extracellular fractions of infected cells were isolated and protein profiles analyzed by shotgun proteomics analysis. Proteins that were significantly expressed in the extracellular fraction compared with the intracellular fraction (I/E) are presented as fold differences. The cutoff is based on P value at $P < 0.0001$, $P < 0.01$ and $P < 0.05$. All the P-values are calculated from mean and SD from Gassian distribution.

	Locus Tag	Gene ID	Gene name	Ratio (I/E)	Function
p value < 0.001	UT76-HP_00965		RNA-binding protein	26.00	RNA binding and processing
	UT76-HP_01100	yccA	membrane protein	21.50	protein synthesis
	UT76-HP_01944	surf1	surfeit locus protein 1	7.99	energy metabolism
	UT76-HP_02249	ank1	ankyrin repeat-containing protein	7.55	effectors and secretion systems
	UT76-HP_01738	prfA	peptide chain release factor 1	5.13	protein synthesis
	UT76-HP_00451	rnpA	ribonuclease P	4.75	RNA binding and processing
	UT76-HP_00496	ubiB	ubiquinone biosynthesis protein UbiB	4.73	oxidation-reduction processes
	UT76-HP_00730		transposase	4.24	transposase
	UT76-HP_02120	lpxK	tetraacyldisaccharide 4'-kinase	4.11	lipid metabolism
	UT76-HP_01600	nuoB	NADH-quinone oxidoreductase subunit B	4.07	oxidation-reduction processes
p value < 0.01	UT76-HP_00411	gstA	glutathione S-transferase	3.22	oxidation-reduction processes
	UT76-HP_01955	dapA	4-hydroxy-tetrahydrodipicolinate synthase	3.21	protein synthesis
	UT76-HP_01609		hypothetical protein	3.18	hypothetical
	UT76-HP_01864	glyQ	glycine--tRNA ligase subunit alpha	3.06	protein synthesis
	UT76-HP_00619	ank13	ankyrin repeat-containing protein 13	3.02	effectors and secretion systems
	UT76-HP_01784	ank13	ankyrin repeat-containing protein 13	2.96	effectors and secretion systems
	UT76-HP_01676	atpF	ATP synthase subunit b	2.59	energy metabolism
	UT76-HP_00502	tpiA	triose-phosphate isomerase	2.53	energy metabolism
	UT76-HP_02059		transposase	2.41	transposase
p value < 0.05	UT76-HP_01078	virB6	type IV secretion protein	2.29	effectors and secretion systems
	UT76-HP_00501	secG	preprotein translocase subunit SecG	2.26	protein synthesis
	UT76-HP_01119		hypothetical protein	2.09	hypothetical
	UT76-HP_00981	yihA	YihA family ribosome biogenesis GTP-binding protein	2.06	protein synthesis
	UT76-HP_00711		transposase	2.02	transposase
	UT76-HP_00021	tsa22	membrane protein	1.99	membrane protein
	UT76-HP_02129		hypothetical protein, Ribonuclease HII	1.96	hypothetical
	UT76-HP_01613	ubiG	bifunctional 3-demethylubiquinone 3-O-methyltransferase/2-octaprenyl-6-hydroxy phenol methylase	1.93	methylation
	UT76-HP_00477		hypothetical protein	1.78	hypothetical
	UT76-HP_00792	tlc	ATP/ADP translocase; ADP,ATP carrier protein	1.78	energy metabolism
	UT76-HP_01099		hypothetical protein	1.76	hypothetical
	UT76-HP_01417	Der	ribosome biogenesis GTPase Der	1.73	protein synthesis

Table 4. Summary of proteins abundant in intracellular bacteria. *O. tsutsugamushi* was infected in L929 cells in independent triplicates. The intracellular and extracellular fractions of infected cells were isolated and protein profiles analyzed by shotgun proteomics analysis. Proteins that were significantly expressed in the intracellular fraction compared with the extracellular fraction (I/E) are presented as fold differences. The cutoff is based on P value at $P < 0.0001$, $P < 0.01$ and $P < 0.05$. All the P-values are calculated from mean and SD from Gassian distribution.

Chapter 5: *O. tsutsugamushi* becomes metabolically active shortly after entry into host cells

This research has been preprinted on bioRxiv under the title of Developmental differentiation in a cytoplasm-dwelling obligate intracellular bacterium: Giengkam S, Wongsantichon J, Atwal S, Jaiyen Y, Goh WI, Wright G, Chung T, Huh H, Lee S, Sobota R, Salje J. Developmental differentiation in a cytoplasm-dwelling obligate intracellular bacterium. bioRxiv. 2020 Jan 1.

5.1 *O. tsutsugamushi* undergoes a lag period upon entry into host cells

Bacteria exhibit an exponential growth phase under normal conditions, however, bacterial growth also presents lag, stationary, and death phases under starvation conditions. The lag phase is defined as a temporary period of nonreplication or a stage during which bacteria have not yet started dividing (298). Bacteria that undergo a lag phase need time to adapt to the new environment and prepare for the first replication before starting exponential growth (299). At this stage, bacteria could repair macromolecular damage and synthesize the precursors or cellular components that are essential for bacterial growth (300). Upon the entry of *O. tsutsugamushi* into new host cells, the metabolically inactive extracellular stage turns into the intracellular stage in a short period. Based on previous work, *Orientia* undergoes a lag phase of 24 hours post infection and starts replication after 24-48 hours post infection (262). However, this study used purified intracellular bacteria only. To identify and difference in the growth of extracellular and intracellular subpopulations during the lag phase, both populations were isolated and propagated in L929 cells. The growth was measured from 0 hour until 7 days post infection by qPCR. The results showed that the bacteria copy number from extracellular and intracellular infections did not significantly change during the first 0 - 24 hours post infection, and DNA replication initiates after 24 hours post infection. This confirms that the extracellular and intracellular populations undergo a lag phase from 0-24 hours post infection (Fig. 23).

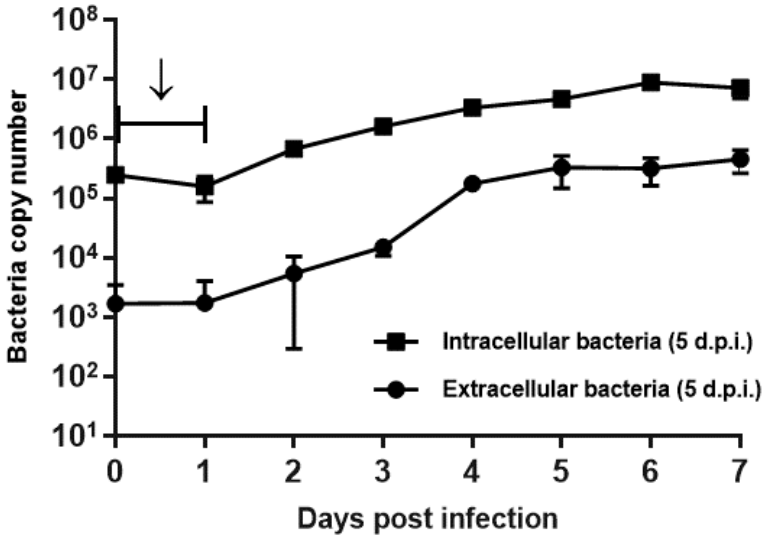

Figure 23. Growth curve shows bacterial replication starts 24 hours post infection. This mark represents the lag phase. Bacteria were harvested at each time point and the bacterial copy number in one well of a 24-well plate measured by qPCR.

5.2 Verifying the metabolic activity of intracellular populations by Click-HPG protein synthesis assay

O. tsutsugamushi starts DNA replication 24 hours post infection, but metabolic activity during the intracellular infection cycle has never been monitored to determine whether *Orientia* initiates protein synthesis before or after the DNA replication process. The alkyne-modified methionine analog, L-homopropargylglycine (HPG), which is incorporated into nascent proteins during active protein synthesis, was used to measure the metabolic activity of the bacteria. A non-toxic HPG probe was directly added to cell culture media (methionine-free media) for 30 minutes before fixation, and further reacted with an azide-conjugated fluorophore under a copper(I)-catalyzed click reaction. The advantage of the click chemistry approach is its use of a fluorescence dye bound to a small molecule without permeabilization of cells and resulting in simple and rapid sample processing. The triazole linkage between alkyne and azide is very stable and specific which allows for the identification of fluorescence signals of individual cell activity.

In this study, alkyne-modified methionine was incorporated with azide-conjugated Alexa Fluor 488 which exhibits a green signal. The intensity of the fluorescence signal corresponds to

the level of translational activity of bacteria at each time point. To observe the metabolic activity of *Orientia* during the early stage of entry, HPG was added to *Orientia* cell culture in L929 cells at 0, 1, 3 hours post infection and further monitored from day 1 to day 7 post infection. Bacteria were co-labeled with a surface protein antigen, TSA56 to demonstrate the whole population. HPG-labeling results revealed that a signal in bacteria is strongly detected under the confocal microscope after incubation with the HPG probe for 30 minutes (Fig. 24), suggesting that bacteria need time to uptake the HPG probe to synthesize new proteins during the translation process. Host cells can uptake the methionine-HPG probe and present a green signal but the bacterial signal is much stronger than the host cell background.

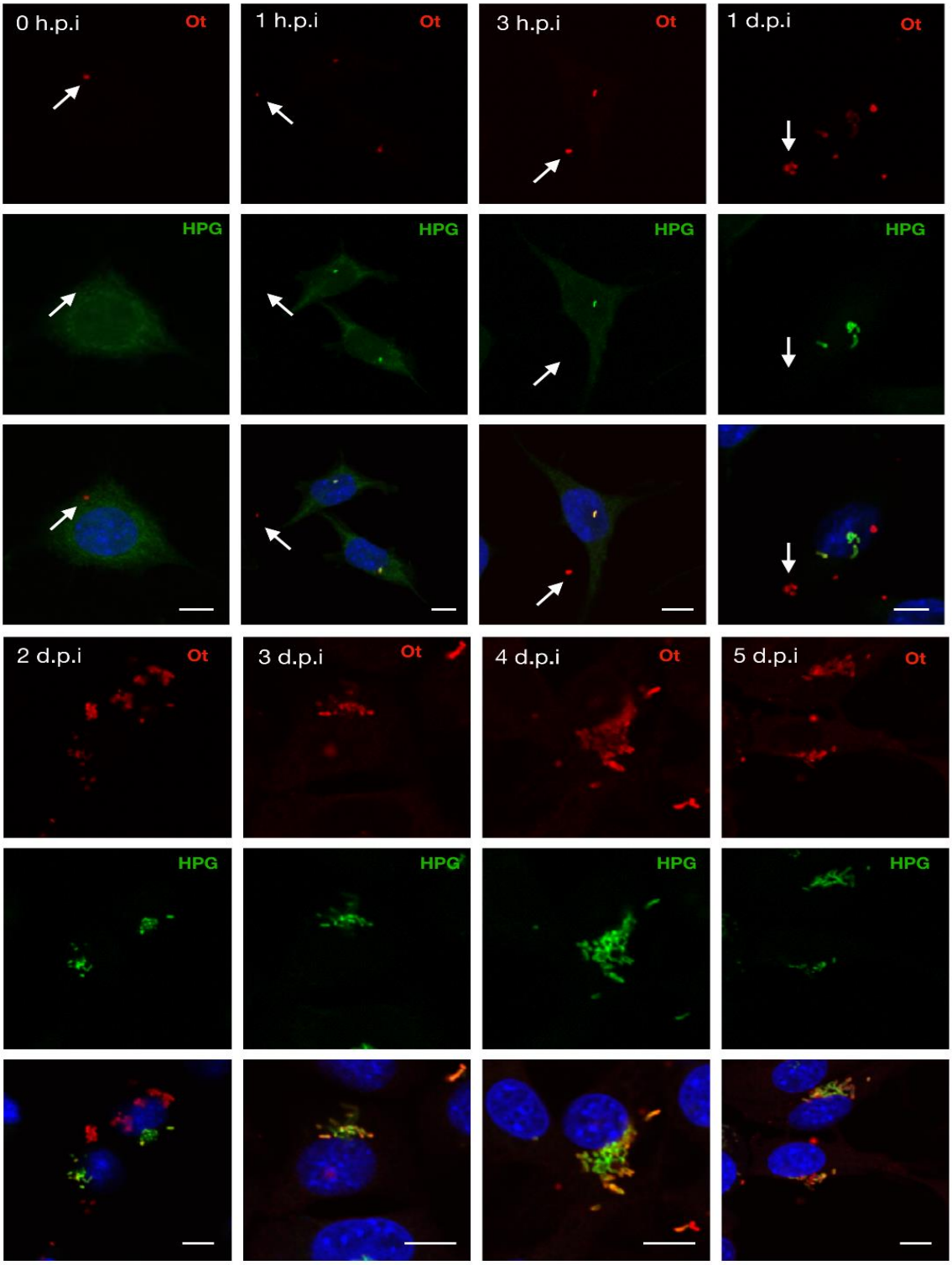

Figure 24. Confocal microscopy images of *Orientia tsutsugamushi* show that *Orientia* becomes metabolically active shortly after entry. A clickable methionine probe (HPG, green) is used to identify metabolically active cells. Bacteria were grown in L929 host cells in the presence of HPG for 30 minutes. Subsequently, cells were fixed and HPG reacted with an azide-conjugated

fluorophore (Alexa Fluor® 488) to reveal cells actively undergoing protein synthesis (green). Bacteria are counterstained with a TSA56 antibody (red), hoescht-labelled DNA (blue). Arrows indicate metabolically inactive bacteria. *Orientia* grown in L929 cells. Scale bar = 10μm.

5.3 Clarification of the stages of *O. tsutsugamushi*

Metabolic activity and DNA synthesis were used as a baseline to classify the stages of *O. tsutsugamushi* during the infection cycle. *Orientia* does not synthesis DNA during 0-24 hours post infection (lag phase), but protein synthesis is already initiated as early as 1 hour post infection. This indicates that *Orientia* is primed for the resumption of metabolic activity upon entry into host cells. This key finding facilitated a classification of three more stages of the early infection cycle as follows, early entry, pre-replicative, and replicative stages. The early entry stage is defined as when *Orientia* had entered into host cells but is metabolically inactive. The pre-replicative stage is the period when *Orientia* is metabolically active but DNA replication has not yet begun. In the replicative stage, *Orientia* exhibits both metabolic activity and DNA replication.

Later in the infection, *Orientia* is still metabolically active as the bacteria located near the host cell membrane are labeled with HPG (Fig. 24). Once bacteria exit host cells, extracellular bacteria could not be labeled with HPG. This finding suggests that extracellular bacteria are metabolically inactive.

Besides clickable methionine (HPG) labeling, which reflects active translation, nucleotide analogs based on click chemistry were used as an alternative tool to study nascent DNA and RNA synthesis during the replication process. Nucleotide labeling could be used to monitor active nucleotide synthesis in the subpopulations, since the measurement by qPCR and RT-qPCR represents only the combined DNA and RNA levels of mixed populations. EdU and EU probes were used to observe DNA and RNA synthesis during *Orientia* infection (0, 1, 3 hours and 3, 5 days post infection). The EdU (5-ethynyl-2´-deoxyuridine) probe, a thymidine analog, is incorporated into DNA during active DNA synthesis. EU (5-ethynyl uridine) probe, a nucleoside analog of uracil, is incorporated into RNA during active RNA synthesis. The labeling was optimized under several conditions, including the probe concentrations, incubation times, probe carriers, and cell permeabilization. The findings revealed that the EdU and EU probes failed to label

Orientia at every time point. However, the host nucleus was clearly labeled with both probes, indicating that the labeling method was successful (Fig. 25). One of the possible reasons is that *O. tsutsugamushi* cannot uptake these unnatural nucleotides. Either the modified nucleotides cannot cross the bacterial cell membrane or the recognition of these analogs during transcription and DNA replication is insufficient (301).

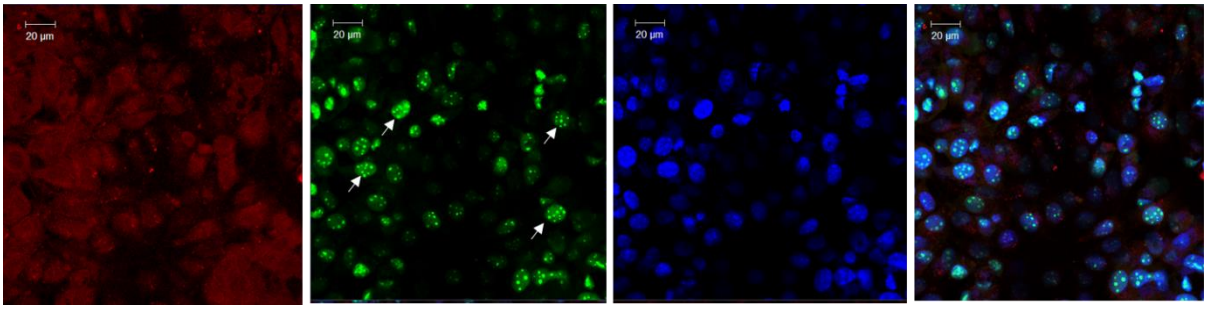

Figure 25. A clickable nucleotide probe (EdU) is used to identify nascent DNA synthesis. *O. tsutsugamushi* was grown in L929 cells for 3 days before labelling with EdU. The EdU probe was incubated with the infected cells for 30 mins, cells were fixed, and EdU was reacted with an azide-conjugated fluorophore to reveal cells actively undergoing DNA synthesis (green). Bacteria are counterstained with a TSA56 antibody (red) and nuclei are labelled with DAPI (blue). Arrows indicate a successful labeling of compact DNA on host nucleus but fail to detect bacterial DNA. Scale bar = 20 µm.

5.4 Protein synthesis of *Orientia* begins immediately upon exit from endosomes

Orientia enters host cells via a clathrin-mediated endocytosis-like mechanism and escapes from the host endocytic pathway by exiting from late endosomes into the cytoplasm. Bacteria escape from the endolysosomal pathway 1 to 2 hours post infection and are co-localized with early and late endosomal markers, EEA1 and LAMP2, respectively (302). Together with the findings in this study (described above in the topic 5.2), this illustrated that metabolic activity is initiated during the early infection (30 min post infection onwards). This leads to the next question; does *Orientia* become metabolically active within the endosome or after release into the host cytoplasm?

Intracellular and extracellular bacteria at 5 days post infection were isolated and used to infect L929 cells. Bacteria were fixed at 15 mins, 30 mins, 1 hour and 24 hours post infection and were labeled with the late endosomal marker LAMP1, *Orientia* maker 16s RNA FISH, and methionine probe HPG (Fig 21). Bacteria that co-labeled with LAMP1 are endosomal localized *Orientia*, and HPG labelling represents metabolic activity. The results (Fig. 27) showed that the majority of bacteria were colocalised with LAMP1 without HPG (2-8%) during 15 -30 min post infection, indicating that bacteria in endosomes are metabolically inactive at the first 15-30 min post infection. The colocalisation of LAMP1 and HPG (2-10%) appeared later, from 30 -60 min post infection, suggesting that *Orientia* may initiate metabolic activity while still intact in endosomes or this perhaps could happen during the lysis of the endosomal membrane. To prove that bacteria inside an endosome could be labeled with HPG, *Salmonella typhimurium* which is known to live in a membrane–bound endosome (Salmonella containing vacuole-SCV) were labeled with HPG probe as a control experiment. Salmonella bacteria were inoculated in growth media overnight and labeled with HPG for 30 min before fixation. HPG successfully labeled Salmonella as shown in figure 28. This result confirms that HPG was able to label bacteria within a membrane-bound vacuolar compartment.

Escape from the vacuole or endosome is a key step for cytosolic pathogens. This process occurs shortly after the invasion, and many pathogens are detected free in the cytoplasm within 30 minutes of entry such as *Shigella flexneri*, *Listeria monocytogenes,* and *Rickettsia coronii* (303). Like other cytosolic pathogens, *O. tsutsugamushi* also escapes endosome within 30-60 minutes. The fast rate of endosomal lysis suggests that bacteria are in a battle for survival. Bacteria must escape before endosome-lysosome fusion to continue their life cycle within the cytosol.

A large number of *Orientia* (70-96%) were HPG positive and LAMP negative at a later time (1- 24 hours post infection). This showed that most bacteria had already escaped from endosome into the cytoplasm. Overall, the labeling pattern of LAMP1 and HPG in infections with intracellular and extracellular bacteria were similar, suggesting that even though bacteria are in different states at the point of infection, the magnitude of escape from the endosome during the early infection is equivalent.

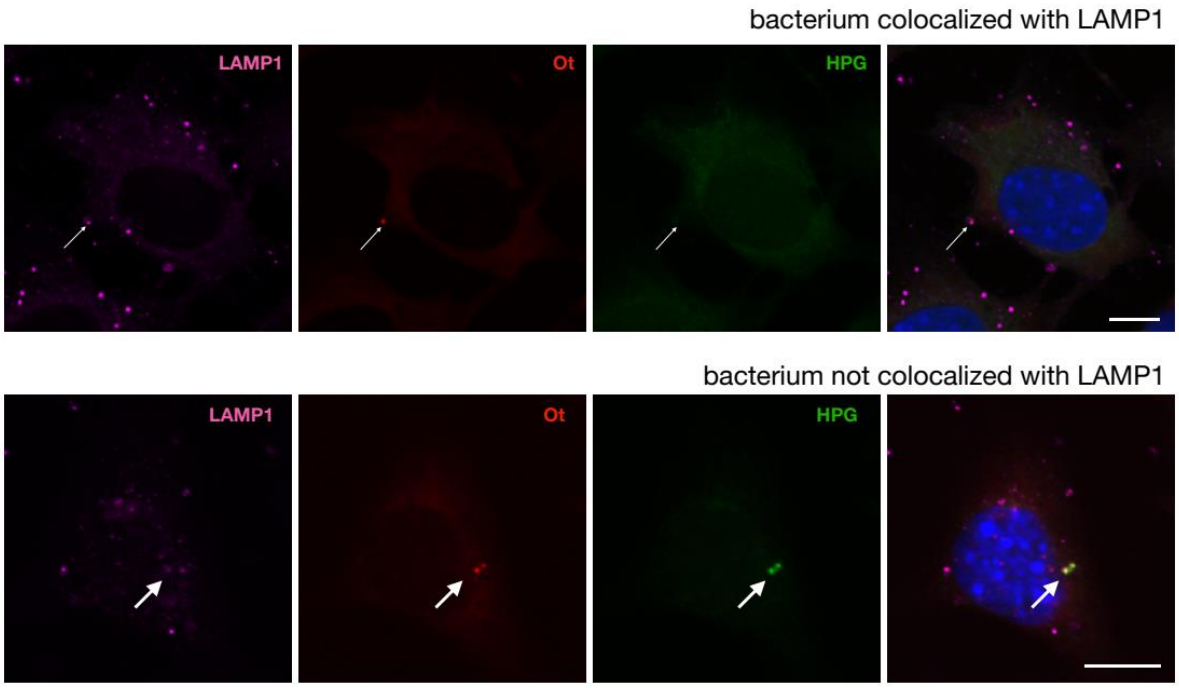

Figure 26. *O. tsutsugamushi* becomes metabolically active shortly after entry. Confocal microscopy images of intracellular *Orientia* 15 mins (upper panel) and 1 hour post infection (lower panel). Late endosomes are labelled with LAMP1 (magenta), *Orientia* is counterstained with 16S RNA FISH probes (red), and metabolic activity is measured with a clickable methionine probe (HPG, green).

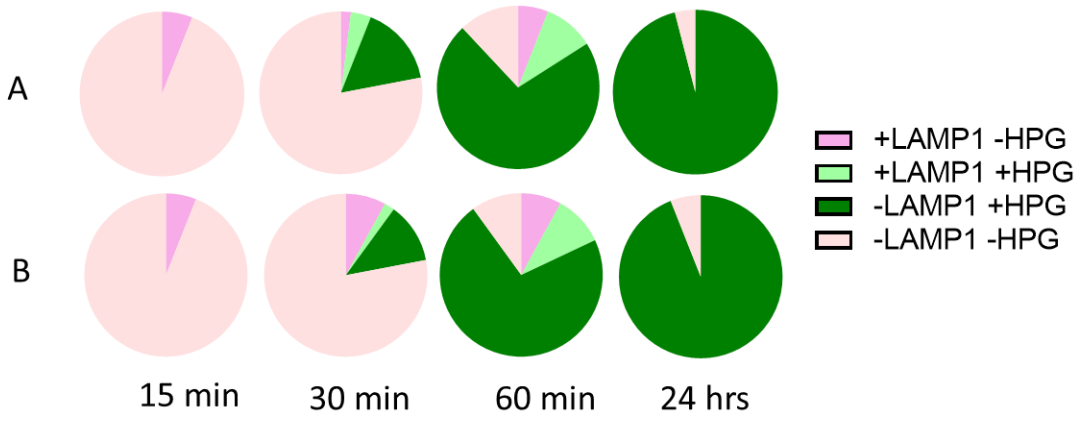

Figure 27. Quantification of confocal data, measuring the fraction of all bacteria (measured by the presence of 16S RNA FISH labelling) that colocalize with LAMP1 and HPG (methionine probe). A= extracellular bacteria used for infection, B= intracellular bacteria used for infection

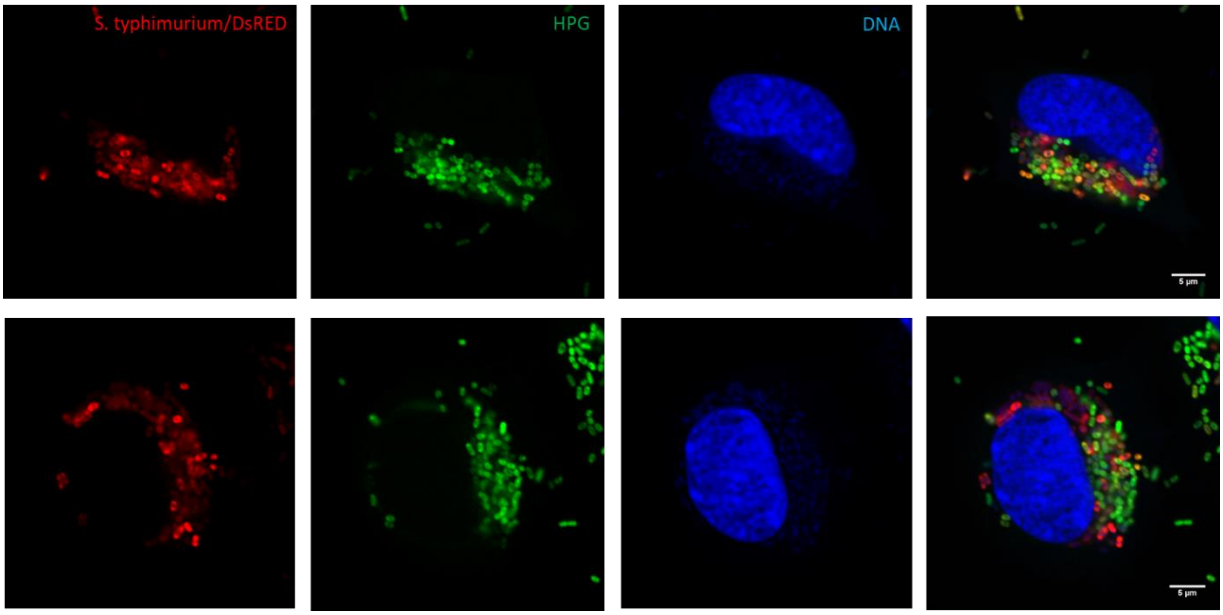

Figure 28. Intracellular *Salmonella* can be labeled with HPG. L929 cells were infected with *Salmonella typhimurium* expressing DsRed (red) for 3 hours and were labeled with the clickable methionine probe HPG (green). This was added to the growth media for 30 mins prior to fixation, and then conjugated to an Alexa488 fluorophore.

5.5 Bacterial activation following entry into host cells is triggered by sensing the reducing environment of the host cytoplasm

The evidence that protein synthesis in *Orientia* begins immediately upon exit from the endosome into the host cytoplasm leads to the next question; what mechanism activates the resumption of metabolic activity in cytoplasmic *Orientia*? TSA56 is one of the major outer membrane proteins of *O. tsutsugamushi*. It has been determined that TSA56 forms a disulfide crosslink network in *Orientia* (44). The sulfur-containing residue cysteine on the bacterial membrane is particularly sensitive to oxidizing molecules, such as reactive oxygen species (ROS), generated by host cells to kill invading pathogens. Several proteins are involved in protecting bacterial cell membranes and repairing proteins from oxidative damage including catalase, peroxiredoxins, superoxide dismutases (SOD), and oxidoreductases (304). For example in *E.coli*, there are two major cysteine-based reducing pathways in the cytoplasm: the flavoenzyme

thioredoxin reductase (trxB) and its redox partners trxA and trxC, and the glutaredoxins and the couple glutathione/glutathione reductase (gor) (305). This leads to the next question: whether TSA56 and other cysteine-related proteins might be oxidized upon release in the reducing environment of the host cytoplasm, and this mechanism might trigger an internal signal to activate the metabolism of *Orientia*.

To answer this question, Buthionine sulphoximine (BSO), which is an inhibitor of gamma-glutamylcysteine synthetase, was used to reduce the tissue glutathione (GSH) level, and this consequently depleted the reducing environment in the host cytoplasm. L929 cells were pretreated with BSO 4 mM and 10 mM for 24 hours before infection with *Orientia*. Bacteria were observed 1, 3, and 24 hours post infection. The HPG probe was added prior to fixation and stained with Azide-488 fluorophore to monitor the metabolic effect. Quantification involved imaging 100 random bacteria at the same imaging setting for each time point. The brightest pixel intensity within the area of the bacterium was measured manually using Fiji ImageJ software. BSO did not affect the infection of *Orientia* in L929 cells. The number of infected intracellular *Orientia* in L929 cells did not significantly reduce in the presence of BSO compared with the untreated control (Fig. 30). The results (Fig. 29) showed that the HPG intensity significantly reduced in the presence of BSO 4 mM and 10 mM, suggesting that the reducing environment mediates the reactivation of *Orientia* after entry into host cells. This may happen by breaking disulfide links between TSA56 and other surface proteins and inducing structural or signaling changes. Another possible mechanism could be redox regulation; the reductive stress in host cytosol might affect the cellular NAD^+/NADH imbalance by either direct or indirect pathways to enhance bacterial glutathione (GSH) synthesis (306). In addition, the enrichment of redox-related gene products (ubiB, nuoB, and gstA) in proteomic profile (Table. 4) are uplregulated in intracellular bacteria. These particular redox-related proteins may play a role in the redox regulation during the early stages of infection.

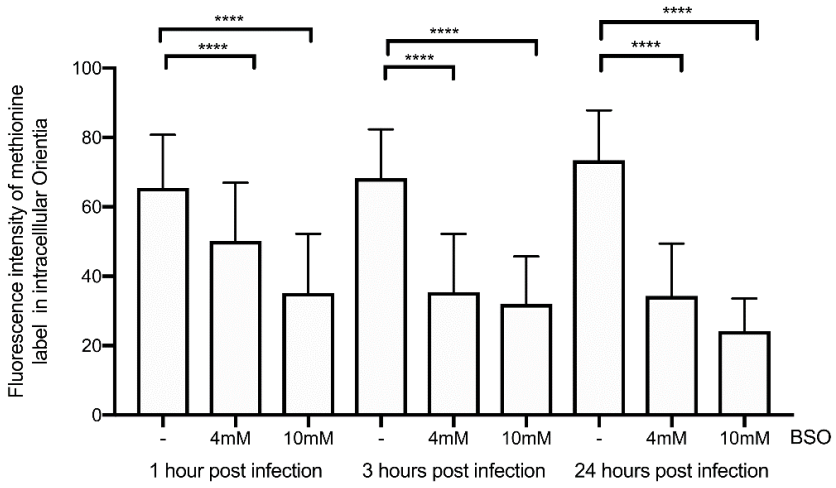

Figure 29. The inhibition of reduced glutathione by BSO leads to reduced metabolic activity in *O. tsutsugamushi*. The fluorescence intensity of HPG-labelled bacteria in confocal microscopy images was quantified at 1, 3 and 24 hours post infection and in the presence of 0, 4 mM or 10 mM BSO. Quantification involved imaging 100 random bacteria at the same imaging setting for each time point. The brightest pixel intensity within the area of the bacterium was measured manually using Fiji ImageJ software.

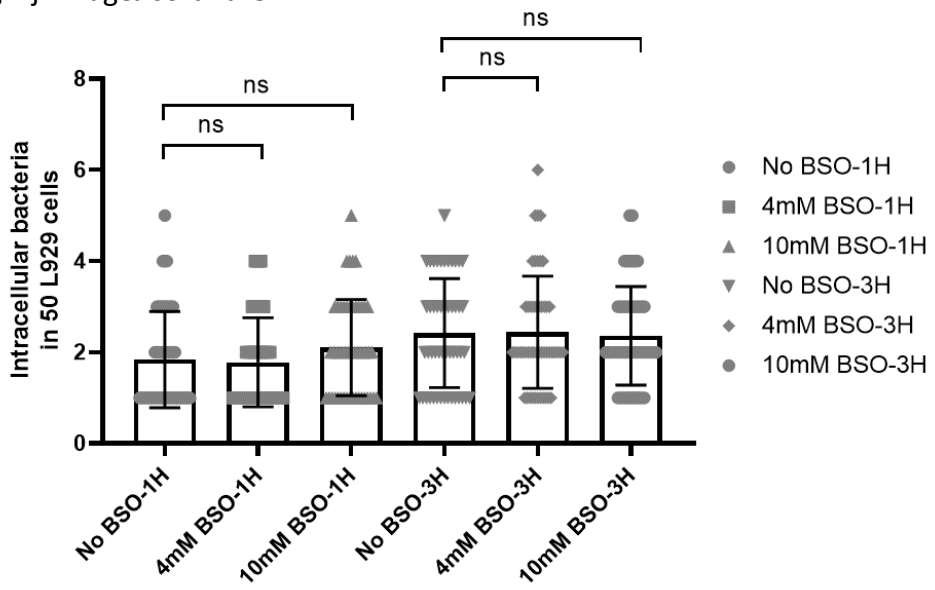

Figure 30. Treatment with BSO does not affect entry of *O. tsutsugamushi* into host cells. Quantification of HPG-label intracellular bacteria 1 hour and 3 hours post infection, assessed by analysis of confocal microscopy images. Quantification involved imaging random bacteria from 50 infected host cells. *O. tsutsugamushi* was infected into L929 cells and treated with no, 4mM or 10mM BSO.

Chapter 6: Discussion of chapters 3-5

By definition intracellular bacteria are organisms that grow and reproduce inside host cells. These have been divided into two distinct groups; facultative intracellular bacteria and obligate intracellular bacteria. Facultative intracellular bacteria such as *Salmonella typhi*, *Mycobacterium* spp., *Listeria monocytogenes*, *Yersinia* spp*., Francisella* spp., *Neisseria meningitides*, and many others, are able to live and reproduce either inside or outside host cells. The obligate intracellular bacteria, for example, *Coxiella burnetti*, *Chlamydia spp.*, and members of the order Rickettsiales (*Anaplasma*, *Ehrlichia* spp., *Wolbachia* spp., *Rickettsia* spp*.,* including *Orientia tsutsugamushi*) are able to grow and reproduce only inside host cells (307). This reflects their intracellular cycle which always depends on the host cells' machinery. The complexity of the developmental cycle in obligate intracellular bacteria is a key challenge to understanding host-pathogen interaction and the mechanism of infection.

Compared with other obligate intracellular bacteria, the life cycle of *O. tsutsugamushi* is relatively little known, including the developmental differentiation which has not been elucidated before. In this thesis, I investigate how *O. tsutsugamushi* differentiates into distinct subpopulations during the course of a 5-7 day infection cycle in host cells. This allows us to classify the *Orientia* infection cycle into 5 distinct stages; stage I-IV (intracellular stage), which represents bacteria located inside host cells and stage V (extracellular stage), which represents bacteria exiting from host cells by budding. This is equivalent to the well-known biphasic life cycle in *Chlamydia,* which exhibits two morphologically and physiologically distinct stages; infectious extracellular and noninfectious intracellular stages, *Orientia* does not undergo the biphasic developmental cycle because it does not present a clear and contrasting biological and physiological specialization. The infection cycle of *Orientia* is unique among the other Rickettsiaceae family. One notable feature is the exit strategy. *Orientia* escapes host cells by a slow budding process in which individual bacteria are encased by host cytoplasmic membrane while other bacteria in the family Rickettsiaceae exit via other mechanisms, such as actin-based protrusion in *Ehrlichia*, *R. rickettsii* and *R. conorii* (56). The membrane-encased exit strategies help bacteria avoid host immune recognition that would normally trigger a lytic type of cell death,

and could promote the uptake by macrophage or phagocytic cells, and thus facilitate the spread of infection. Upon exit, membrane–bound *Orientia* in the extracellular phase are able to infect cells and this could promote systemic dissemination during infection.

Based on the host-dependent life cycle of *O. tsutsugamushi* the growth of *Orientia* relies on the host cells to supply metabolism processes with ATP and intermediate molecules. *Orientia* cannot carry out energy metabolism when it lives outside of the host cell because *Orientia* lacks several key components involved in metabolic pathways, for example, the absence of functional pyruvate dehydrogenase for producing acetyl-CoA which is an essential coenzyme in several biosynthetic pathways, missing enzymes involved in the pentose phosphate pathway which is a key metabolite in the synthesis of nucleotides, and lack of many genes involved in amino acid metabolism i.e. lysine, histidine, tryptophan, tyrosine, and phenylalanine (54). Thus, the extracellular stage V was expected to be metabolically inactive. This was proven using clickable-methionine (HPG) labeling as a reporter of active protein synthesis in intracellular pathogens (190). The HPG probe never labeled the extracellular bacteria. This confirms that extracellular *Orientia* is metabolically inactive. It is important to note that both intracellular and extracellular populations are mainly distinguished by the metabolic activity using a clickable-methionine probe (HPG) and the active protein synthesis is detected by imaged-based analysis. This method is fast, non-toxic, and sensitive. However, it cannot detect the extracellular populations which present low metabolic activity. Additionally, the antibodies (anti-TSA56, anti-human) and RNA-FISH (16srRNA) probe were used in this study to represent the whole population of *Orientia*. However, these antibodies and the RNA-FISH probe were not able to label all subpopulations of bacteria. Therefore, the antibodies and probe against specific proteins in *Orientia* are required further validation to represent the whole *Orientia* population.

The extracellular stage V could be equivalent to the stationary phase in free-living bacteria. Upon exit, extracellular bacteria have to cope with stress conditions such as nutrient limitation, pH, and osmolality imbalances by altering cell membranes, changing cell morphology, and activation of stringent response mechanisms to survive. When *Orientia* enters into stage V, the cell membrane of extracellular bacteria is highly cross-linked. This corresponds to proteomics

profiles that show TSA56 is enriched in the extracellular stage. TSA56 is the major surface protein of *O. tsutsugamushi* harboring three cysteine residues and forms disulfide crosslink networks (98). By microscopy, the intensity of TSA56 labeling in extracellular bacteria is always brighter than intracellular populations. In addition, the membrane-integrated dsbB proteins are found in extracellular bacteria. DsbB functions by cooperation with ubiquinone and dsbA to generate disulfide bonds which impact protein folding in the periplasmic space (308). This could suggest that *O. tsutsugamushi* regulates disulfide bond formation of surface or periplasmic proteins.

The morphology of *Orientia* bacteria becomes smaller and round (coccoid form) after exit. The reduction in cell size upon entry to the stationary phase can be explained as a result of two distinct processes; reductive division and dwarfing. DNA replication and cell division are initiated at the same time during the transition to the stationary phase. Due to a lack of nutrients at the stationary phase, bacteria cannot divide but the DNA synthesis is continued because of the previous initiation of DNA replication. Bacterial cells may consist of two or even more than two chromosomes. Unlike reductive division, in the dwarfing process there is a steady reduction of the cell size via degradation of cellular components such as a cytoplasmic membrane or cell wall. This process occurs after the completion of the reductive division and is activated by starvation (309, 310). Morphological alteration in extracellular *Orientia* (stage V) may progress through either reductive division or dwarfing mechanisms.

When bacteria enter the stationary phase, the cells have to regulate the transcription process through either activation of the genes required for survival or suppression of unnecessary genes. In *E. coli*, around 20% of genes are found to be highly expressed in the stationary phase, for instance, DNA repair, glycogen synthesis, heat-resistance, osmotic tolerance, etc. (215). The mechanism of regulating the expression of extracellular-stage genes is unknown. Stage V *O. tsutsugamushi* may activate the stress response mechanisms via a group of genes related to stringent response and dormancy (SpoT, RpoH, and obgE) which were enriched in extracellular populations. These genes have been found to upregulate at the stationary phase in *E. coli* and *S. typhimurium* (282, 283, 311). *Orientia* encodes two main sigma factors, RpoD and RpoH. The role of RpoH/heat shock-type σ factors is to maintain protein-folding homeostasis under high

temperature, functioning as a starvation sigma factor that regulates the response from stress during the stationary phase (215, 312, 313). This suggests that RpoH may regulate the gene expression of extracellular stage bacteria. At the translation level, the ribosomal assembly may be regulated by ObgE which prevents the association of 50S and 30S subunits to form 70S ribosome, resulting in blocking of the translation process. ObgE also has GTPase activity and is inhibited by (p)ppGpp to prevent correcting ribosome maturation during starvation (284). In addition, ribosomal proteins (rmpA; 50S ribosomal protein L27, RplX; 50S ribosomal protein L24 and RbfA; ribosome-binding factor) are present in extracellular fractions. These proteins may play a role in ribosomal inactivation and reactivation during dormancy.

Genes involved in changing the DNA structure, YbaB/EbfC, are enriched in the extracellular fraction. EbfC is a DNA-binding protein. It can form a homodimer or higher structures such as tetramers and octamers with DNA called nucleoprotein complex resulting in the condensation of the nucleoid (286). This protein has similar functions in DNA compaction to protect DNA from damage during the stationary phase (309). Likewise, *Orientia* may control the nucleoid condensation through the EbfC gene for DNA protection and regulation of gene expression.

ScaC plays a role in adhesion and entry (98), and is upregulated in extracellular fraction. ScaC is an important gene in the extracellular stage and exhibits as a marker gene during the maturation stage. It was selectively expressed on surface-residing bacteria during the transition from stage IV (maturation stage) to stage V (extracellular stage), though the role of ScaC in budding out of host cells is unknown. The mechanism that triggers the activation of transition into stage IV and V is unknown. Starvation conditions could trigger the essential genes through RpoH regulator. The other genes that could be alternative markers of the maturation stage are TSA47 and TSA22. These genes encode major outer membrane proteins and also present differential expression among the subpopulations. In addition, Tpr8 could be an ideal marker protein for the maturation stage due to high expression in the extracellular fraction.

In the proteomic profiles, peptidoglycan related genes (MurC, MurE) are abundant in the extracellular fraction and the qPCR results illustrated that peptidoglycan biosynthesis genes are upregulated during early infection. This suggests that cell wall synthesis is an important process in the early stage of intracellular growth. Tetratricopeptide (TPR)-repeat proteins (TPR-3 and TPR-

8) were enriched in the extracellular stage. TPR forms a scaffold on which other proteins may assemble. TPR-containing proteins are involved in several cellular functions, for instance, cell cycle control, transcription, protein folding, and protein transport (314). It has been shown that *O. tsutsugamushi* encodes TPR proteins and may interfere with host cell metabolism through DDx3 RNA helicase after secretion into the host cytosol (60, 315). Given the presence of TPR proteins in extracellular bacteria, TPR might play a role in host-pathogen interaction in the early stage of infection. A group of genes related to energy metabolism (*nuoA, nuoD, idh*) and lipid metabolism (*fabI*) are upregulated in the extracellular fraction. This indicates that the extracellular bacteria activate metabolic related genes to facilitate infectivity when entering into new host cells.

Another important protein that is enriched in the intracellular fraction is Ank (Ankyrin-repeat)-containing proteins (Ank1, Ank13). This protein is present in multiple copies in the genome of *O. tsutsugamushi* (60) and has been shown to be exported as an effector protein into host cells through the type IV secretion system in intracellular pathogens (293-296). It is possible that Ank-containing proteins in intracellular bacteria play an important role as a virulence factor acting against host defense mechanisms during the infection cycle.

The proteomic profile of some subpopulations might not be presented in this study, particulary bacteria which are located at the surface of the host cells and attached to membranes deu to the limitation of the purification processes. Those bacteria might have been pelleted with host cell debris after the lysis step and lost.

The intracellular bacteria can be divided into four different stages (I-IV) based on metabolic activity and DNA synthesis. Stages II-IV represent the metabolically active bacteria and stages III-IV represent bacteria that undergo DNA replication. Several genes involved in protein synthesis, energy metabolism, and lipid metabolism are upregulated in intracellular bacteria. At this stage, the transcriptional and translational processes are activated during the active growth of bacterial cells. As *Orientia* exits the endosome into the host cytosol, it experiences a rapid change from an oxidizing to a reducing environment in the host cytosol. This study found that the metabolic activity of *Orientia* significantly diminishes when the degree of reducing environment is

decreased due to the inhibition of host glutathione (GSH) pools via BSO. Therefore, the reducing environment in the host cytoplasm triggers the activation of metabolic activity after entry into host cells. This host-derived GSH mechanism has been shown to trigger virulence factor and metabolic adaptation in other intracellular pathogens such as *Listeria monocytogenes* and *Burkholderia pseudomallei* (306, 316). Other possible factors that could trigger *Orientia* activation are redox stress and pH level. To understand the complex interaction between the host microenvironment and bacteria, future research in this area is needed.

Orientia is generally described as having a coccobacillus shape with size 1-2 µM, however, this study shows that the morphology of intracellular bacteria (Stage II-IV) changes over time with considerable variation. *Orientia* presents as a coccoid bacterium and becomes elongated with a length up to 5 µM during active growth. Multiple septa were not found in elongated bacteria, suggesting that bacteria could grow continuously without cell division, though the number of nucleoids in one cell has never been measured. The morphology of *Orientia* does not change when grown in different cell lines (L929 and Ptk2). The mechanism of elongation in *O. tsutsugamushi* is unknown. In *Rickettsia* spp., *R. felis* has been found to exhibit a 'long-form' when propagated in a tick-derived cell line, and filamentous forms have been reported in *R. prowazekii* (75, 317). Given that nutrient availability, cell density, and host cell types may contribute to a long-form in *Rickettsia* spp., the elongation seen in *Orientia* might result from unfavorable environmental conditions such as limited nutrients or a change of pH rather than a distinct stage in the developmental cycle. The high infectivity of long-form *R. felis* promotes the entry into host cells and long-form bacteria are more stable than short-form. This suggests that the variation of cell morphology may contribute differently to virulence and invasion. Likewise, the elongated *Orientia* in this study becomes rod-shaped rather than round-shaped. The elongated shape of rod-bacterium may promote adherence during infection, while a small and round shape may allow for a better escape from the complement, a component of the host immune system, and allows bacteria to form a packed colony in a restricted host cell volume. In addition, a low amount of peptidoglycan-like structure in the surface membrane of elongated cells may help to avoid host immune recognition by immune system elements such as NOD1, a receptor of the innate immune system that senses fragments of bacterial peptidoglycan (105). However, the

distribution of peptidoglycan along the length of elongated cells is unknown. *Orientia* aggregates commonly form near the nucleus during binary fission. One study has proposed that *Orientia* secretes the polysaccharide polymer which promotes aggregation along with bacterial microcolony (157). In this work, the super-resolution imaging techniques (SIM and STORM) were used for studying bacterial shape and morphology. However, the aggregated bacteria are difficult to measure and quantify precisely by SIM and STORM.

Both extracellular and intracellular stages of *Orientia tsutsugamushi* are infectious. This feature is different from the biphasic life cycle of *Anaplasma spp*., *Ehrlichia spp*. and others which present infectious extracellular and noninfectious intracellular stages. *Orientia* exhibits broad cellular tropism in which bacteria can infect several cell types, such as endothelial cells, macrophages, dendritic cells, and cardiac myocytes, and leads to multiple organs being affected during a disseminated infection (9). The infectious extracellular stage in *O. tsutsugamushi* may promote systematic dissemination during infection, though, the mechanisms of dissemination to cause systemic infection is unknown. In common with most intracellular life cycles, the intracellular pathogen is thought to infect the cell, replicate, re-enter the extracellular space and repeat the process. However, re-entering extracellular space risks exposure of the bacteria to host immune systems (i.e. antibodies, complement) and other factors that inhibit bacterial growth or block entry into new cells. To avoid this risk, intracellular pathogens prefer to transfer directly from infected cells to uninfected cells (318). Many intracellular bacterial pathogens, for example, *Listeria monocytogenes*, *Shigella flexneri*, and *Rickettsia* spp,. are known to transfer directly from cell to cell through an actin-based motility (ABM) process (319). Intracellular *Orientia* may also spread through a cell to cell transfer mechanism. Intracellular stage bacteria may mediate local disseminated infection via cell to cell transfer mechanism, and the infectiousness of extracellular stage bacteria may mediate systemic dissemination.

Chapter 7: Developing genetic tools for *O. tsutsugamushi.*

In this study a transposon-based vector (pCis-mRuby2-MurAHimar) was introduced into *O. tsutsugamushi* via electrotransformation. To improve the transformation efficiency, this vector was modified from pCis-mCherrySS-Himar, which has been successfully used in *Anaplasma phagocytophilum* (223), by replacing the promoters for antibiotic selection and fluorescent protein expression with a strong *Orientia tsutsugamushi* promoter. The vector "pCis-mRuby2-MurA-Himar" only requires the expression of the Himar I transposase without additional host factors and encodes integrated elements containing the Himar repeated cassette, a fluorescent protein (mRuby2) and MurA (fosfomycin resistant gene). The integrated elements are driven by the strong promoter "Eftu", a translation elongation factor which constantly expresses in *O. tsutsugamushi* (63). The transposon vector is expected to generate a single-insertion mutant in the *Orientia* chromosome.

7.1 Introducing transposon-based vector into *O. tsutsugamushi*

7.1.1 Optimizing the electroporation and other related conditions of *O. tsutsugamushi*

To find the optimal sucrose concentrations for the preparation of electrocompetent cells, purified bacteria were resuspended in different sucrose concentrations (Fig. 31A). The bacterial growth was monitored for seven days post infection by qPCR using the TSA47 gene. The optimal sucrose concentration range that does not affect *Orientia* growth is 200 mM to 300 mM. Using a high sucrose concentration (500 mM) reduces bacteria growth compared with the control. In this study, sucrose 300 mM was used for all transformation experiments.

Voltage and number of pulses are important factors for plasmid uptake during electroporation. The voltage generates a membrane potential which causes reversible cellular membrane breakdown which results in "pore formation" in cellular membranes, and these pores allow small molecules, i.e. DNA, RNA, protein, plasmid, to enter the cells (320). To measure plasmid uptake into the cells, *Orientia* was electroporated with two voltages (1.2 kV and 2 kV) and the plasmid uptake level was measured by qPCR (Fig. 31B). Use of a 2 kV voltage was associated with higher plasmid uptake than using 1.2 kV. At 2kV, multiple pulses improved

plasmid uptake around 20 fold compared with a single pulse. Because applying multiple pulses gradually increases cell membrane permeability and the cell membrane is less damaged, this allows small DNA molecules to pass through the membrane easily. However, using high voltage with multiple pulses is still harmful to cells, potentially leading to cell death. Thus, using a low voltage (1.2 kV) with multiple pulses is the optimal condition in this experiment to achieve the maximum transfection efficiency (Fig. 31C).

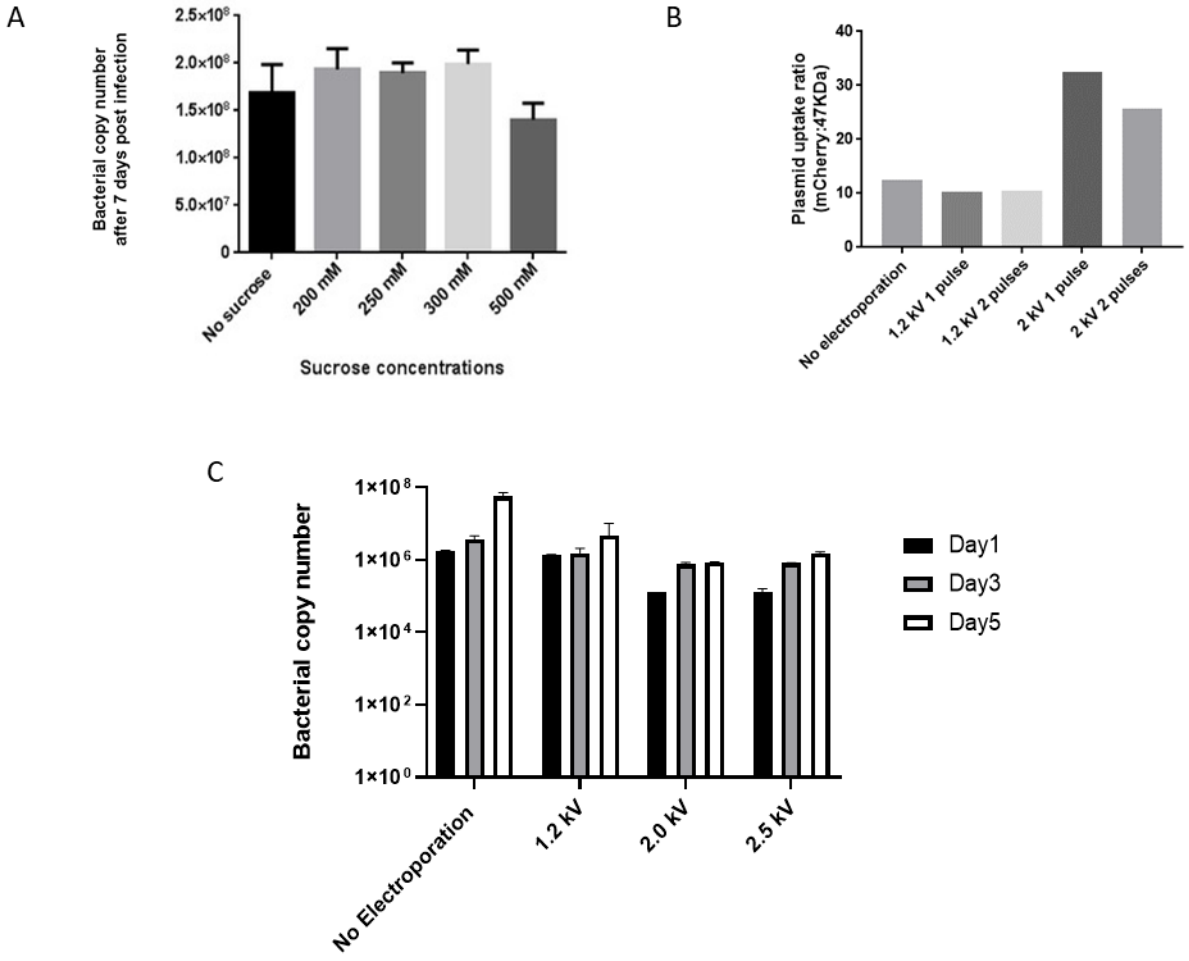

Figure 31. (A) Optimizing sucrose to affect *Orientia* growth seven days post infection. Bacteria level was determined by qPCR using the TSA47 gene. (B) Plasmid uptake ratio between fluorescence gene and TSA47 gene. (C) Measuring the voltage to affect bacterial growth (1, 3, 5 days post infection).

7.1.2 Optimizing antibiotic selection of *O. tsutsugamushi*

The MIC (Minimum Inhibitory Concentration) of fosfomycin was optimized to find the concentration that could inhibit the growth of *Orientia* wild type strain. Bacteria were incubated with antibiotics for seven days and the growth was measured by qPCR. The results (Fig. 32A) showed that fosfomycin 40 µg/ml inhibits *Orientia* growth as the MIC of fosfomycin is approximately equal to the MIC of chloramphenicol, the first drug used to treat scrub typhus in patients. However, the MIC cannot inhibit the bacterial population to the minimum baseline (zero copies). It was decided to increase the fosfomycin concentration to about 10-fold of MIC to enhance the selection of the transformants. The day after electroporation, fosfomycin was added to transformant and was left for seven days. Bacteria were harvested to check the bacterial level and the fluorescence marker gene (mRuby) by qPCR. The result showed that no positive transformants were obtained in these experiments (Fig. 32B). This could be because the antibiotics (fosfomycin) chosen were not strong enough to suppress wild type growth.

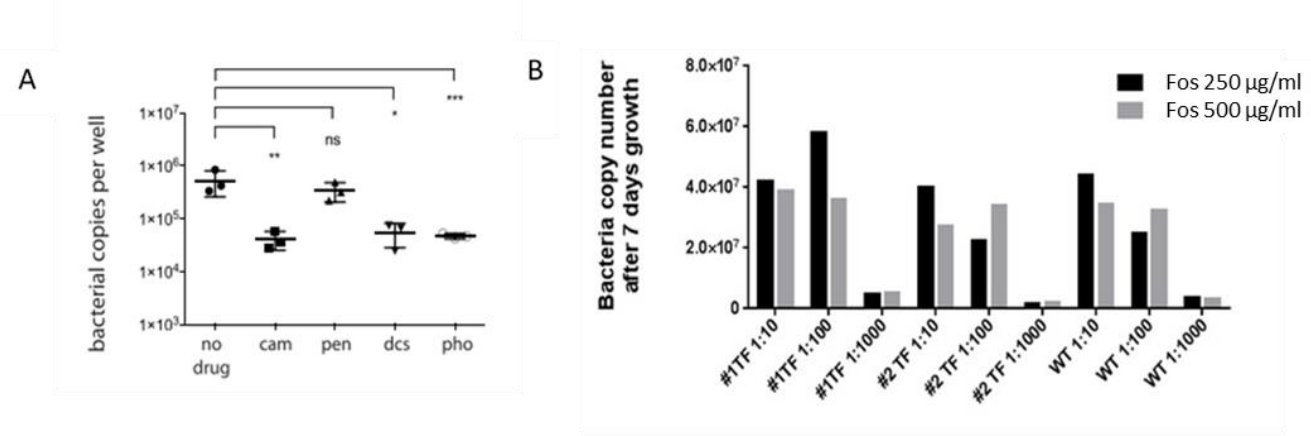

Figure 32. (A) Bacterial copy number after seven days growth in the presence of different drugs. cam = Chloramphenicol, dsc = D-cycloserine, fos = fosfomycin, pen = Penicillin. (B) Transformant was measured by qPCR of TSA47 gene to see the inhibition after treatment with fosfomycin.

7.2 Bridge nucleic acid (BNA) technology

Since the transformation approach failed to manipulate the *Orientia* genome, BNA technology was chosen for downregulation of specific genes in *O. tsutsugamushi* due to its high efficiency in knocking-down the targeted genes. In this study, 2',4'-BNA^{NC} (Fig.8) was designed to target TSA56, a major surface protein in *Orientia*, and BNA was expected to reduce the protein expression of TSA56, resulting in reduced infection of host cells. The BNA oligomer was synthesized by Bio Synthesis (Lewisville, TX). The oligomer was designed complementary to the DNA region of the *tsa56* gene which is approximately 300 bp from the start codon and conjugated with cell-penetrating peptide or carrier peptide (CPP, KFFKFFKFFK) to increase uptake of BNA through both host and bacterial membrane (321).

The specificity of BNA was determined *in vitro* using a PCR inhibition assay. The BNA concentration was varied before adding to the PCR reaction, which contained *Orientia* gDNA (0.125 ng), 56kDa primers (10 µM) that flanking BNA region, and 1x of Taq master mix (Qiagen). The result (Fig. 33) showed that BNA at 25 µM completely inhibited the amplification of the *tsa56* gene as assessed by PCR. This means BNA has a high binding affinity to the *tsa56* gene and has the potential to inhibit transcription of TSA56 *in vivo*.

BNA was further studied to determine whether it specifically binds to mRNA and inhibits the transcription process. To prove transcription inhibition, BNA was added into RT-PCR reactions during cDNA synthesis and the reduction of cDNA product was observed by RT-PCR. The *tsa56* gene was amplified from the cDNA samples to determine the inhibition pattern. The results (Fig. 36) showed that there was no PCR product of *tsa56* gene in the presence of BNA. This suggested that BNA can also bind to mRNA of TSA56 gene and blocks the transcription process.

The BNA inhibition in *Orientia* was further determined in *vivo* using the electroporation technique. BNA 15 µM and BNA 50 µM were delivered into competent cells with voltage 1.2 kV, single pulse. Electroporated bacteria were incubated with host cells (L929) for three days. The expression of TSA56 was observed by western blot. The preliminary results (Fig. 34A) showed that BNA 15 µM reduced TSA56 expression compared with the control (No BNA/DNA), while

there was no reduction of TSA56 expression with a high concentration of BNA (50 μM). This may be due to self-complementary among BNA itself. The result from western blot (Fig.35B) suggests that BNA could bind to the DNA strand and/or mRNA resulting in inhibition of *tsa56* transcription or translation. However, the mechanism of BNA binding is still unclear and needs further investigation.

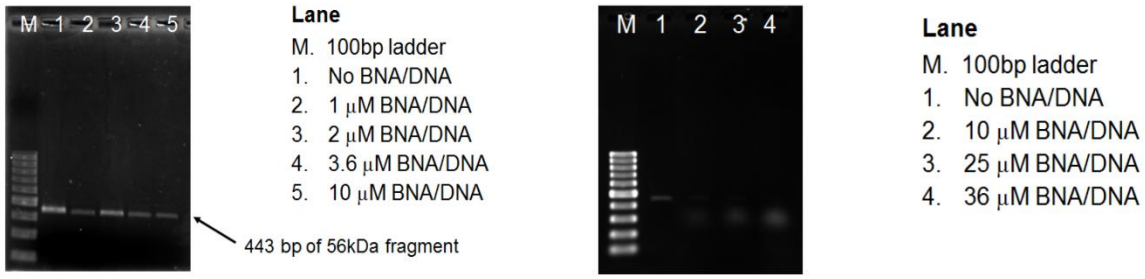

Figure 33. PCR inhibition by BNA. BNA was diluted to different concentrations prior adding into PCR reaction. The optimal Tm is 55°C with 35 amplification cycles. The PCR product size of targeted gene (*tsa56*) is 443 bp.

A

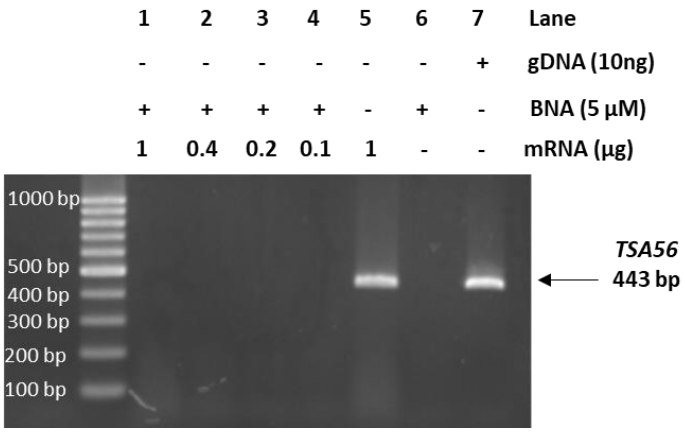

B

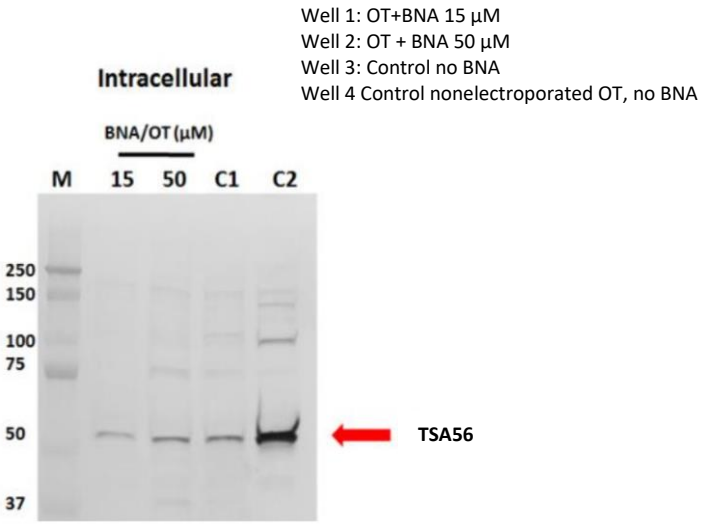

Figure 34. BNA inhibition assays. A. RT-PCR inhibition assay. BNA was added into the RT-PCR reaction in order to see whether BNA could bind to mRNA and inhibit cDNA synthesis. The *tsa56* gene was amplified from cDNA samples. B. Western blot *O. tsutsugamushi* in the presence of BNA, using a monoclonal antibody against TSA56 protein. The protein loading volume was normalized by qPCR of TSA47.

7.3 Discussion

The approaches to genetic manipulation for obligate intracellular bacteria are still limited compared to the number of methods that are available for free-living bacteria. Fortunately, the successful transformation via electroporation in many obligate intracellular bacteria (i.e. *Coxiella, Anaplasma*, and *Rickettsia*) has enabled genetic manipulation to be achieved and shown that it is possible within this class of organism (261, 322, 323). The HimarI transposon has been used in generating transformants expressing GFP and mcherry for studying host-pathogen interaction. For example, HimarI inactivated a novel virulence gene (*sca2*) in *Rickettsia rickettsii* (260), and in *Rickettsia prowazekii* disrupted the *pld* gene associated with phagosomal escape, using transformation (324).

Using electrotransformation with a transposon-based vector (pCis-mRuby2-MurA-Himar) I was unable to successfully effect integration into the *Orientia tsutsugamushi* genome. Possible reasons why transformation was unsuccessful in *Orientia* include: (i) the *Orientia* genome contains many mobile genetic elements that may randomly insert gene/foreign DNA from its chromosome and reduce the stability of transformants. (ii) The efficiency of the transformant is low as *Orientia* requires long term propagation for one week. (iii) The antibiotics chosen were not strong enough to select transformants and could not suppress wild type growth. Therefore, transformants as a minority population cannot compete with the remaining wild type. This would be one reason for transformant loss during subculture selection. (iv) Lack of suitable plasmid for *Orientia*. Until now, there has been no plasmid/vector which has been used successfully for *Orientia* transformation. The inserted elements in the vector, such as strong promoters and fluorescent proteins, might need further development to see whether they are suitable for use with *Orientia* or not.

Another major barrier of transformation in *Orientia* is the delivery of plasmid into bacterial cells. This process is important to improve the efficiency of the transformants. In future work, the plasmid could be mixed with dendrimers or alternative molecules that facilitate the plasmids to penetrate into host cells and bacterial cells and subsequently allow the transforming plasmid to integrate into the bacterial genome.

BNA technology is a new tool for down-regulation of targeted genes. Preliminary results show that an appropriately designed BNA could bind to *Orientia* DNA and RNA, and inhibit the expression of TSA56 *in vitro* and *in vivo*. BNA could be used as an alternative tool for studying virulence and the intracellular life cycle of *Orientia.* BNA inhibition in *Orientia* has never been tested before. This is a challenging technique that still requires further optimization. In this first observation of BNA inhibition in *O. tsutsugamushi*, BNA has strong inhibition *in vitro* and mild inhibition *in vivo*. However, the inhibition pattern and mechanism *in vivo* requires more study and needs to be repeated to determine whether the inhibition occurred or not.

Chapter 8: Dual RNA-seq provides insight into the biology of the neglected intracellular human pathogen *O. tsutsugamushi*

The research in this chapter has been published in Nature Communications under the title of Dual RNA-seq of Orientia tsutsugamushi informs on host-pathogen interactions for this neglected intracellular human pathogen, Mika-Gospodorz B, Giengkam S, Westermann AJ, Wongsantichon J, Kion-Crosby W, Chuenklin S, et al. Nature Communications. 2020;11(1):1-14.

8.1 Growth of *Orientia tsutsugamushi* strain Karp and UT176

Two clinical isolates of *Orientia tsutsugamushi,* Karp, and UT176, were used in this study. Karp was taken from a patient in New Guinea in 1943 (325), and UT176 was taken from a patient in northern Thailand in 2004 (326). Based on whole-genome sequencing, UT176 is closely related to Karp, sharing *tsa56* sequence similarity of about 95% (327). HUVEC (human umbilical vein endothelial) cells were chosen because of the similarity of cell types related to early and advanced infection in human.

Since Karp and UT176 have never been propagated in HUVEC cells, growth curves of both strains were measured over the 7-day infection cycle by qPCR (Fig. 35). The growth curve showed that the doubling time of Karp (19 hours) is faster than UT176 (27 hours), suggesting that the growth rate of Karp is slightly faster than UT176. Based on the model of variation in virulence, a high growth rate of bacteria tends to increase host mortality (virulence)(328). This implies that the virulence of Karp may be higher than that of UT176.

Infection of both strains was further observed by confocal microscopy using metabolic probe (HPG) labeling (Fig. 36-37). The bacterial number increases over time and presents a heavy infection at 5-7 days post infection. To get enough RNA yield from the bacteria, the 5-day time point was chosen for RNA isolation, as a high bacterial load at this stage does not damage host cell integrity.

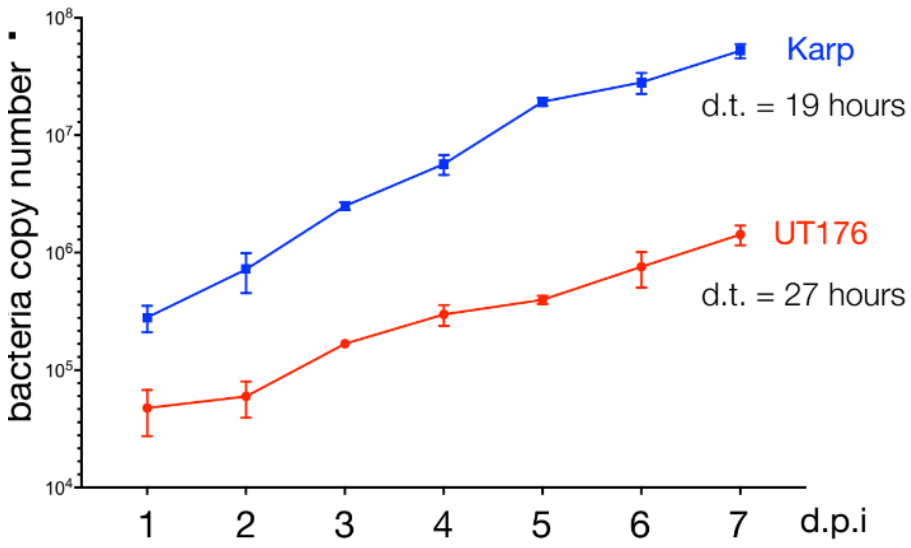

Figure 35. Growth curve showing replication of *Orientia* in HUVEC cells. Bacteria were grown in 24-well plates and the total bacterial copy number per well as measured by qPCR. Bacteria were added at a MOI of 8:1 (UT176) and 25:1 (Karp). Mean and SD from three independent replicates.

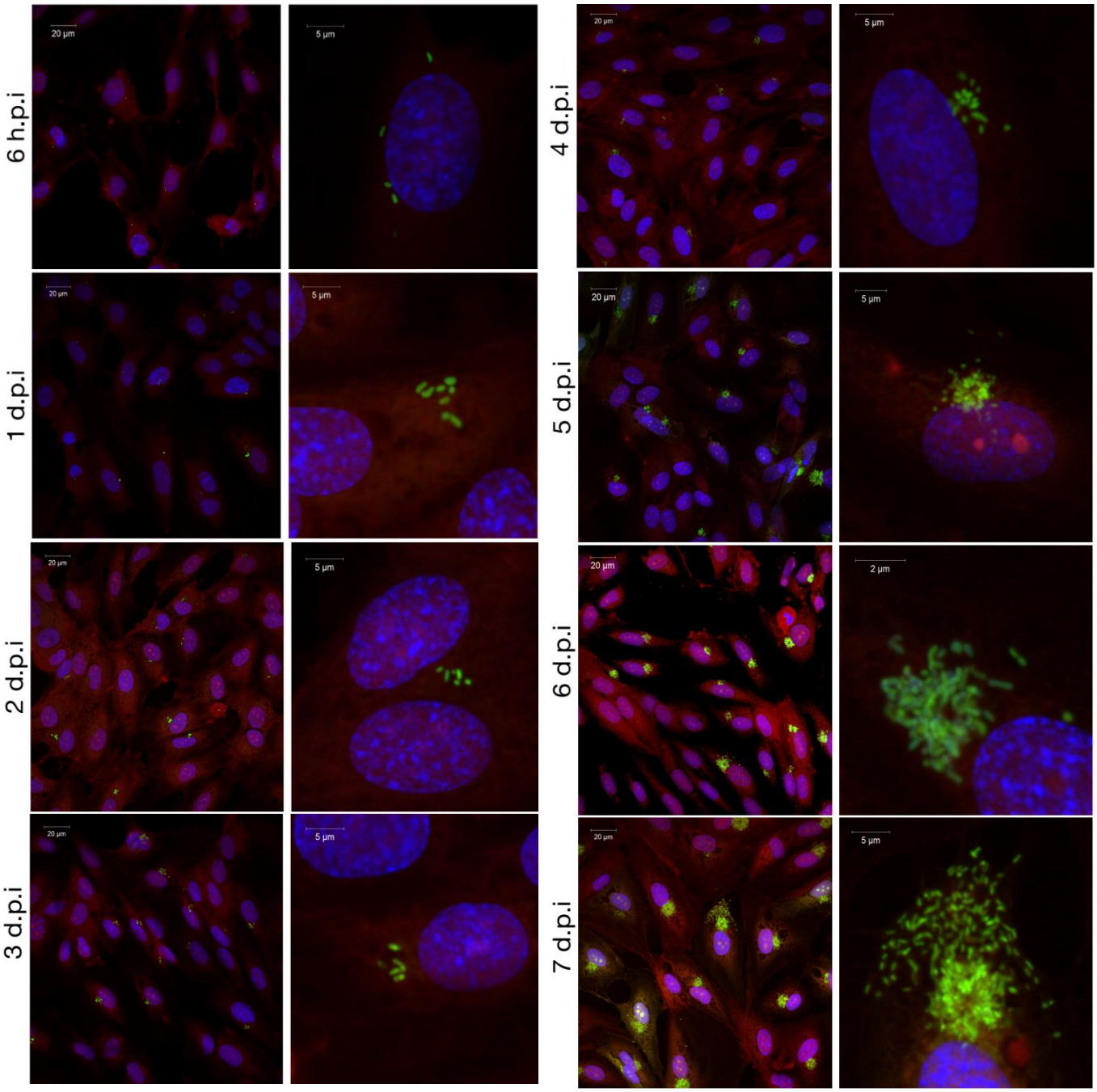

Figure 36. *O. tsutsugamushi* strain Karp time course. Confocal microscopy images of bacteria in HUVEC cells at 0-7 days post infection. The images are shown at each time point. Blue = DAPI (DNA), Red = Evans blue (host cells), green = *Orientia* labelled with Alexa488-click-methionine.

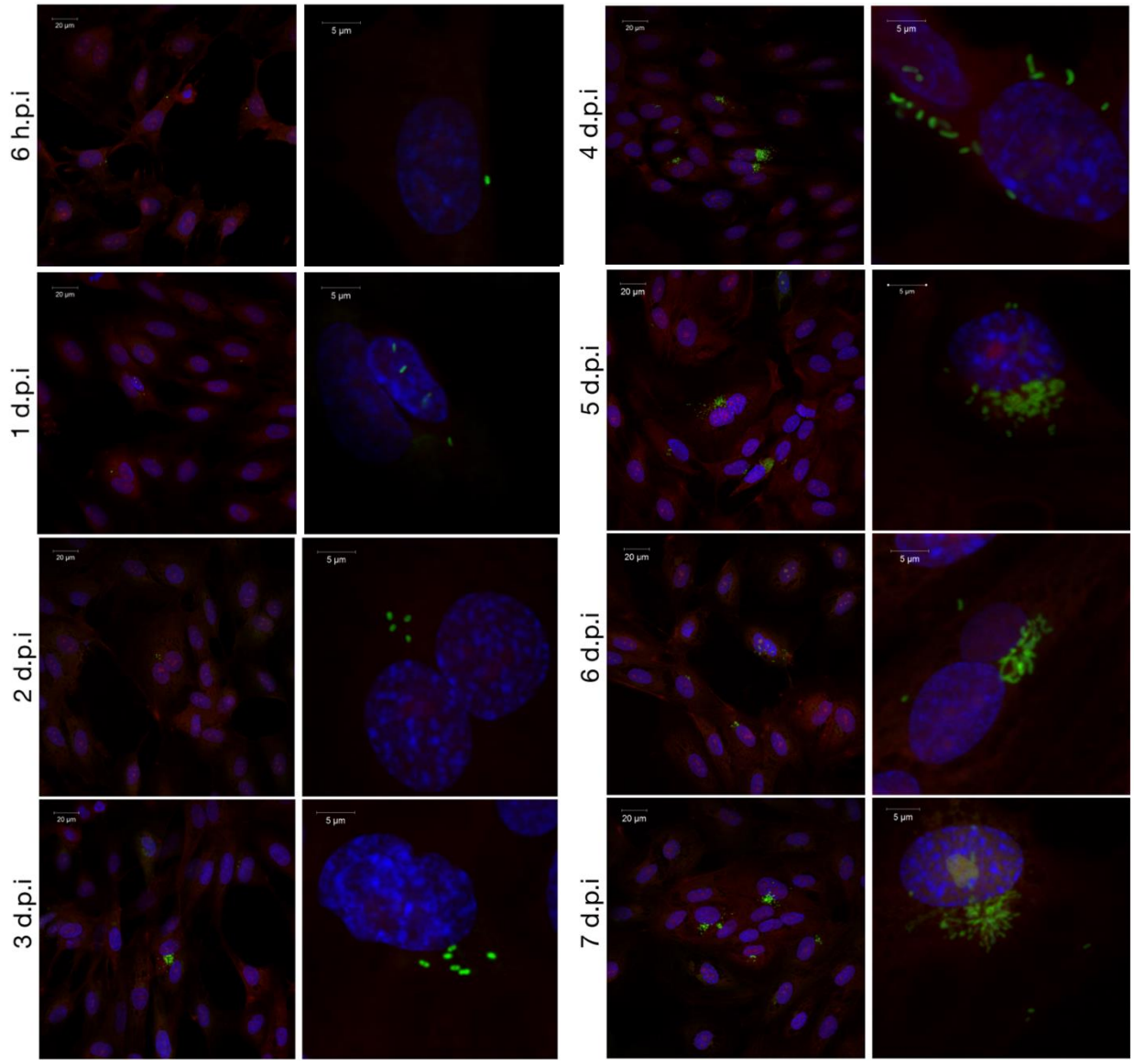

Figure 37. *O. tsutsugamushi* strain UT176 time course. Confocal microscopy images of bacteria in HUVEC cells at 0-7 days post infection. Two representative images are shown at each time point. Blue = DAPI (DNA), Red = Evans blue (host cells), green = *Orientia* labelled with Alexa488-click-methionine.

8.2 An overview of experiment and Dual RNA-seq outline

O. tsutsugamushi strains Karp and UT176 were propagated in human umbilical vein endothelial cells (HUVEC) for 5 days. Control uninfected HUVEC cells were grown in parallel. Five days post infection, total RNA was isolated followed by depletion of rRNA (ribosomal RNA). rRNA-free RNA was converted to cDNA and sequenced to approximately 35 million reads per library using Illumina technology (Fig. 38). Reads were mapped to the completed genomes of Karp, UT176, and the human genome, in parallel.

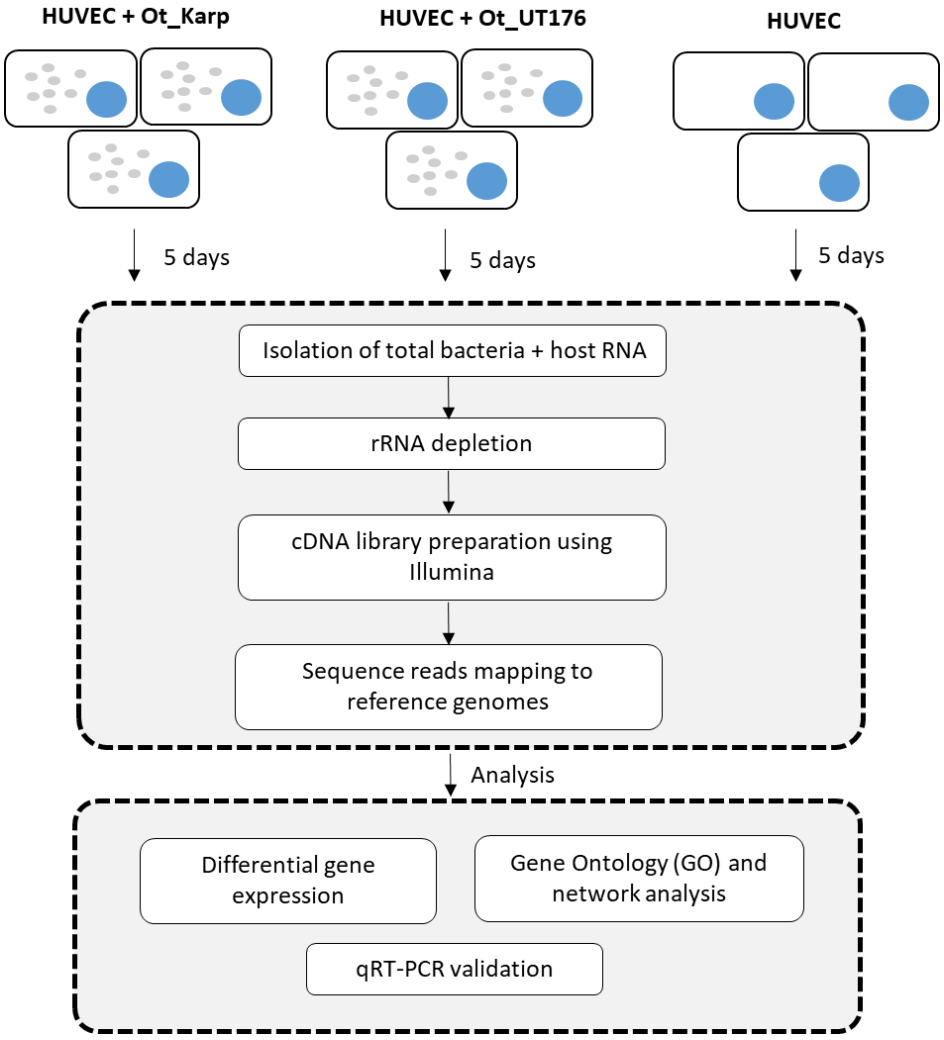

Figure 38. The experimental overview and analysis of dual RNA-seq data.

8.3 Dual RNA-seq of *Orientia tsutsugamushi* infecting endothelial cells

Bacterial reads of each condition were observed as shown in Fig. 39. HUVEC infected with Karp and HUVEC infected with UT176 exhibit bacterial reads as a percentage of total cDNA of about 17.1 – 17.5% and 2.8-4.9%, respectively. This may be due to differences in both cell entry and growth rate between Karp and UT176. Read mapping to coding sequences (CDSs) were abundant in both the HUVEC data and bacterial reads, which allows for the performance of differential expression analysis.

Dual RNA-seq also detects several non-coding RNA classes from both bacteria and host (Fig. 40). Although non-coding RNA (ncRNAs) are thought not to translate into proteins, they may have other functions (329). It has been demonstrated that ncRNAs are involved in internal signals that control the different levels of gene expression, transcription, RNA splicing, including chromosome segregation and stress responses (330-332). Generally, bacterial genomes encode several ncRNAs. The most conserved ncRNAs include abundant housekeeping ncRNAs, the RNA components of ribonuclease P (RNaseP), the signal recognition particle (SRP), and transfer-messenger RNA (tmRNA). Of those found in the Karp transcriptome data, tmRNA was shown to be expressed at unusually high levels, between 4.6% and 13% of total bacterial reads (Fig. 40). This suggests that tmRNA plays an essential role in *Orientia* survival in mammalian cells.

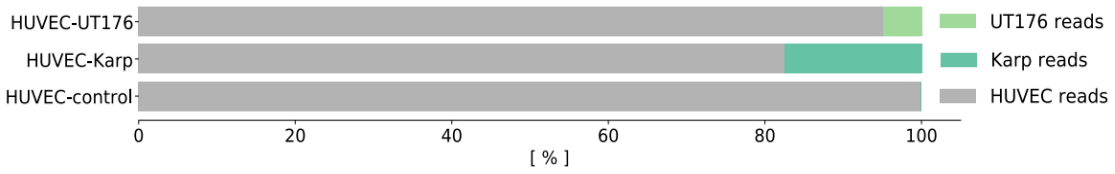

Figure 39. RNA mapping statistics showing the fraction of host and *Orientia* RNA for each condition. The mean of three independent experiments is shown.

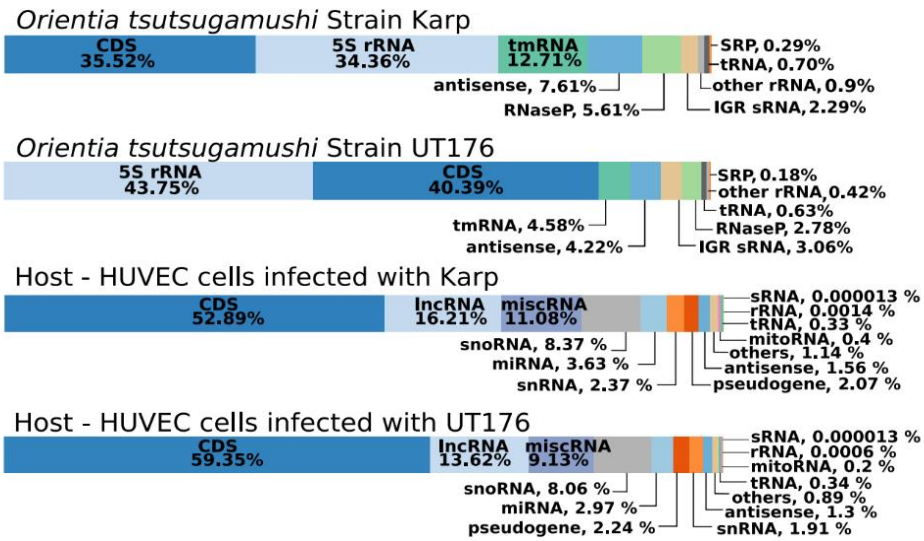

Figure 40. Percentage of RNA-seq reads assigned to different classes of RNA in Karp, UT176 and HUVEC.

8.4 Differential expression of genes in Karp and UT176

Orientia is a genetically intractable bacteria, leading to little information about its antigenic surface proteins and effectors. This is a major barrier to the study of virulence mechanisms in *Orientia*. As much of the diversity of the *Orientia* genome is a result of gene duplication, any differences in virulence between strains may be caused by differences in expression. To demonstrate this hypothesis, differential expression analysis of Karp and UT176 at five days post infection in HUVEC cells was performed. Pathway and gene ontology (GO) analyses of differentially expressed genes showed that most pathways were up-regulated in Karp compared with UT176, which is involved in DNA replication and metabolism (Fig. 41A). This data is consistent with the higher growth rate in Karp.

At the gene level, many surface proteins (TSA22, TSA56), autotransporter protein (ScaE), and effectors proteins (Anks) were differentially regulated between the two strains (Fig. 41B). LogFC of *ScaE*, *tsa56*, and *tsa22* in Karp over UT176 is 1.4, 3.08, and 3.86, respectively. Also, the *ScaD* level was increased in UT176 (0.99 logFC) compared with Karp. The different levels of expression of these surface proteins may affect the interaction with host cells through the

binding of host cell receptors (i.e., integrin, fibronectin), or activation of innate and adaptive immune receptors.

Based on recently published genome data, Karp and UT176 contain 33(Ank)/29(TPR), and 21(Ank)/22(TPR), respectively (60). Ank and TPR genes in Karp and UT176 were compared. The results showed that *ank2, ank3*, *ank12*, and two copies of *tpr8* were upregulated in UT176 with a log FC > 1.5, while *ank6, tpr1, tpr3,* and *tpr5* were upregulated in Karp with a log FC > 1.5. Anks are the key virulence factor in the intracellular pathogen, and some Anks function as effectors in eukaryotic cells (66, 333). However, many Anks are uncharacterized. When these *ank* genes ectopically express, the protein products of *ank* are localized to the endoplasmic reticulum or host cytoplasm (68). A recent report demonstrated that Ank6 blocks the accumulation of NFkB subunit (p65) in the nucleus and inhibits its transcriptional activation (334). The function of other differentially expressed Anks is unknown. Furthermore, Ank interacts directly with host proteins which may result in changing downstream mechanisms in the host response.

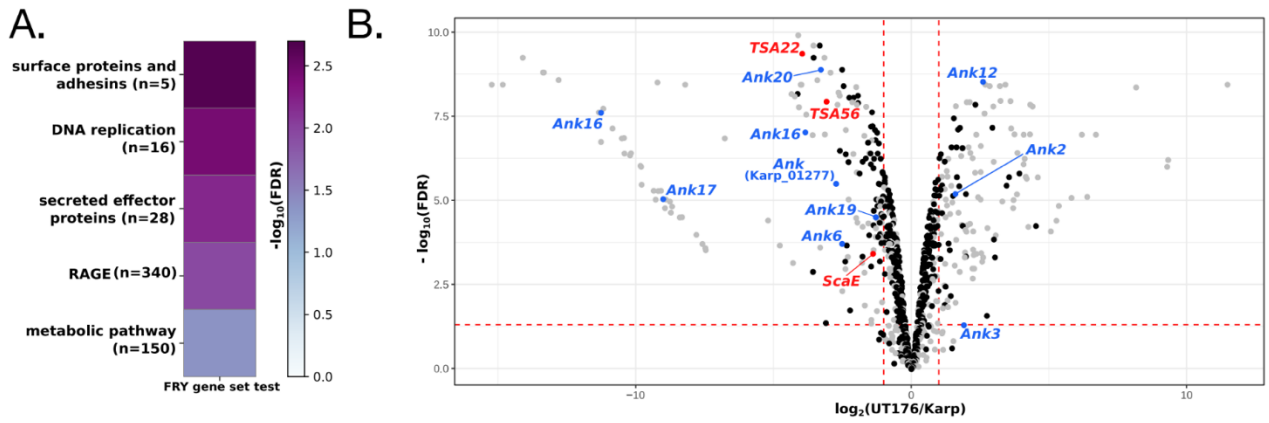

Figure 41. Differential bacterial expression. A. Heatmap demonstrating pathways enriched in differentially expressed genes. All illustrated groups are more highly expressed in Karp. B. Volcano plot representing differential expression of bacterial genes in Karp and UT176. Bacterial surface genes (red) and ankyrin repeat containing effector proteins (blue) with log fold change ≥1 are highlighted.

8.5 Differential host response to Karp and UT176

The inflammatory response activated by *Orientia* infection plays a key role in virulence during the infection. A network map of proinflammatory cytokines and chemokines in response to Karp and UT176 in HUVEC cells was produced (Fig. 42). Most of the genes involved in cytokine, chemokines, and cytokine receptors were differentially up-regulated in UT176 infection compared with Karp. UT176 strongly induced IL6-mediated proinflammatory response (Fig. 42A), while IL33 (Fig. 42B) was specifically up-regulated in Karp infection (5.1 logFC higher in Karp-infected HUVEC cells). IL33 has been shown to be involved in pathogenicity in a mouse model of *Orientia* infection using Karp strain (335). The mutant *IL33*$^{-/-}$ gene in mice presented less severe disease symptoms, while mice recombinant IL33 (rIL33) strikingly increased severity and mortality. The difference in the inflammatory response is likely to relate to bacterial virulence. The reduction of IL33 in low virulence UT176 strain could suggest that cytokine (IL33) are involved in the pathogenesis of scrub typhus.

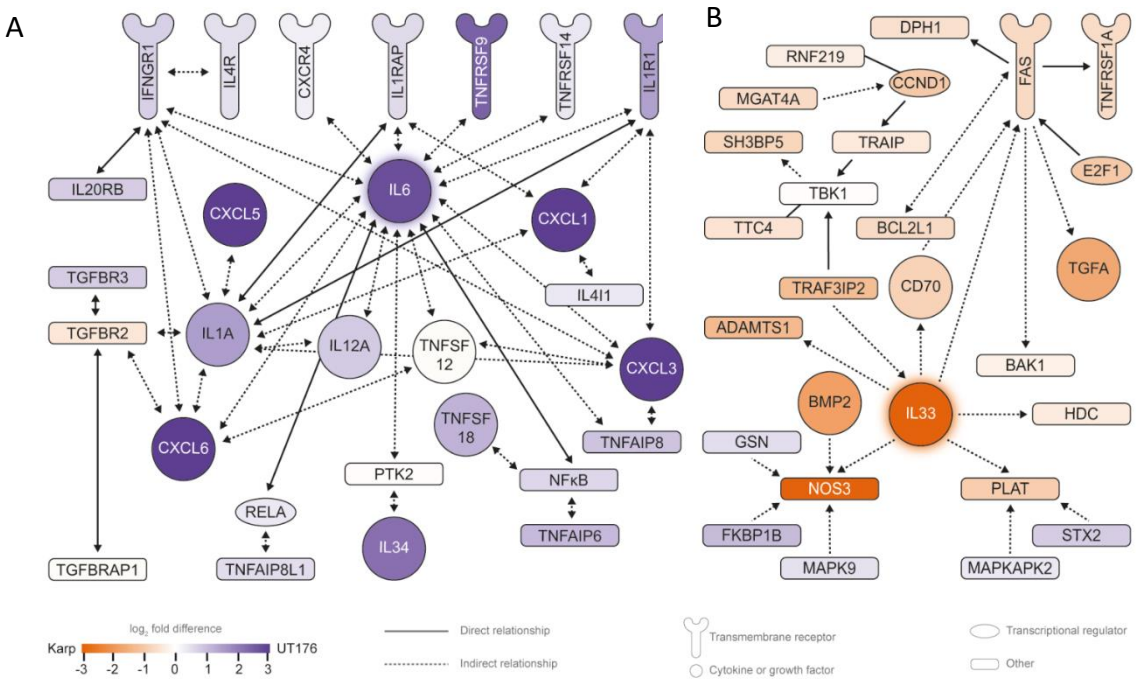

Figure 42. Karp and UT176 lead to up-regulation of distinct networks in HUVECs. A. Up-regulation of multiple proinflammatory chemokines and cytokines in HUVECs infected with UT176. B. Induction of the IL33-FAS-mediated anoikis network in Karp infected HUVEC cells.

8.6 Karp and UT176 are different in virulent in a mouse model

To investigate whether Karp and UT176 exhibit differences in virulence in a host, a mouse infection model of scrub typhus was used. Freshly isolated bacteria ($1.25x10^6$ copies) were intravenously inoculated into female C57BL/6NJcl mice (6-8 weeks, 8 mice per group) and the disease symptoms were monitored for 12 days before euthanasia. Karp-infected animals were found to have more severe clinical symptoms (Fig. 43B) and lower weight gain over 12 days (Fig. 43A) compared to UT176-infected mouse. This evidence suggests that Karp is more virulent than UT176 in a mouse infection model.

Bacteria were isolated from blood and tissue from lung, liver, spleen, and kidneys, and the bacterial load was measured by qPCR. The bacterial copies number in blood (Fig. 43C) and tissues (Fig. 43D) was strikingly higher in Karp-infected mice. The mouse tissues were stained by hematoxylin and eosin, and the tissue injury was subsequently carried out by histopathological scoring (Fig. 43E). Lesion scoring of Karp-infected mice was significantly more severe in lung, liver, spleen, and kidney than UT176-infected mice. The histology of airway and gas exchange areas (alveolus) of all infected mice was microscopically observed and in each group. The results (Fig. 43F) illustrated diffuse thickening of alveolar septa, and infiltration of macrophages and lymphocytes in both Karp- and UT176-infected mice, however, the severity of white blood cells infiltrate condition was more predominantly shown in Karp-infected mice. Even though the pathological injuries of tissues were only observed at a single time point (12 days), the differences of pathological profiles could suggest that the disease dynamics ae different between the two strains.

Together the virulence data from mouse and observations in HUVEC cells including the differential host response to Karp- and UT176-infected mice and specific adaptive immune response networks illustrate that Karp exhibited higher virulence than UT176.

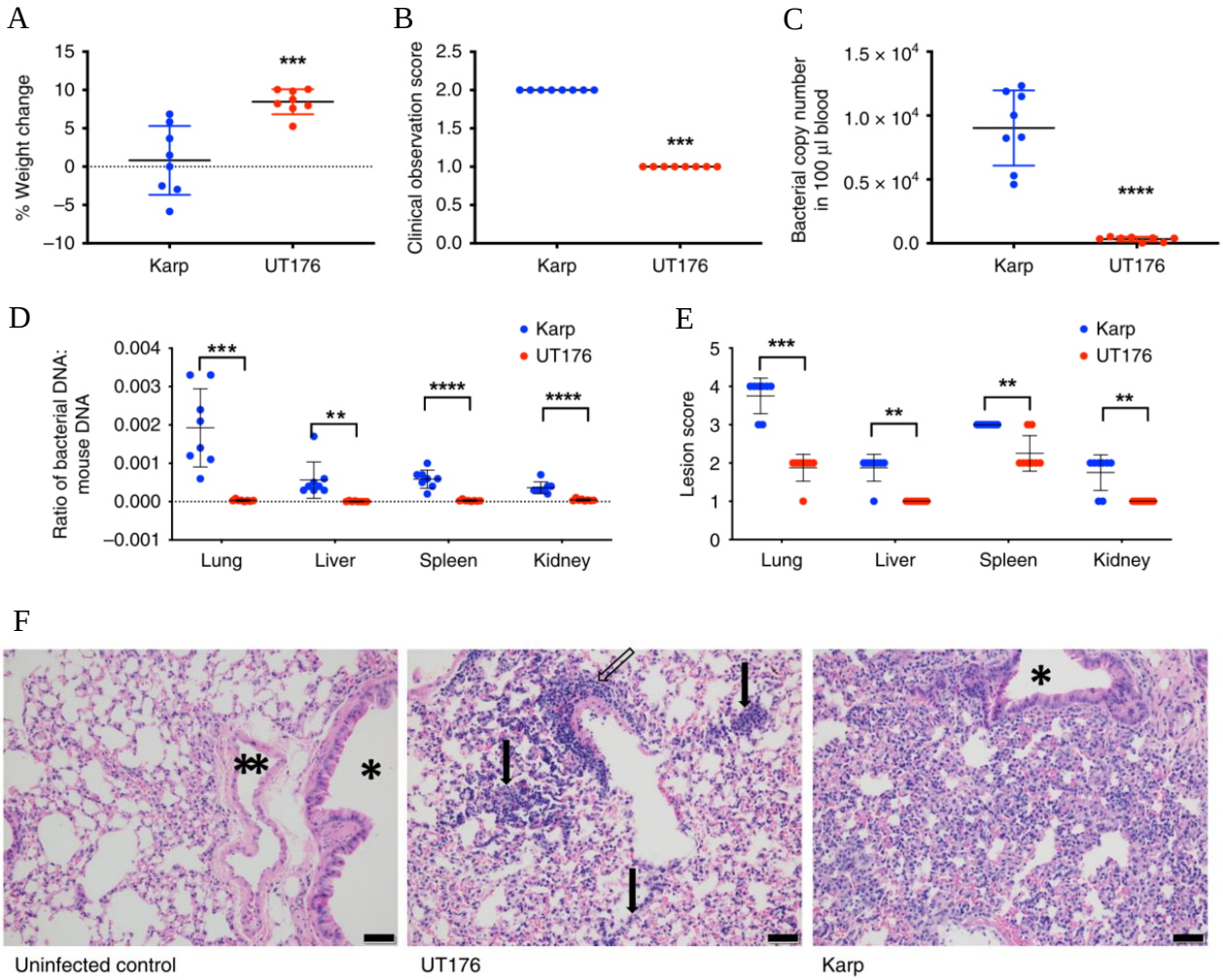

Figure 43. A mouse infection model showing that Karp is more virulent than UT176. A. Weight change over 12 days of infection. B. Clinical observation score of mice 12 days post infection. This number is a composite score based on appetite, activity, and hair coat with higher numbers representing low appetite, low activity, and ruffled fur. C Bacterial genome copy number in 100 µl blood taken from euthanized mice 12 days post infection, measured by qPCR. D. The ratio of bacterial genome copy number to mouse genome copy number in lung, liver, spleen, and kidney of euthanized mice 12 days post infection, measured by qPCR. E. Lesion scores of hematoxylin and eosin-stained lung, liver, spleen, and kidneys of euthanized mice 12 days post infection. Scores range from 0 to 5 with 0 representing normal tissue and 5 representing severe lesion

damage. All graphs show mean and standard deviation. Statistical significance is calculated using unpaired Student t-test in GraphPad Prism software. **p ≤ 0.01 ***p ≤ 0.001 ****p ≤ 0.0001. F. Images of hematoxylin and eosin-stained lung tissue of mice infected with buffer, UT176 or Karp. Scale bars = 50 µm. * indicates airway and ** indicates blood vessel. Uninfected control: airway, blood vessel, and alveoli all appear normal. UT176-infected lungs: there are diffuse thickening and infiltration of alveolar septa with a mixed population of macrophages and lymphocytes (arrows). There is also mild perivascular lymphohistiocytic inflammation (open arrow). Karp-infected lungs: there is diffuse moderate thickening and infiltration of alveolar septa with a mixed population of macrophages and lymphocytes. The airway (*) is unaffected and normal.

8.7 Discussion

The goal of the work in this chapter was to determine which bacterial and host genes are expressed during *Orientia tsutsugamushi* infection of cultured cells, to observe differences in gene expression between two different clinical isolates, and to determine the relative virulence of these isolates in a mouse infection model.

The genome size of *Orientia* is 1.9-2.5 Mbp, almost 50% of which consists of repetitive regions of more than 1,000 bp in length (60). The complexity of rearrangements in the *Orientia* genome creates genome instability which makes it difficult to study the transcriptional profile. Dual RNA-seq provided the transcriptomic profiles which included protein-coding genes and also ncRNAs, tmRNA, and operonic transcripts. tmRNA is known to be associated with the virulence in pathogens, for example, *ssrA* (known as tmRNA) contributes to the pathogenesis of *Salmonella Typhimurium* (336) and *Francisella tularensis* (337). These studies demonstrated that tmRNA is involved in the growth, resistance to stress conditions, and may affect the expression of virulence genes. Future work could determine the role of tmRNA and other ncRNA in *Orientia tsutsugamushi* infection.

The comparative genomics of *Orientia* reveals that the diversity in the *Orientia* genome arises from many gene duplications rather than the acquisition of new genes (70). This is likely to reflect the environmental niches associated with an obligate intracellular lifestyle. As a

consequence, strain-specific differences are likely to be associated with the relative gene expression rather than the absence or presence of virulence genes. Differential expression of genes in Karp and UT176 identified specific genes, especially Anks, TPR, and surface proteins that are associated with putative virulence differences between two strains.

The differential response of endothelial cells to Karp and UT176 demonstrated that the inflammatory response is a key driver of virulence during *Orientia* infection. The IL6-mediated proinflammatory response was strongly upregulated in UT176 whereas IL33 was induced in Karp. The stimulation of proinflammatory responses during Karp and UT176 infection has also been shown previously (118, 338, 339). It is important to note that this study cannot distinguish between the differential host responses to actively replicating bacteria and non-replicating bacteria.

Mouse model of *Orientia* infection was used in this study for understanding the pathogenesis correlating with human infections. The intraveneous inoculation was selected to inoculate bacteria in mice because the needle inoculation route is the most closely similar to the natural vector transmission. Even though natural chigger-bite infection would be ideal to monitor bacteria dissemination and host-pathogen interactions, the natural infection has several limitations, such as the limited access to infect *Leptotrombidium* mite, difficulty to maintain bacteria when they are outside host cells, and inability to control the dose of bacterial transmission (340). The infection of C57Bl/6 mice with *O. tsutsugamushi* Karp and UT176 strains results in sublethal disease which is supported by the evidence of weight loss and the presence of bacteria in target organs (lung, liver, spleen, and kidney) including, the clinical signs, bacterial load in blood, as well as the histopathologic events. Karp-infected mice significantly presented more severe symptoms and weight loss compared to UT176-infected mice. The lung inflammation was observed in all *Orientia*-infected mice, however, the accumulation of lymphocytes and macrophage including the thickening of alveolar septa were more presented in Karp-infected mice. The evidence in the mouse model indicated that Karp exhibited higher virulence than UT176.

Chapter 9: Overall conclusions and future directions

Characterization of *O. tsutsugamushi* subpopulations (extracellular and intracellular populations)

The first research question was to understand how *O. tsutsugamushi* differentiates into distinct subpopulations between intracellular and extracellular populations. Both populations were characterized by observing the different degrees of morphology, protein profiles, and infectivity. The results from confocal microscopy, SIM, and STORM imaging, demonstrated that the morphology of extracellular *Orientia* bacteria is small and round throughout the infection cycle. The shape of intracellular bacteria has more variation and presents as small and round at early infection and becomes elongated during days 1 - 7 post infection. The septum in elongated bacteria was not found. The elongation process may occur when the bacterial replication is initiated without dividing due to changing host environment conditions. *Orientia* forms large aggregates near the nucleus of host cells. Due to this biological reason, it is difficult to precisely measure the shape and size of individual bacteria in a pack-microcolony. Using the Shotgun proteomics, the protein profiles of both populations at the mid stage (day 3- day5) of infection were different but were similar to each other at the late stage. Similar to the protein profile, the infectivity is slightly different among both populations at mid stage but similar at the late stage of infection (day 6-day7).

O. tsutsugamushi differentiates into a specific maturation stage (extracellular stage)

The first key finding led to the second research question of how *O. tsutsugamushi* differentiates into a specific maturation stage (extracellular stage). A marker gene (*ScaC*) of the maturation stage was used to identify the transition-maturation stage of *Orientia*. By using fluorescent labelling, ScaC is only present in subpopulations that are located at the host membrane; bacteria which have just entered the cell and budding bacteria at the maturation stage. The labelling of bacteria by the ScaC antibody in this section should improve by colabelling anti-ScaC with the plasma membrane dye (CellMask). This will provide a clear image of bacteria at the surface of host cells.

***O. tsutsugamushi* becomes metabolically active shortly after entry into host cells**

The third research question focused on how *O. tsutsugamushi* senses the entry into the host cytoplasm. The findings illustrated that the extracellular bacteria are metabolically inactive and they start being active shortly after exiting the endosome. This process is regulated by the reducing environment of the host cytoplasm.

The findings in chapters 3-5 allow us to distinguish the stages of growth in intracellular bacteria. The differences in metabolic activity, replication, and infectivity drive the progression of cellular infection through five distinct stages during the 5-7 days infection cycle; stage I (Early entry), stage II (Pre-replicative), stage III (Replicative), stage IV (Maturation) and stage V (Extracellular)(figure 44).

The metabolic activity of intracellular and extracellular populations is based on their ability to incorporate a methionine derivative (HPG) into nascent proteins and subsequently measured by using click chemistry. In this work, the metabolically active bacteria were identified by the intensity of fluorescence of HPG. However, some subpopulations that present a low metabolic level will not be detected by this method.

Upon entry at 0-3 hours post infection, bacterial stage I has not yet undergone DNA and protein synthesis. Once bacteria are released from the endosome at 3-24 hours post infection (stage II), protein synthesis is active but DNA synthesis has not yet initiated. Bacteria move to the perinuclear region for replication (stage III) during 1-5 days post infection and start DNA and protein synthesis. In stage IV, the bacteria relocate from the perinuclear region to the host membrane, and become mature before exiting at 3-6 days post infection. ScaC, a marker for the maturation of intracellular bacteria, is present on the bacterial surface membrane at this stage. The mature bacteria (stage IV) is metabolically active but the status of DNA synthesis is still unknown. After exiting the host cell, the intracellular bacteria enters the extracellular stage (Stage V) when both DNA and protein synthesis are terminated.

The active DNA synthesis during stage IV needs to be examined further because of the following limitation of the methods used: the measurement of active DNA and RNA synthesis via

clickable DNA and RNA probes failed because *Orientia* may not uptake the synthetic DNA/RNA nucleotides; and the isolation of stage IV bacteria from the other stages is very difficult due to the short duration of the maturation stage and the issue of mixing of different subpopulations. The intracellular stages III-IV and extracellular stage V are infectious, but the infectivity of intracellular stage I and II are unknown because it is difficult to isolate bacteria during this short period of the infection.

In these research studies I describe bacterial differentiation in *O. tsutsugamushi,* leading to a greater understanding of the infection cycle and the regulation and mechanism of differentiation in scrub typhus. This new model system also provides us a fundamental understanding of bacterial development that could stimulate new therapeutic approaches to disease treatment.

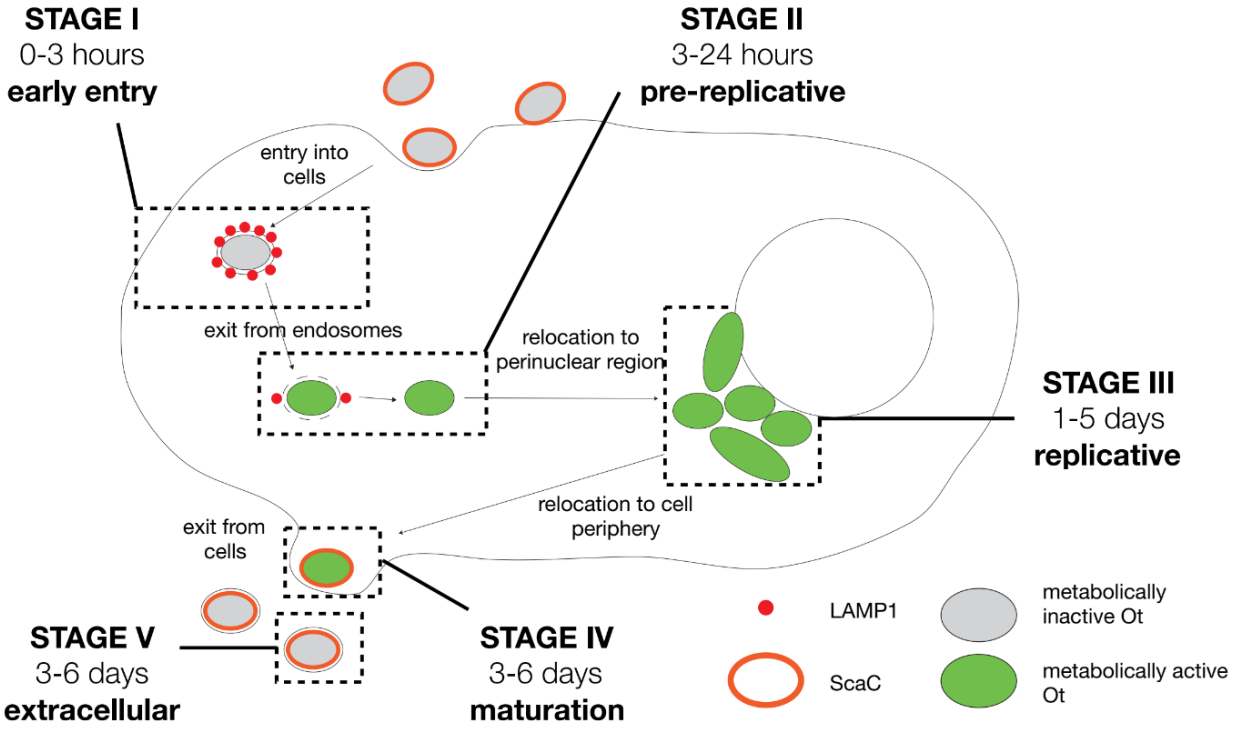

Stage	Name	Time	Protein synthesis?	DNA synthesis?	Location	Infectious?
I	Early entry	0-3 hours	NO	NO	intra	?
II	Pre-replicative	3-24 hours	YES	NO	intra	?
III	Replicative	1-5 days	YES	YES	intra	YES
IV	Maturation	3-6 days	YES	?	intra	
V	Extracellular	3-6 days	NO	NO	extra	YES

Figure 44. An overview of the distinct stages in the intracellular lifecycle of *O. tsutsugamushi*.

Summary of studies to develop genetic tools in *O. tsutsugamushi*

The modified transposon-based transformation vector (pCis-mRuby2-MurA-HimarI) was used for attempted molecular manipulation of *Orientia tsutsugamushi*. Electroporation was used to introduce the vector into *O. tsutsugamushi*. However, the transposon and transposase did not successfully integrate into the genome. There were several limitations that need further development such as low transformation efficiencies, appropriateness of the vector, optimisation of antibiotic selection, isolation of null mutants, etc.

Given that transformation failed, use of BNA (bridge nucleic acid), a DNA analog, was chosen as an alternative approach to disrupt the target gene of *Orientia tsutsugamushi*. This study aimed to downregulate the major surface protein TSA56 in *Orientia.* BNA efficiently bound both targeted DNA and RNA as assessed by PCR. BNA was introduced into *Orientia* via electroporation and the immunoblot result demonstrated strong inhibition of DNA.

Dual RNA-seq provides insight into the biology of the neglected intracellular human pathogen *Orientia tsutsugamushi*.

Dual RNA-seq is a novel approach for studying the mechanism of gene regulation of the genetically intractable bacteria *Orientia tsutsugamushi*, during infection in cultured human endothelial cells. RNA-seq data from infection using two clinical isolates infection, Karp and UT176, in HUVEC cells provided evidence of the transcriptional architecture, gene expression, and the discovery of distinct immune response networks in response to the infection in HUVEC cells. The relative induction of cytokine IL6 and IL33 based on gene networks in the host might predict relative virulence and this correlates with our findings in a mouse infection model.

Future directions

The finding that during infection *Orientia* exists in five distinct subpopulations leads to several further questions about the infection mechanisms deployed by each stage. Much is still unknown and remains to be elucidated. How does *Orientia* escape from the phagosome? What are the unknown mechanisms that trigger the relocation of *Orientia* from the perinuclear region to adjacent to the host membrane? Which pathway controls the expression of ScaC, a marker for the maturation stage, during intracellular stages? What is the difference in the infection mechanism between intracellular and extracellular stages? Do intracellular bacteria infect the next cell without budding out and by what mechanisms and does intracellular bacteria become inactive or remain active when invading the next cells? How stable are host membranes in membrane-bound budding bacteria? Does membrane-bound *Orientia* re-infect the same host cells or prefer to infect new uninfected cells? If the membrane-bound *Orientia* enters into new cells, what mechanisms trigger the lysis from the endosome? How do bacteria regulate the progression between the stages? *Orientia* can replicate in several cell types and present a different level of pathogenicity in human and animal models; how might the behavior of the different bacterial stages differ by bacterial strain and host cell types? Lastly, is the timing of distinct bacterial stages important to differences in virulence? All these questions could facilitate future work with *Orientia* to elucidate disease mechanisms and contribute a better understanding of important aspects of host-pathogen interaction.

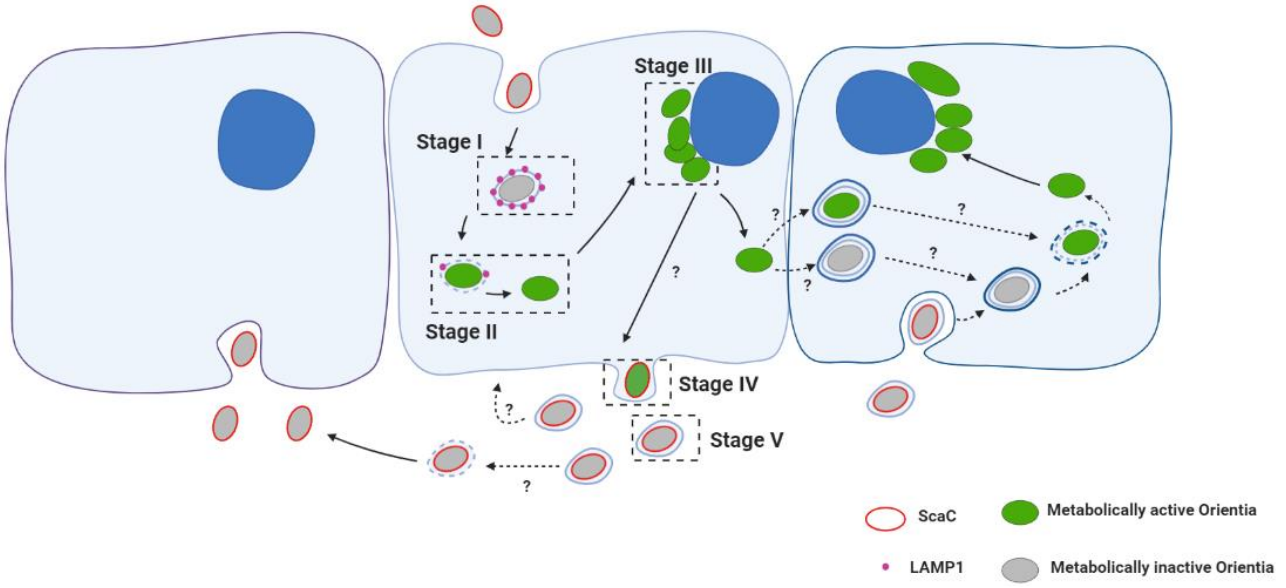

Figure 45 A summary of unknown mechanisms in the intracellular infection cycle of *O. tsutsugamushi*.

Since BNA can be used to inhibit both the transcriptional and translational process, BNA can be used for further studies. Firstly, the inhibition pattern of TSA56 in the presence of BNA throughout the *Orientia* life cycle and the reduction of TSA56 can be further monitored using immunofluorescence labeling. Secondly, there is an alternative way to improve a strong inhibition by using multiple BNA/DNA oligomers to target a single gene or using a single BNA/DNA oligomer to target multiple genes. Lastly, BNA can be used to inhibit or interfere with the virulence genes which are putatively involved in pathogenesis during the infection.

The findings of the dual RNA-seq work could facilitate subsequent studies on the regulation of gene expression and mechanisms of pathogenesis in *Orientia*, such as studying the association between *Orientia* strains and host immune response by screening panels of *Orientia* strains and applying genome/transcriptome analysis or through use of immunomodulating agents (i.e., monoclonal antibodies, cytokines) that target a specific part of the immune system on host cells.

Appendix 1

List of figures

Appendix 2

List of tables

Appendix 3

References

1. Takaaki Y, Taiji Y. Scrub Typhus in Japan. Am J Clin Microbiol Antimicrob 2019; 2 (3).1042.
2. Watt G, Parola P. Scrub typhus and tropical rickettsioses. Current opinion in infectious diseases. 2003;16(5):429-36.
3. Jiang J, Richards AL. Scrub typhus: no longer restricted to the Tsutsugamushi Triangle. Tropical medicine and infectious disease. 2018;3(1):11.
4. Phupong V, Srettakraikul K. Scrub typhus during pregnancy: a case report and review of the literature. Southeast Asian Journal of Tropical Medicine & Public Health. 2004;35(2):358-60.
5. Tamura A. Tsutsugamushi Disease: An Overview: University of Tokyo Press; 1995.
6. Kelly DJ, Fuerst PA, Ching W-M, Richards AL. Scrub typhus: the geographic distribution of phenotypic and genotypic variants of Orientia tsutsugamushi. Clinical Infectious Diseases. 2009;48(Supplement_3):S203-S30.
7. Roberts L, Gan E, Rapmund G, Chan C, Ramasamy S, Walker J, et al. Identification of Rickettsia tsutsugamushi in the life stages of Leptotrombidium fletcheri with isolation and immunofluorescence techniques. Annals of the New York Academy of Sciences. 1975;266(1):73-9.
8. Diaz JH. Mite-Transmitted Dermatoses and Infectious Diseases in Returning Travelers. Journal of travel medicine. 2010;17(1):21-31.
9. Paris DH, Phetsouvanh R, Tanganuchitcharnchai A, Jones M, Jenjaroen K, Vongsouvath M, et al. Orientia tsutsugamushi in human scrub typhus eschars shows tropism for dendritic cells and monocytes rather than endothelium. PLoS neglected tropical diseases. 2012;6(1).
10. Liu Y-X, Cao W-C, Gao Y, Zhang J-L, Yang Z-Q, Zhao Z-T, et al. Orientia tsutsugamushi in eschars from scrub typhus patients. Emerging infectious diseases. 2006;12(7):1109.
11. Frances S, Watcharapichat P, Phulsuksombati D, Tanskul P. Transmission of Orientia tsutsugamushi, the aetiological agent for scrub typhus, to co-feeding mites. Parasitology. 2000;120(6):601-7.
12. Walker J, Chan C, Manikumaran C, Elisberg B. Attempts to infect and demonstrate transovarial transmission of R. tsutsugamushi in three species of Leptotrombidium mites. Annals of the New York Academy of Sciences. 1975;266(1):80-90.
13. Jeong YJ, Kim S, Wook YD, Lee JW, Kim K-I, Lee SH. Scrub typhus: clinical, pathologic, and imaging findings. Radiographics. 2007;27(1):161-72.
14. Traub R, Wisseman Jr CL. Ecological considerations in scrub typhus: 2. Vector species. Bulletin of the World Health Organization. 1968;39(2):219.
15. Kawamori F, Akiyama M, Sugieda M, Kanda T, Akahane S, Uchikawa K, et al. Epidemiology of Tsutsugamushi disease in relation to the serotypes of Rickettsia tsutsugamushi isolated from patients, field mice, and unfed chiggers on the eastern slope of Mount Fuji, Shizuoka Prefecture, Japan. Journal of clinical microbiology. 1992;30(11):2842-6.
16. Gurung S, Pradhan J, Bhutia P. Outbreak of scrub typhus in the North East Himalayan region-Sikkim: an emerging threat. Indian journal of medical microbiology. 2013;31(1):72.
17. Paris DH, Shelite TR, Day NP, Walker DH. Unresolved problems related to scrub typhus: a seriously neglected life-threatening disease. The American journal of tropical medicine and hygiene. 2013;89(2):301-7.
18. Weitzel T, Dittrich S, López J, Phuklia W, Martinez-Valdebenito C, Velásquez K, et al. Endemic scrub typhus in South America. New England Journal of Medicine. 2016;375(10):954-61.
19. Osuga K, Kimura M, Goto H, Shimada K, Suto T. A case of Tsutsugamushi disease probably contracted in Africa. European Journal of Clinical Microbiology and Infectious Diseases. 1991;10(2):95-6.

20. Izzard L, Fuller A, Blacksell SD, Paris DH, Richards AL, Aukkanit N, et al. Isolation of a novel Orientia species (O. chuto sp. nov.) from a patient infected in Dubai. Journal of clinical microbiology. 2010;48(12):4404-9.
21. Rajapakse S, Rodrigo C, Fernando D. Scrub typhus: pathophysiology, clinical manifestations and prognosis. Asian Pacific journal of tropical medicine. 2012;5(4):261-4.
22. Kim D-M, Won KJ, Park CY, Yu KD, Kim HS, Yang TY, et al. Distribution of eschars on the body of scrub typhus patients: a prospective study. The American journal of tropical medicine and hygiene. 2007;76(5):806-9.
23. Chi W-C, Huang J-J, Sung J-M, Lan R-R, Ko W-C, Chen F-F. Scrub typhus associated with multiorgan failure: a case report. Scandinavian journal of infectious diseases. 1997;29(6):634-5.
24. Taylor AJ, Paris DH, Newton PN. A systematic review of mortality from untreated scrub typhus (Orientia tsutsugamushi). PLoS neglected tropical diseases. 2015;9(8).
25. Hu J, Tan Z, Ren D, Zhang X, He Y, Bao C, et al. Clinical characteristics and risk factors of an outbreak with scrub typhus in previously unrecognized areas, Jiangsu province, China 2013. PloS one. 2015;10(5).
26. Xu G, Walker DH, Jupiter D, Melby PC, Arcari CM. A review of the global epidemiology of scrub typhus. PLoS neglected tropical diseases. 2017;11(11):e0006062.
27. Lim C, Paris DH, Blacksell SD, Laongnualpanich A, Kantipong P, Chierakul W, et al. How to determine the accuracy of an alternative diagnostic test when it is actually better than the reference tests: a re-evaluation of diagnostic tests for scrub typhus using Bayesian LCMs. PloS one. 2015;10(5).
28. Koh GC, Maude RJ, Paris DH, Newton PN, Blacksell SD. Diagnosis of scrub typhus. The American journal of tropical medicine and hygiene. 2010;82(3):368-70.
29. Blacksell SD, Bryant NJ, Paris DH, Doust JA, Sakoda Y, Day NP. Scrub typhus serologic testing with the indirect immunofluorescence method as a diagnostic gold standard: a lack of consensus leads to a lot of confusion. Clinical infectious diseases. 2007;44(3):391-401.
30. Lee K-D, Moon C, Oh WS, Sohn KM, Kim B-N. Diagnosis of scrub typhus: introduction of the immunochromatographic test in Korea. The Korean journal of internal medicine. 2014;29(2):253.
31. La Scola B, Raoult D. Laboratory diagnosis of rickettsioses: current approaches to diagnosis of old and new rickettsial diseases. Journal of clinical microbiology. 1997;35(11):2715.
32. Coleman RE, Sangkasuwan V, Suwanabun N, Eamsila C, Mungviriya S, Devine P, et al. Comparative evaluation of selected diagnostic assays for the detection of IgG and IgM antibody to Orientia tsutsugamushi in Thailand. The American journal of tropical medicine and hygiene. 2002;67(5):497-503.
33. Blacksell SD, Tanganuchitcharnchai A, Nawtaisong P, Kantipong P, Laongnualpanich A, Day NP, et al. Diagnostic accuracy of the InBios scrub typhus detect enzyme-linked immunoassay for the detection of IgM antibodies in Northern Thailand. Clin Vaccine Immunol. 2016;23(2):148-54.
34. Paris DH, Blacksell SD, Newton PN, Day NP. Simple, rapid and sensitive detection of Orientia tsutsugamushi by loop-isothermal DNA amplification. Transactions of the Royal Society of Tropical Medicine and Hygiene. 2008;102(12):1239-46.
35. Murai K, Tachibana N, Okayama A, Shishime E, Tsuda K, Oshikawa T. Sensitivity of polymerase chain reaction assay for Rickettsia tsutsugamushi in patients' blood samples. Microbiology and immunology. 1992;36(11):1145-53.
36. Horinouchi H, Murai K, Okayama A, Nagatomo Y, Tachibana N, Tsubouchi H. Genotypic identification of Rickettsia tsutsugamushi by restriction fragment length polymorphism analysis of DNA amplified by the polymerase chain reaction. The American journal of tropical medicine and hygiene. 1996;54(6):647-51.
37. Richards AL. Worldwide detection and identification of new and old rickettsiae and rickettsial diseases. FEMS Immunology & Medical Microbiology. 2012;64(1):107-10.

38. Walsh DS, Myint KS, Kantipong P, Jongsakul K, Watt G. Orientia tsutsugamushi in peripheral white blood cells of patients with acute scrub typhus. The American journal of tropical medicine and hygiene. 2001;65(6):899-901.
39. Kim D-M, Byun JN. Effects of antibiotic treatment on the results of nested PCRs for scrub typhus. Journal of clinical microbiology. 2008;46(10):3465-6.
40. Rajapakse S, Rodrigo C, Fernando SD. Drug treatment of scrub typhus. Tropical doctor. 2011;41(1):1-4.
41. Watt G, Chouriyagune C, Ruangweerayud R, Watcharapichat P, Phulsuksombati D, Jongsakul K, et al. Scrub typhus infections poorly responsive to antibiotics in northern Thailand. The Lancet. 1996;348(9020):86-9.
42. Perter D, Friedel H, Mctwsh D. Azithromycin a review of its antimicrobial activity, pharmacokinetic properties and clinical efficiency. Drugs. 1992;44(5):750.
43. Chanta C, Phloenchaiwanit P. Randomized controlled trial of azithromycin versus doxycycline or chloramphenicol for treatment of uncomplicated pediatric scrub typhus. J Med Assoc Thai. 2015;98(8):756-60.
44. Atwal S, Giengkam S, Chaemchuen S, Dorling J, Kosaisawe N, VanNieuwenhze M, et al. Evidence for a peptidoglycan-like structure in Orientia tsutsugamushi. Molecular microbiology. 2017.
45. Strickman D, Sheer T, Salata K, Hershey J, Dasch G, Kelly D, et al. In vitro effectiveness of azithromycin against doxycycline-resistant and-susceptible strains of Rickettsia tsutsugamushi, etiologic agent of scrub typhus. Antimicrobial agents and chemotherapy. 1995;39(11):2406-10.
46. Wangrangsimakul T, Phuklia W, Newton PN, Richards AL, Day NP. Scrub typhus and the misconception of doxycycline resistance. Clinical Infectious Diseases. 2019.
47. Bourgeois AL, Olson JG, Fang RC, Huang J, Wang CL, Chow L, et al. Humoral and cellular responses in scrub typhus patients reflecting primary infection and reinfection with Rickettsia tsutsugamushi. The American journal of tropical medicine and hygiene. 1982;31(3):532-40.
48. Phuklia W, Panyanivong P, Sengdetka D, Sonthayanon P, Newton PN, Paris DH, et al. Novel high-throughput screening method using quantitative PCR to determine the antimicrobial susceptibility of Orientia tsutsugamushi clinical isolates. 2018;74(1):74-81.
49. Sharma R. Scrub typhus: prevention and control. JK Science. 2010;12(2):91.
50. Chattopadhyay S, Richards AL. Scrub typhus vaccines: past history and recent developments. Human vaccines. 2007;3(3):73-80.
51. Tamura A, Ohashi N, Urakami H, Miyamura SJIJoS, Microbiology E. Classification of Rickettsia tsutsugamushi in a New Genus, Orientia gen. nov., as Orientia tsutsugamushi comb. nov. 1995;45(3):589-91.
52. Eremeeva ME, Madan A, Shaw C, Tang K, Dasch GA. New Perspectives on Rickettsial Evolution from New Genome Sequences of Rickettsia, particularly R. canadensis, and Orientia tsutsugamishi. ANNALS-NEW YORK ACADEMY OF SCIENCES. 2005;1063:47.
53. Merhej V, Raoult D. Rickettsial evolution in the light of comparative genomics. Biological Reviews. 2011;86(2):379-405.
54. Min C-K, Yang J-S, Kim S, Choi M-S, Kim I-S, Cho N-H. Genome-based construction of the metabolic pathways of Orientia tsutsugamushi and comparative analysis within the Rickettsiales order. Comparative and functional genomics. 2008;2008.
55. Cho N-H, Kim H-R, Lee J-H, Kim S-Y, Kim J, Cha S, et al. The Orientia tsutsugamushi genome reveals massive proliferation of conjugative type IV secretion system and host–cell interaction genes. Proceedings of the National Academy of Sciences. 2007;104(19):7981-6.
56. Hybiske K, Stephens RS. Exit strategies of intracellular pathogens. Nature Reviews Microbiology. 2008;6(2):99-110.

57. Bern M, Goldberg D. Automatic selection of representative proteins for bacterial phylogeny. BMC evolutionary biology. 2005;5(1):34.
58. Sakharkar KR, Dhar PK, Chow VT. Genome reduction in prokaryotic obligatory intracellular parasites of humans: a comparative analysis. International journal of systematic and evolutionary microbiology. 2004;54(6):1937-41.
59. Williamson CH, Sanchez A, Vazquez A, Gutman J, Sahl JW. Bacterial genome reduction as a result of short read sequence assembly. bioRxiv. 2016:091314.
60. Batty EM, Chaemchuen S, Blacksell S, Richards AL, Paris D, Bowden R, et al. Long-read whole genome sequencing and comparative analysis of six strains of the human pathogen *Orientia tsutsugamushi*. PLoS Negl Trop Dis. 2018;12(6):e0006566.
61. Salje J. Orientia tsutsugamushi: A neglected but fascinating obligate intracellular bacterial pathogen. PLoS pathogens. 2017;13(12):e1006657.
62. Gillespie JJ, Joardar V, Williams KP, Driscoll T, Hostetler JB, Nordberg E, et al. A Rickettsia genome overrun by mobile genetic elements provides insight into the acquisition of genes characteristic of an obligate intracellular lifestyle. Journal of bacteriology. 2012;194(2):376-94.
63. Nakayama K, Yamashita A, Kurokawa K, Morimoto T, Ogawa M, Fukuhara M, et al. The Whole-genome sequencing of the obligate intracellular bacterium Orientia tsutsugamushi revealed massive gene amplification during reductive genome evolution. DNA Res. 2008;15(4):185-99.
64. Ogata H, Renesto P, Audic S, Robert C, Blanc G, Fournier P-E, et al. The genome sequence of Rickettsia felis identifies the first putative conjugative plasmid in an obligate intracellular parasite. PLoS biology. 2005;3(8).
65. Min C-K, Kwon Y-J, Ha N-Y, Cho B-A, Kim J-M, Kwon E-K, et al. Multiple Orientia tsutsugamushi ankyrin repeat proteins interact with SCF1 ubiquitin ligase complex and eukaryotic elongation factor 1 α. PLoS One. 2014;9(8).
66. Al-Khodor S, Price CT, Kalia A, Kwaik YA. Functional diversity of ankyrin repeats in microbial proteins. Trends in microbiology. 2010;18(3):132-9.
67. Beyer AR, VieBrock L, Rodino KG, Miller DP, Tegels BK, Marconi RT, et al. Orientia tsutsugamushi strain Ikeda ankyrin repeat-containing proteins recruit SCF1 ubiquitin ligase machinery via poxvirus-like F-box motifs. Journal of bacteriology. 2015;197(19):3097-109.
68. VieBrock L, Evans SM, Beyer AR, Larson CL, Beare PA, Ge H, et al. Orientia tsutsugamushi ankyrin repeat-containing protein family members are Type 1 secretion system substrates that traffic to the host cell endoplasmic reticulum. Frontiers in cellular and infection microbiology. 2015;4:186.
69. Koo J-E, Koh Y-S. Structural and transcriptional analysis of gene clusters for a type IV secretion system in Orientia tsutsugamushi. World Journal of Microbiology and Biotechnology. 2010;26(4):753-9.
70. Fleshman A, Mullins K, Sahl J, Hepp C, Nieto N, Wiggins K, et al. Comparative pan-genomic analyses of Orientia tsutsugamushi reveal an exceptional model of bacterial evolution driving genomic diversity. Microbial genomics. 2018;4(9).
71. Baldridge GD, Burkhardt N, Herron MJ, Kurtti TJ, Munderloh UG. Analysis of fluorescent protein expression in transformants of Rickettsia monacensis, an obligate intracellular tick symbiont. Applied and environmental microbiology. 2005;71(4):2095-105.
72. Beare PA, Sandoz KM, Omsland A, Rockey DD, Heinzen RA. Advances in genetic manipulation of obligate intracellular bacterial pathogens. Frontiers in microbiology. 2011;2.
73. Paris DH, Richards AL, Day NP. Orientia. Molecular Medical Microbiology: Elsevier; 2015. p. 2057-96.
74. Urakami H, Tsuruhara T, Tamura A. Electron microscopic studies on intracellular multiplication of Rickettsia tsutsugamushi in L cells. Microbiol Immunol. 1984;28(11):1191-201.

75. Sunyakumthorn P, Bourchookarn A, Pornwiroon W, David C, Barker SA, Macaluso KR. Characterization and growth of polymorphic Rickettsia felis in a tick cell line. Appl Environ Microbiol. 2008;74(10):3151-8.
76. Stork E, Wisseman C. Growth of Rickettsia prowazeki in enucleated cells. Infection and immunity. 1976;13(6):1743-8.
77. Amano K, Tamura A, Ohashi N, Urakami H, Kaya S, Fukushi K. Deficiency of peptidoglycan and lipopolysaccharide components in Rickettsia tsutsugamushi. Infect Immun. 1987;55(9):2290-2.
78. Silverman DJ, Wisseman C. Comparative ultrastructural study on the cell envelopes of Rickettsia prowazekii, Rickettsia rickettsii, and Rickettsia tsutsugamushi. Infection and immunity. 1978;21(3):1020-3.
79. Silverman D, Wisseman C, Waddell A, Jones M. External layers of Rickettsia prowazekii and Rickettsia rickettsii: occurrence of a slime layer. Infection and immunity. 1978;22(1):233-46.
80. Choi M-S, Seong S-Y, Kang J-S, Kim Y-W, Huh M-S, Kim I-S. Homotypic and heterotypic antibody responses to a 56-kilodalton protein of Orientia tsutsugamushi. Infection and immunity. 1999;67(11):6194-7.
81. Lin C-C, Chou C-H, Lin T-C, Yang M-C, Cho C-L, Chang C-H, et al. Molecular characterization of three major outer membrane proteins, TSA56, TSA47 and TSA22, in Orientia tsutsugamushi. International journal of molecular medicine. 2012;30(1):75-84.
82. Ching W-M, Wang H, Eamsila C, Kelly D, Dasch G. Expression and refolding of truncated recombinant major outer membrane protein antigen (r56) of Orientia tsutsugamushi and its use in enzyme-linked immunosorbent assays. Clin Diagn Lab Immunol. 1998;5(4):519-26.
83. Blacksell SD, Luksameetanasan R, Kalambaheti T, Aukkanit N, Paris DH, McGready R, et al. Genetic typing of the 56-kDa type-specific antigen gene of contemporary Orientia tsutsugamushi isolates causing human scrub typhus at two sites in north-eastern and western Thailand. FEMS Immunology & Medical Microbiology. 2008;52(3):335-42.
84. Park CS, Kim IC, Lee JB, Choi MS, Choi SB, Chang WH, et al. Analysis of antigenic characteristics of Rickettsia tsutsugamushi Boryong strain and antigenic heterogeneity of Rickettsia tsutsugamushi using monoclonal antibodies. Journal of Korean medical science. 1993;8(5):319-24.
85. Hickman CJ, Stover C, Joseph SW, Oaks EV. Murine T-cell response to native and recombinant protein antigens of Rickettsia tsutsugamushi. Infection and immunity. 1993;61(5):1674-81.
86. Choi S, Jeong HJ, Hwang K-J, Gill B, Ju YR, Lee YS, et al. A recombinant 47-kDa outer membrane protein induces an immune response against Orientia tsutsugamushi strain Boryong. The American journal of tropical medicine and hygiene. 2017;97(1):30-7.
87. Jiang J, Paris DH, Blacksell SD, Aukkanit N, Newton PN, Phetsouvanh R, et al. Diversity of the 47-kD HtrA nucleic acid and translated amino acid sequences from 17 recent human isolates of Orientia. Vector-Borne and Zoonotic Diseases. 2013;13(6):367-75.
88. Chen H-W, Zhang Z, Huber E, Chao C-C, Wang H, Dasch GA, et al. Identification of cross-reactive epitopes on the conserved 47-kilodalton antigen of Orientia tsutsugamushi and human serine protease. Infection and immunity. 2009;77(6):2311-9.
89. Yu Y, Wen B, Wen B, Niu D, Chen M, Qiu L. Induction of protective immunity against scrub typhus with a 56-kilodalton recombinant antigen fused with a 47-kilodalton antigen of Orientia tsutsugamushi Karp. The American journal of tropical medicine and hygiene. 2005;72(4):458-64.
90. Hickman CJ, Stover CK, Joseph SW, Oaks EV. Molecular cloning and sequence analysis of a Rickettsia tsutsugamushi 22 kDa antigen containing B-and T-cell epitopes. Microbial pathogenesis. 1991;11(1):19-31.
91. Ge H, Tong M, Li A, Mehta R, Ching W-M. Cloning and sequence analysis of the 22-kDa antigen genes of Orientia tsutsugamushi strains Kato, TA763, AFSC 7, 18-032460, TH1814, and MAK 119. NAVAL MEDICAL RESEARCH CENTER SILVER SPRING MD; 2005.

92. Ngwamidiba M, Blanc G, Ogata H, RAOULT D, FOURNIER PE. Phylogenetic Study of Rickettsia Species Using Sequences of the Autotransporter Protein-Encoding Gene sca2. Annals of the New York Academy of Sciences. 2005;1063(1):94-9.
93. Uchiyama T, Kawano H, Kusuhara Y. The major outer membrane protein rOmpB of spotted fever group rickettsiae functions in the rickettsial adherence to and invasion of Vero cells. Microbes and infection. 2006;8(3):801-9.
94. Li H, Walker DH. rOmpA is a critical protein for the adhesion ofRickettsia rickettsiito host cells. Microbial pathogenesis. 1998;24(5):289-98.
95. Koralur MC, Ramaiah A, Dasch GA. Detection and distribution of Sca autotransporter protein antigens in diverse isolates of Orientia tsutsugamushi. PLoS neglected tropical diseases. 2018;12(9):e0006784.
96. Henderson IR, Nataro JP. Virulence functions of autotransporter proteins. Infection and immunity. 2001;69(3):1231-43.
97. Ha N-Y, Sharma P, Kim G, Kim Y, Min C-K, Choi M-S, et al. Immunization with an autotransporter protein of Orientia tsutsugamushi provides protective immunity against scrub typhus. PLoS neglected tropical diseases. 2015;9(3).
98. Ha N-Y, Cho N-H, Kim Y-S, Choi M-S, Kim I-S. An autotransporter protein from Orientia tsutsugamushi mediates adherence to nonphagocytic host cells. Infection and immunity. 2011;79(4):1718-27.
99. Nagano I, Kasuya S, Noda N, Yamashita T. Virulence in mice of Orientia tsutsugamushi isolated from patients in a new endemic area in Japan. Microbiology and immunology. 1996;40(10):743-7.
100. Groves MG, Osterman JV. Host defenses in experimental scrub typhus: genetics of natural resistance to infection. Infection and immunity. 1978;19(2):583-8.
101. Cho BA, Cho NH, Min CK, Kim SY, Yang JS, Lee JR, et al. Global gene expression profile of Orientia tsutsugamushi. Proteomics. 2010;10(8):1699-715.
102. Audia JP, Winkler HH. Study of the five Rickettsia prowazekii proteins annotated as ATP/ADP translocases (Tlc): only Tlc1 transports ATP/ADP, while Tlc4 and Tlc5 transport other ribonucleotides. Journal of Bacteriology. 2006;188(17):6261-8.
103. Braeken K, Moris M, Daniels R, Vanderleyden J, Michiels J. New horizons for (p) ppGpp in bacterial and plant physiology. Trends in microbiology. 2006;14(1):45-54.
104. Zientz E, Dandekar T, Gross R. Metabolic interdependence of obligate intracellular bacteria and their insect hosts. Microbiol Mol Biol Rev. 2004;68(4):745-70.
105. Diaz FE, Abarca K, Kalergis AM. An Update on Host-Pathogen Interplay and Modulation of Immune Responses during Orientia tsutsugamushi Infection. Clin Microbiol Rev. 2018;31(2).
106. Koo J-E, Hong H-J, Dearth A, Kobayashi KS, Koh Y-S. Intracellular invasion of Orientia tsutsugamushi activates inflammasome in ASC-dependent manner. PLoS One. 2012;7(6).
107. Antosz H, Osiak M. NOD1 and NOD2 receptors: integral members of the innate and adaptive immunity system. Acta Biochimica Polonica. 2013;60(3).
108. Moreira L, Zamboni DS. NOD1 and NOD2 signaling in infection and inflammation. Frontiers in immunology. 2012;3:328.
109. Kumar H, Kawai T, Akira S. Pathogen recognition by the innate immune system. International reviews of immunology. 2011;30(1):16-34.
110. Kawai T, Akira S. Toll-like receptors and their crosstalk with other innate receptors in infection and immunity. Immunity. 2011;34(5):637-50.
111. Netea MG, Simon A, van de Veerdonk F, Kullberg B-J, Van der Meer JW, Joosten LA. IL-1β processing in host defense: beyond the inflammasomes. PLoS pathogens. 2010;6(2).
112. Nurieva RI, Chung Y. Understanding the development and function of T follicular helper cells. Cellular & molecular immunology. 2010;7(3):190-7.

113. Khan N, Gowthaman U, Pahari S, Agrewala JN. Manipulation of costimulatory molecules by intracellular pathogens: veni, vidi, vici!! PLoS pathogens. 2012;8(6).
114. Lehar SM, Bevan MJ. Polarizing a T-cell response. Nature. 2004;430(6996):150-1.
115. Choi J-H, Cheong T-C, Ha N-Y, Ko Y, Cho C-H, Jeon J-H, et al. Orientia tsutsugamushi subverts dendritic cell functions by escaping from autophagy and impairing their migration. PLoS neglected tropical diseases. 2013;7(1).
116. Chu H, Park S-M, Cheon IS, Park M-Y, Shim B-S, Gil B-C, et al. Orientia tsutsugamushi infection induces CD4+ T cell activation via human dendritic cell activity. J Microbiol Biotechnol. 2013;23(8):1159-66.
117. Gorvel L, Textoris J, Banchereau R, Amara AB, Tantibhedhyangkul W, von Bargen K, et al. Intracellular bacteria interfere with dendritic cell functions: role of the type I interferon pathway. PLoS One. 2014;9(6).
118. Cho N-H, Seong S-Y, Huh M-S, Han T-H, Koh Y-S, Choi M-S, et al. Expression of chemokine genes in murine macrophages infected with Orientia tsutsugamushi. Infection and immunity. 2000;68(2):594-602.
119. Koo JE, Yun JH, Lee KH, Hyun JW, Kang HK, Jang WJ, et al. Activation of mitogen-activated protein kinases is involved in the induction of interferon β gene in macrophages infected with Orientia tsutsugamushi. Microbiology and immunology. 2009;53(2):123-9.
120. Kim M-J, Kim M-K, Kang J-S. Orientia tsutsugamushi inhibits tumor necrosis factor α production by inducing interleukin 10 secretion in murine macrophages. Microbial pathogenesis. 2006;40(1):1-7.
121. Meghari S, Bechah Y, Capo C, Lepidi H, Raoult D, Murray PJ, et al. Persistent Coxiella burnetii infection in mice overexpressing IL-10: an efficient model for chronic Q fever pathogenesis. PLoS pathogens. 2008;4(2).
122. Sing A, Roggenkamp A, Geiger AM, Heesemann J. Yersinia enterocolitica evasion of the host innate immune response by V antigen-induced IL-10 production of macrophages is abrogated in IL-10-deficient mice. The Journal of Immunology. 2002;168(3):1315-21.
123. Otterdal K, Janardhanan J, Astrup E, Ueland T, Prakash JA, Lekva T, et al. Increased endothelial and macrophage markers are associated with disease severity and mortality in scrub typhus. Journal of Infection. 2014;69(5):462-9.
124. Cho K-A, Jun YH, Suh JW, Kang J-S, Choi HJ, Woo S-Y. Orientia tsutsugamushi induced endothelial cell activation via the NOD1-IL-32 pathway. Microbial pathogenesis. 2010;49(3):95-104.
125. Page AV, Liles WC. Biomarkers of endothelial activation/dysfunction in infectious diseases. Virulence. 2013;4(6):507-16.
126. Chousterman BG, Swirski FK, Weber GF, editors. Cytokine storm and sepsis disease pathogenesis. Seminars in immunopathology; 2017: Springer.
127. Soong L, Wang H, Shelite TR, Liang Y, Mendell NL, Sun J, et al. Strong type 1, but impaired type 2, immune responses contribute to Orientia tsutsugamushi-induced pathology in mice. PLoS neglected tropical diseases. 2014;8(9).
128. Valbuena G, Walker DH. Approaches to vaccines against Orientia tsutsugamushi. Frontiers in cellular and infection microbiology. 2013;2:170.
129. Alberts B, Johnson A, Lewis J, Raff M, Roberts K, Walter P. Chapter 24: The adaptive immune system. Molecular Biology of the Cell. 2002.
130. Seong S-Y, Kim HR, Huh M, Park S, Kang J, Han T, et al. Induction of neutralizing antibody in mice by immunization with recombinant 56 kDa protein of Orientia tsutsugamushi. Vaccine. 1997;15(16):1741-7.
131. Ha N-Y, Kim Y, Min C-K, Kim H-I, Yen NTH, Choi M-S, et al. Longevity of antibody and T-cell responses against outer membrane antigens of Orientia tsutsugamushi in scrub typhus patients. Emerging microbes & infections. 2017;6(1):1-8.

132. Metzemaekers M, Vanheule V, Janssens R, Struyf S, Proost P. Overview of the mechanisms that may contribute to the non-redundant activities of interferon-inducible CXC chemokine receptor 3 ligands. Frontiers in immunology. 2018;8:1970.
133. Henderson B, Nair S, Pallas J, Williams MA. Fibronectin: a multidomain host adhesin targeted by bacterial fibronectin-binding proteins. FEMS microbiology reviews. 2011;35(1):147-200.
134. Martinez JJ, Seveau S, Veiga E, Matsuyama S, Cossart P. Ku70, a component of DNA-dependent protein kinase, is a mammalian receptor for Rickettsia conorii. Cell. 2005;123(6):1013-23.
135. Yáñez D, Izquierdo M, Ruiz-Perez F, Nataro JP, Girón JA, Vidal RM, et al. The role of fibronectin in the adherence and inflammatory response induced by enteroaggregative Escherichia coli on epithelial cells. Frontiers in cellular and infection microbiology. 2016;6:166.
136. Menzies BE. The role of fibronectin binding proteins in the pathogenesis of Staphylococcus aureus infections. Current opinion in infectious diseases. 2003;16(3):225-9.
137. Van Putten JP, Duensing TD, Cole RL. Entry of OpaA+ gonococci into HEp-2 cells requires concerted action of glycosaminoglycans, fibronectin and integrin receptors. Molecular microbiology. 1998;29(1):369-79.
138. Lee J-H, Cho N-H, Kim S-Y, Bang S-Y, Chu H, Choi M-S, et al. Fibronectin facilitates the invasion of Orientia tsutsugamushi into host cells through interaction with a 56-kDa type-specific antigen. The Journal of infectious diseases. 2008;198(2):250-7.
139. Cho B-A, Cho N-H, Seong S-Y, Choi M-S, Kim I-S. Intracellular invasion by Orientia tsutsugamushi is mediated by integrin signaling and actin cytoskeleton rearrangements. Infection and immunity. 2010;78(5):1915-23.
140. Christianson HC, Belting M. Heparan sulfate proteoglycan as a cell-surface endocytosis receptor. Matrix Biology. 2014;35:51-5.
141. Ihn K-S, Han S-H, Kim H-R, Huh M-S, Seong S-Y, Kang J-S, et al. Cellular invasion of Orientia tsutsugamushi requires initial interaction with cell surface heparan sulfate. Microbial pathogenesis. 2000;28(4):227-33.
142. Kim H-R, Choi M-S, Kim I-S. Role of Syndecan-4 in the cellular invasion of Orientia tsutsugamushi. Microbial pathogenesis. 2004;36(4):219-25.
143. Morgan MR, Humphries MJ, Bass MD. Synergistic control of cell adhesion by integrins and syndecans. Nature reviews Molecular cell biology. 2007;8(12):957-69.
144. Wennerberg K, Rossman KL, Der CJ. The Ras superfamily at a glance. Journal of cell science. 2005;118(5):843-6.
145. Clapham DE. Calcium signaling. Cell. 2007;131(6):1047-58.
146. Ko Y, Cho N-H, Cho B-A, Kim I-S, Choi M-S. Involvement of Ca2+ signaling in intracellular invasion of non-phagocytic host cells by Orientia tsutsugamushi. Microbial pathogenesis. 2011;50(6):326-30.
147. Chu H, Lee J-H, Han S-H, Kim S-Y, Cho N-H, Kim I-S, et al. Exploitation of the endocytic pathway by Orientia tsutsugamushi in nonprofessional phagocytes. Infection and immunity. 2006;74(7):4246-53.
148. Schmid J. The acidic environment in endocytic compartments. Biochemical Journal. 1994;303(Pt 2):679.
149. Ko Y, Choi JH, Ha NY, Kim IS, Cho NH, Choi MS. Active escape of Orientia tsutsugamushi from cellular autophagy. Infect Immun. 2013;81(2):552-9.
150. Uchiyama T, Kishi M, Ogawa M. Restriction of the growth of a nonpathogenic spotted fever group rickettsia. FEMS Immunology & Medical Microbiology. 2012;64(1):42-7.
151. Ogawa M, Yoshimori T, Suzuki T, Sagara H, Mizushima N, Sasakawa C. Escape of intracellular Shigella from autophagy. Science. 2005;307(5710):727-31.
152. Dortet L, Mostowy S, Louaka AS, Gouin E, Nahori M-A, Wiemer EA, et al. Recruitment of the major vault protein by InlK: a Listeria monocytogenes strategy to avoid autophagy. PLoS pathogens. 2011;7(8).

153. Kim S-W, Ihn K-S, Han S-H, Seong S-Y, Kim I-S, Choi M-S. Microtubule-and dynein-mediated movement oforientia tsutsugamushi to the microtubule organizing center. Infection and immunity. 2001;69(1):494-500.
154. Rikihisa Y, Ito S. Intracellular localization of Rickettsia tsutsugamushi in polymorphonuclear leukocytes. J Exp Med. 1979;150(3):703-8.
155. Wesolowski J, Weber MM, Nawrotek A, Dooley CA, Calderon M, Croix CMS, et al. Chlamydia hijacks ARF GTPases to coordinate microtubule posttranslational modifications and Golgi complex positioning. MBio. 2017;8(3):e02280-16.
156. Beyer AR, Rodino KG, VieBrock L, Green RS, Tegels BK, Oliver Jr LD, et al. Orientia tsutsugamushi Ank9 is a multifunctional effector that utilizes a novel GRIP-like Golgi localization domain for Golgi-to-endoplasmic reticulum trafficking and interacts with host COPB2. Cellular microbiology. 2017;19(7):e12727.
157. Lee S-M, Kim M-K, Kim M-J, Kang J-S. Novel polysaccharide antigen of Orientia tsutsugamushi revealed by a monoclonal antibody. FEMS microbiology letters. 2009;297(1):95-100.
158. Schaechter M, Bozeman F, Smadel J. Study on the growth of rickettsiae: II. Morphologic observations of living rickettsiae in tissue culture cells. Virology. 1957;3(1):160-72.
159. Ewing E, Takeuchi A, Shirai A, Osterman JV. Experimental infection of mouse peritoneal mesothelium with scrub typhus rickettsiae: an ultrastructural study. Infection and immunity. 1978;19(3):1068-75.
160. Hybiske K, Stephens RS. Mechanisms of host cell exit by the intracellular bacterium Chlamydia. Proceedings of the National Academy of Sciences. 2007;104(27):11430-5.
161. Brown D, London E. Functions of lipid rafts in biological membranes. Annual review of cell and developmental biology. 1998;14(1):111-36.
162. Shin J-S, Gao Z, Abraham SN. Involvement of cellular caveolae in bacterial entry into mast cells. Science. 2000;289(5480):785-8.
163. Norkin LC, Wolfrom SA, Stuart ES. Association of caveolin with Chlamydia trachomatis inclusions at early and late stages of infection. Experimental cell research. 2001;266(2):229-38.
164. Kim MJ, Kim MK, Kang JS. Involvement of lipid rafts in the budding-like exit of Orientia tsutsugamushi. Microb Pathog. 2013;63:37-43.
165. Justice SS, Harrison A, Becknell B, Mason KM. Bacterial differentiation, development, and disease: mechanisms for survival. FEMS Microbiol Lett. 2014;360(1):1-8.
166. Collier J. Cell division control in Caulobacter crescentus. Biochimica et Biophysica Acta (BBA)-Gene Regulatory Mechanisms. 2019;1862(7):685-90.
167. Gober JW, Marques MVJMMBR. Regulation of cellular differentiation in Caulobacter crescentus. 1995;59(1):31-47.
168. Poindexter JSJTpvPa, subclasses b. Dimorphic prosthecate bacteria: the genera Caulobacter, Asticcacaulis, Hyphomicrobium, Pedomicrobium, Hyphomonas and Thiodendron. 2006:72-90.
169. Hughes V, Jiang C, Brun Y. Caulobacter crescentus. Current biology: CB. 2012;22(13):R507.
170. Weigel W, Dersch P. Phenotypic heterogeneity: a bacterial virulence strategy. Microbes and infection. 2018;20(9-10):570-7.
171. Davis KM, Isberg RR. Defining heterogeneity within bacterial populations via single cell approaches. Bioessays. 2016;38(8):782-90.
172. Henderson IR, Owen P, Nataro JP. Molecular switches—the ON and OFF of bacterial phase variation. Molecular microbiology. 1999;33(5):919-32.
173. Van Der Woude MW, Bäumler AJ. Phase and antigenic variation in bacteria. Clinical microbiology reviews. 2004;17(3):581-611.
174. Bayliss CD, Field D, Moxon ER. The simple sequence contingency loci of Haemophilus influenzae and Neisseria meningitidis. The Journal of clinical investigation. 2001;107(6):657-66.

175. Borges V, Pinheiro M, Antelo M, Sampaio DA, Vieira L, Ferreira R, et al. Chlamydia trachomatis in vivo to in vitro transition reveals mechanisms of phase variation and down-regulation of virulence factors. PloS one. 2015;10(7).
176. Rejmanek D, Foley P, Barbet A, Foley J. Antigen variability in Anaplasma phagocytophilum during chronic infection of a reservoir host. Microbiology. 2012;158(Pt 10):2632.
177. Errington J. From spores to antibiotics via the cell cycle. Microbiology. 2010;156(1):1-13.
178. Abdelrahman YM, Belland RJ. The chlamydial developmental cycle. FEMS Microbiol Rev. 2005;29(5):949-59.
179. Minnick MF, Raghavan R. Developmental biology of Coxiella burnetii. Adv Exp Med Biol. 2012;984:231-48.
180. Rikihisa Y. Mechanisms of obligatory intracellular infection with Anaplasma phagocytophilum. Clin Microbiol Rev. 2011;24(3):469-89.
181. Zhang JZ, Popov VL, Gao S, Walker DH, Yu XJ. The developmental cycle of Ehrlichia chaffeensis in vertebrate cells. Cell Microbiol. 2007;9(3):610-8.
182. Elfving K, Lukinius A, Nilsson K. Life cycle, growth characteristics and host cell response of Rickettsia helvetica in a Vero cell line. Exp Appl Acarol. 2012;56(2):179-87.
183. Serra DO, Hengge R. Stress responses go three dimensional–the spatial order of physiological differentiation in bacterial macrocolony biofilms. Environmental microbiology. 2014;16(6):1455-71.
184. Huber D, von Voithenberg LV, Kaigala G. Fluorescence in situ hybridization (FISH): History, limitations and what to expect from micro-scale FISH? Micro and Nano Engineering. 2018;1:15-24.
185. Poppert S, Essig A, Marre R, Wagner M, Horn M. Detection and differentiation of chlamydiae by fluorescence in situ hybridization. Appl Environ Microbiol. 2002;68(8):4081-9.
186. Roostalu J, Jõers A, Luidalepp H, Kaldalu N, Tenson T. Cell division in Escherichia colicultures monitored at single cell resolution. BMC microbiology. 2008;8(1):68.
187. Manina G, Dhar N, McKinney JD. Stress and host immunity amplify Mycobacterium tuberculosis phenotypic heterogeneity and induce nongrowing metabolically active forms. Cell host & microbe. 2015;17(1):32-46.
188. Helaine S, Thompson JA, Watson KG, Liu M, Boyle C, Holden DW. Dynamics of intracellular bacterial replication at the single cell level. Proceedings of the National Academy of Sciences. 2010;107(8):3746-51.
189. McClure EE, Chavez ASO, Shaw DK, Carlyon JA, Ganta RR, Noh SM, et al. Engineering of obligate intracellular bacteria: progress, challenges and paradigms. Nat Rev Microbiol. 2017;15(9):544-58.
190. Atwal S, Giengkam S, Jaiyen Y, Feaga HA, Dworkin J, Salje JJJoMM. Clickable methionine as a universal probe for labelling intracellular bacteria. 2020;169:105812.
191. Dewachter L, Verstraeten N, Fauvart M, Michiels J. An integrative view of cell cycle control in Escherichia coli. FEMS microbiology reviews. 2018;42(2):116-36.
192. Wang JD, Levin PA. Metabolism, cell growth and the bacterial cell cycle. Nature Reviews Microbiology. 2009;7(11):822-7.
193. Xu Z-Q, Dixon NE. Bacterial replisomes. Current opinion in structural biology. 2018;53:159-68.
194. Chiaramello AE, Zyskind JW. Coupling of DNA replication to growth rate in Escherichia coli: a possible role for guanosine tetraphosphate. Journal of bacteriology. 1990;172(4):2013-9.
195. Ferullo DJ, Lovett ST. The stringent response and cell cycle arrest in Escherichia coli. PLoS genetics. 2008;4(12).
196. Quon KC, Yang B, Domian IJ, Shapiro L, Marczynski GT. Negative control of bacterial DNA replication by a cell cycle regulatory protein that binds at the chromosome origin. Proceedings of the National Academy of Sciences. 1998;95(1):120-5.

197. Ryan KR, Judd EM, Shapiro L. The CtrA response regulator essential for Caulobacter crescentus cell-cycle progression requires a bipartite degradation signal for temporally controlled proteolysis. Journal of molecular biology. 2002;324(3):443-55.
198. Laub MT, Chen SL, Shapiro L, McAdams HH. Genes directly controlled by CtrA, a master regulator of the Caulobacter cell cycle. Proceedings of the National Academy of Sciences. 2002;99(7):4632-7.
199. Skerker JM, Shapiro L. Identification and cell cycle control of a novel pilus system in Caulobacter crescentus. The EMBO journal. 2000;19(13):3223-34.
200. Thanbichler M. Synchronization of chromosome dynamics and cell division in bacteria. Cold Spring Harbor perspectives in biology. 2010;2(1):a000331.
201. Gonzalez MD, Beckwith J. Divisome under construction: distinct domains of the small membrane protein FtsB are necessary for interaction with multiple cell division proteins. Journal of bacteriology. 2009;191(8):2815-25.
202. Morcinek-Orłowska J, Galińska J, Glinkowska MK. When size matters–coordination of growth and cell cycle in bacteria-Review. Acta Biochimica Polonica. 2019;66(2):139-46.
203. Sundararajan K, Miguel A, Desmarais SM, Meier EL, Huang KC, Goley ED. The bacterial tubulin FtsZ requires its intrinsically disordered linker to direct robust cell wall construction. Nature communications. 2015;6(1):1-14.
204. Thanbichler M, Shapiro L. MipZ, a spatial regulator coordinating chromosome segregation with cell division in Caulobacter. Cell. 2006;126(1):147-62.
205. Kiekebusch D, Michie KA, Essen L-O, Löwe J, Thanbichler M. Localized dimerization and nucleoid binding drive gradient formation by the bacterial cell division inhibitor MipZ. Molecular cell. 2012;46(3):245-59.
206. Otten C, Brilli M, Vollmer W, Viollier PH, Salje J. Peptidoglycan in obligate intracellular bacteria. Molecular microbiology. 2018;107(2):142-63.
207. Liechti G, Kuru E, Packiam M, Hsu Y-P, Tekkam S, Hall E, et al. Pathogenic Chlamydia lack a classical sacculus but synthesize a narrow, mid-cell peptidoglycan ring, regulated by MreB, for cell division. PLoS pathogens. 2016;12(5).
208. Ellermeyer SF, Pilyugin SS. A size-structured model of bacterial growth and reproduction. Journal of biological dynamics. 2012;6(2):131-47.
209. Maier RM, Pepper IL. Bacterial growth. Environmental microbiology: Elsevier; 2015. p. 37-56.
210. Jaishankar J, Srivastava P. Molecular basis of stationary phase survival and applications. Frontiers in microbiology. 2017;8:2000.
211. Loewen PC, Hu B, Strutinsky J, Sparling R. Regulation in the rpoS regulon of Escherichia coli. Canadian journal of microbiology. 1998;44(8):707-17.
212. Potvin E, Sanschagrin F, Levesque RC. Sigma factors in Pseudomonas aeruginosa. FEMS microbiology reviews. 2008;32(1):38-55.
213. Alvarez-Martinez CE, Baldini RL, Gomes SL. A Caulobacter crescentus extracytoplasmic function sigma factor mediating the response to oxidative stress in stationary phase. Journal of bacteriology. 2006;188(5):1835-46.
214. Lourenço RF, Kohler C, Gomes SL. A two-component system, an anti-sigma factor and two paralogous ECF sigma factors are involved in the control of general stress response in Caulobacter crescentus. Molecular microbiology. 2011;80(6):1598-612.
215. Jaishankar J, Srivastava P. Molecular Basis of Stationary Phase Survival and Applications. Front Microbiol. 2017;8:2000.
216. O'Connor TJ, Adepoju Y, Boyd D, Isberg RR. Minimization of the Legionella pneumophila genome reveals chromosomal regions involved in host range expansion. Proceedings of the National Academy of Sciences. 2011;108(36):14733-40.

217. Asif A, Mohsin H, Tanvir R, Rehman Y. Revisiting the mechanisms involved in calcium chloride induced bacterial transformation. Frontiers in microbiology. 2017;8:2169.
218. Wang Y, Kahane S, Cutcliffe LT, Skilton RJ, Lambden PR, Clarke IN. Development of a transformation system for Chlamydia trachomatis: restoration of glycogen biosynthesis by acquisition of a plasmid shuttle vector. PLoS pathogens. 2011;7(9).
219. Gérard HC, Mishra MK, Mao G, Wang S, Hali M, Whittum-Hudson JA, et al. Dendrimer-enabled DNA delivery and transformation of Chlamydia pneumoniae. Nanomedicine: Nanotechnology, Biology and Medicine. 2013;9(7):996-1008.
220. Oki AT, Seidman D, Lancina III MG, Mishra MK, Kannan RM, Yang H, et al. Dendrimer-enabled transformation of Anaplasma phagocytophilum. Microbes and infection. 2015;17(11-12):817-22.
221. Tam JE, Davis CH, Wyrick PB. Expression of recombinant DNA introduced into Chlamydia trachomatis by electroporation. Canadian Journal of Microbiology. 1994;40(7):583-91.
222. Rachek LI, Tucker AM, Winkler HH, Wood DO. Transformation of Rickettsia prowazekiito Rifampin Resistance. Journal of bacteriology. 1998;180(8):2118-24.
223. Felsheim RF, Herron MJ, Nelson CM, Burkhardt NY, Barbet AF, Kurtti TJ, et al. Transformation of Anaplasma phagocytophilum. BMC biotechnology. 2006;6(1):42.
224. Long SW, Whitworth TJ, Walker DH, YU XJ. Overcoming barriers to the transformation of the genus Ehrlichia. Annals of the New York Academy of Sciences. 2005;1063(1):403-10.
225. Choi K-H, Kim K-J. Applications of transposon-based gene delivery system in bacteria. J Microbiol Biotechnol. 2009;19(3):217-28.
226. Abdur Rahman S, Seki S, Utsuki K, Obika S, Miyashita K, Imanishi T. 2′, 4′-BNA NC: a novel bridged nucleic acid analogue with excellent hybridizing and nuclease resistance profiles. Nucleosides, Nucleotides, and Nucleic Acids. 2007;26(10-12):1625-8.
227. Wang G, Xu XS. Peptide nucleic acid (PNA) binding-mediated gene regulation. Cell Res. 2004;14(2):111-6.
228. Soler-Bistué A, Zorreguieta A, Tolmasky ME. Bridged nucleic acids reloaded. Molecules. 2019;24(12):2297.
229. Singh RP, Oh B-K, Choi J-W. Application of peptide nucleic acid towards development of nanobiosensor arrays. Bioelectrochemistry. 2010;79(2):153-61.
230. Good L, Awasthi SK, Dryselius R, Larsson O, Nielsen PE. Bactericidal antisense effects of peptide-PNA conjugates. Nat Biotechnol. 2001;19(4):360-4.
231. Pelc RS, McClure JC, Kaur SJ, Sears KT, Rahman MS, Ceraul SM. Disrupting protein expression with peptide nucleic acids reduces infection by obligate intracellular Rickettsia. PloS one. 2015;10(3):e0119283.
232. Humphrys MS, Creasy T, Sun Y, Shetty AC, Chibucos MC, Drabek EF, et al. Simultaneous transcriptional profiling of bacteria and their host cells. PloS one. 2013;8(12).
233. La M-V, Raoult D, Renesto P. Regulation of whole bacterial pathogen transcription within infected hosts. FEMS microbiology reviews. 2008;32(3):440-60.
234. Shendure J. The beginning of the end for microarrays? Nature methods. 2008;5(7):585-7.
235. Canales RD, Luo Y, Willey JC, Austermiller B, Barbacioru CC, Boysen C, et al. Evaluation of DNA microarray results with quantitative gene expression platforms. Nature biotechnology. 2006;24(9):1115-22.
236. Gershon D. More than gene expression. Nature. 2005;437(7062):1195-6.
237. Choudhuri S. Bioinformatics for beginners: genes, genomes, molecular evolution, databases and analytical tools: Elsevier; 2014.
238. Bertone P, Stolc V, Royce TE, Rozowsky JS, Urban AE, Zhu X, et al. Global identification of human transcribed sequences with genome tiling arrays. Science. 2004;306(5705):2242-6.

239. Kronstad JW. Serial analysis of gene expression in eukaryotic pathogens. Infectious Disorders-Drug Targets (Formerly Current Drug Targets-Infectious Disorders). 2006;6(3):281-97.
240. Westermann AJ, Gorski SA, Vogel J. Dual RNA-seq of pathogen and host. Nature reviews Microbiology. 2012;10(9):618.
241. Cloonan N, Forrest AR, Kolle G, Gardiner BB, Faulkner GJ, Brown MK, et al. Stem cell transcriptome profiling via massive-scale mRNA sequencing. Nature methods. 2008;5(7):613.
242. Mortazavi A, Williams BA, McCue K, Schaeffer L, Wold B. Mapping and quantifying mammalian transcriptomes by RNA-Seq. Nature methods. 2008;5(7):621.
243. Trapnell C, Williams BA, Pertea G, Mortazavi A, Kwan G, Van Baren MJ, et al. Transcript assembly and quantification by RNA-Seq reveals unannotated transcripts and isoform switching during cell differentiation. Nature biotechnology. 2010;28(5):511.
244. Westermann AJ, Forstner KU, Amman F, Barquist L, Chao Y, Schulte LN, et al. Dual RNA-seq unveils noncoding RNA functions in host-pathogen interactions. Nature. 2016;529(7587):496-501.
245. Westermann AJ, Barquist L, Vogel J. Resolving host–pathogen interactions by dual RNA-seq. PLoS pathogens. 2017;13(2):e1006033.
246. Conesa A, Madrigal P, Tarazona S, Gomez-Cabrero D, Cervera A, McPherson A, et al. A survey of best practices for RNA-seq data analysis. Genome biology. 2016;17(1):13.
247. Li B, Ruotti V, Stewart RM, Thomson JA, Dewey CN. RNA-Seq gene expression estimation with read mapping uncertainty. Bioinformatics. 2010;26(4):493-500.
248. Mavromatis C, Bokil NJ, Totsika M, Kakkanat A, Schaale K, Cannistraci CV, et al. The co-transcriptome of uropathogenic E scherichia coli-infected mouse macrophages reveals new insights into host–pathogen interactions. Cellular microbiology. 2015;17(5):730-46.
249. Krzywinski M, Altman N. Points of significance: Analysis of variance and blocking. Nature Publishing Group; 2014.
250. Huber W, Carey VJ, Gentleman R, Anders S, Carlson M, Carvalho BS, et al. Orchestrating high-throughput genomic analysis with Bioconductor. Nature methods. 2015;12(2):115.
251. Robinson MD, McCarthy DJ, Smyth GK. edgeR: a Bioconductor package for differential expression analysis of digital gene expression data. Bioinformatics. 2010;26(1):139-40.
252. Love MI, Huber W, Anders S. Moderated estimation of fold change and dispersion for RNA-seq data with DESeq2. Genome biology. 2014;15(12):550.
253. Law CW, Chen Y, Shi W, Smyth GK. voom: Precision weights unlock linear model analysis tools for RNA-seq read counts. Genome biology. 2014;15(2):R29.
254. Consortium GO. Gene ontology consortium: going forward. Nucleic acids research. 2015;43(D1):D1049-D56.
255. Kanehisa M, Sato Y, Kawashima M, Furumichi M, Tanabe M. KEGG as a reference resource for gene and protein annotation. Nucleic acids research. 2016;44(D1):D457-D62.
256. Rahmatallah Y, Emmert-Streib F, Glazko G. Gene set analysis approaches for RNA-seq data: performance evaluation and application guideline. Briefings in Bioinformatics. 2016;17(3):393-407.
257. Marbach D, Costello JC, Küffner R, Vega NM, Prill RJ, Camacho DM, et al. Wisdom of crowds for robust gene network inference. Nature methods. 2012;9(8):796.
258. Tuncbag N, McCallum S, Huang S-sC, Fraenkel E. SteinerNet: a web server for integrating 'omic'data to discover hidden components of response pathways. Nucleic acids research. 2012;40(W1):W505-W9.
259. Rienksma RA, Suarez-Diez M, Mollenkopf H-J, Dolganov GM, Dorhoi A, Schoolnik GK, et al. Comprehensive insights into transcriptional adaptation of intracellular mycobacteria by microbe-enriched dual RNA sequencing. BMC genomics. 2015;16(1):34.
260. Kleba B, Clark TR, Lutter EI, Ellison DW, Hackstadt T. Disruption of the Rickettsia rickettsii Sca2 autotransporter inhibits actin-based motility. Infection and immunity. 2010;78(5):2240-7.

261. Felsheim RF, Chávez ASO, Palmer GH, Crosby L, Barbet AF, Kurtti TJ, et al. Transformation of Anaplasma marginale. Veterinary parasitology. 2010;167(2-4):167-74.
262. Giengkam S, Blakes A, Utsahajit P, Chaemchuen S, Atwal S, Blacksell SD, et al. Improved Quantification, Propagation, Purification and Storage of the Obligate Intracellular Human Pathogen Orientia tsutsugamushi. PLoS Negl Trop Dis. 2015;9(8):e0004009.
263. Schindelin J, Arganda-Carreras I, Frise E, Kaynig V, Longair M, Pietzsch T, et al. Fiji: an open-source platform for biological-image analysis. Nature methods. 2012;9(7):676-82.
264. Batish M, Raj A, Tyagi S. Single molecule imaging of RNA in situ. RNA Detection and Visualization: Springer; 2011. p. 3-13.
265. Wang M, Herrmann CJ, Simonovic M, Szklarczyk D, von Mering C. Version 4.0 of PaxDb: protein abundance data, integrated across model organisms, tissues, and cell-lines. Proteomics. 2015;15(18):3163-8.
266. Yamanaka M, Smith NI, Fujita KJM. Introduction to super-resolution microscopy. 2014;63(3):177-92.
267. Patterson G, Davidson M, Manley S, Lippincott-Schwartz J. Superresolution imaging using single-molecule localization. Annual review of physical chemistry. 2010;61:345-67.
268. Jimenez A, Friedl K, Leterrier C. About samples, giving examples: optimized single molecule localization microscopy. Methods. 2020;174:100-14.
269. Xu J, Ma H, Liu Y. Stochastic Optical Reconstruction Microscopy (STORM). Curr Protoc Cytom. 2017;81:12 46 1-12 46 27.
270. Yang DC, Blair KM, Salama NR. Staying in shape: the impact of cell shape on bacterial survival in diverse environments. Microbiology and Molecular Biology Reviews. 2016;80(1):187-203.
271. Dalia AB, Weiser JN. Minimization of bacterial size allows for complement evasion and is overcome by the agglutinating effect of antibody. Cell host & microbe. 2011;10(5):486-96.
272. Weiser JN. The battle with the host over microbial size. Current opinion in microbiology. 2013;16(1):59-62.
273. Khatoon Z, McTiernan CD, Suuronen EJ, Mah T-F, Alarcon EIJH. Bacterial biofilm formation on implantable devices and approaches to its treatment and prevention. 2018;4(12):e01067.
274. Urakami H, Ohashi N, Tsuruhara T, Tamura AJI, immunity. Characterization of polypeptides in Rickettsia tsutsugamushi: effect of preparative conditions on migration of polypeptides in polyacrylamide gel electrophoresis. 1986;51(3):948-52.
275. Lee S-M, Kwon HY, Im J-H, Baek JH, Kang J-S, Lee J-S. Identification of outer membrane vesicles derived from Orientia tsutsugamushi. Journal of Korean medical science. 2015;30(7):866-70.
276. Hamkalo BA, Elgin SC. Functional organization of the nucleus: a laboratory guide: Academic Press; 1992.
277. Wood TK, Knabel SJ, Kwan BW. Bacterial persister cell formation and dormancy. Appl Environ Microbiol. 2013;79(23):7116-21.
278. Li Y, Zhang YJAa, chemotherapy. PhoU is a persistence switch involved in persister formation and tolerance to multiple antibiotics and stresses in Escherichia coli. 2007;51(6):2092-9.
279. Zhang L, Chiang W-C, Gao Q, Givskov M, Tolker-Nielsen T, Yang L, et al. The catabolite repression control protein Crc plays a role in the development of antimicrobial-tolerant subpopulations in Pseudomonas aeruginosa biofilms. 2012;158(12):3014-9.
280. Lewis K. Persister cells, dormancy and infectious disease. Nat Rev Microbiol. 2007;5(1):48-56.
281. Välikangas T, Suomi T, Elo LL. A systematic evaluation of normalization methods in quantitative label-free proteomics. Briefings in bioinformatics. 2018;19(1):1-11.
282. Magnusson LU, Farewell A, Nystrom T. ppGpp: a global regulator in Escherichia coli. Trends Microbiol. 2005;13(5):236-42.

283. Testerman TL, Vazquez-Torres A, Xu Y, Jones-Carson J, Libby SJ, Fang FCJMm. The alternative sigma factor σE controls antioxidant defences required for Salmonella virulence and stationary-phase survival. 2002;43(3):771-82.
284. Bennison DJ, Irving SE, Corrigan RMJC. The Impact of the Stringent Response on TRAFAC GTPases and Prokaryotic Ribosome Assembly. 2019;8(11):1313.
285. reguFeng B, Mandava CS, Guo Q, Wang J, Cao W, Li N, et al. Structural and functional insights into the mode of action of a universally conserved Obg GTPase. 2014;12(5).
286. Jutras BL, Bowman A, Brissette CA, Adams CA, Verma A, Chenail AM, et al. EbfC (YbaB) is a new type of bacterial nucleoid-associated protein and a global regulator of gene expression in the Lyme disease spirochete. 2012;194(13):3395-406.
287. Flores-Rios R, Quatrini R, Loyola A. Endogenous and Foreign Nucleoid-Associated Proteins of Bacteria: Occurrence, Interactions and Effects on Mobile Genetic Elements and Host's Biology. Comput Struct Biotechnol J. 2019;17:746-56.
288. Sikorski RS, Michaud WA, Hieter PJM, Biology C. p62cdc23 of Saccharomyces cerevisiae: a nuclear tetratricopeptide repeat protein with two mutable domains. 1993;13(2):1212-21.
289. Schultz J, Marshall-Carlson L, Carlson MJM, Biology C. The N-terminal TPR region is the functional domain of SSN6, a nuclear phosphoprotein of Saccharomyces cerevisiae. 1990;10(9):4744-56.
290. Hase T, Riezman H, Suda K, Schatz GJTEj. Import of proteins into mitochondria: nucleotide sequence of the gene for a 70-kd protein of the yeast mitochondrial outer membrane. 1983;2(12):2169-72.
291. Hirano T, Hiraoka Y, Yanagida MJTJoCB. A temperature-sensitive mutation of the Schizosaccharomyces pombe gene nuc2+ that encodes a nuclear scaffold-like protein blocks spindle elongation in mitotic anaphase. 1988;106(4):1171-83.
292. Voronin DA, Kiseleva EV. [Functional role of proteins containing ankyrin repeats]. Tsitologiia. 2007;49(12):989-99.
293. Pan X, Luhrmann A, Satoh A, Laskowski-Arce MA, Roy CR. Ankyrin repeat proteins comprise a diverse family of bacterial type IV effectors. Science. 2008;320(5883):1651-4.
294. Park J, Kim KJ, Choi Ks, Grab DJ, Dumler JSJCm. Anaplasma phagocytophilum AnkA binds to granulocyte DNA and nuclear proteins. 2004;6(8):743-51.
295. Iturbe-Ormaetxe I, Burke GR, Riegler M, O'Neill SLJJob. Distribution, expression, and motif variability of ankyrin domain genes in Wolbachia pipientis. 2005;187(15):5136-45.
296. Walker T, Klasson L, Sebaihia M, Sanders MJ, Thomson NR, Parkhill J, et al. Ankyrin repeat domain-encoding genes in the wPip strain of Wolbachia from the Culex pipiens group. 2007;5(1):39.
297. Belland RJ, Zhong G, Crane DD, Hogan D, Sturdevant D, Sharma J, et al. Genomic transcriptional profiling of the developmental cycle of Chlamydia trachomatis. Proceedings of the National Academy of Sciences. 2003;100(14):8478-83.
298. Bertrand RL. Lag phase is a dynamic, organized, adaptive, and evolvable period that prepares bacteria for cell division. Journal of bacteriology. 2019;201(7).
299. Himeoka Y, Kaneko KJPRX. Theory for transitions between exponential and stationary phases: universal laws for lag time. 2017;7(2):021049.
300. Rolfe MD, Rice CJ, Lucchini S, Pin C, Thompson A, Cameron AD, et al. Lag phase is a distinct growth phase that prepares bacteria for exponential growth and involves transient metal accumulation. Journal of bacteriology. 2012;194(3):686-701.
301. Feldman AW, Fischer EC, Ledbetter MP, Liao J-Y, Chaput JC, Romesberg FEJJotACS. A tool for the import of natural and unnatural nucleoside triphosphates into bacteria. 2018;140(4):1447-54.
302. Chu H, Lee JH, Han SH, Kim SY, Cho NH, Kim IS, et al. Exploitation of the endocytic pathway by Orientia tsutsugamushi in nonprofessional phagocytes. Infect Immun. 2006;74(7):4246-53.

303. Ray K, Marteyn B, Sansonetti PJ, Tang CM. Life on the inside: the intracellular lifestyle of cytosolic bacteria. Nat Rev Microbiol. 2009;7(5):333-40.
304. Arts IS, Gennaris A, Collet J-FJFl. Reducing systems protecting the bacterial cell envelope from oxidative damage. 2015;589(14):1559-68.
305. Hatahet F, Boyd D, Beckwith JJBeBA-P, Proteomics. Disulfide bond formation in prokaryotes: history, diversity and design. 2014;1844(8):1402-14.
306. Portman JL, Dubensky SB, Peterson BN, Whiteley AT, Portnoy DAJM. Activation of the Listeria monocytogenes virulence program by a reducing environment. 2017;8(5):e01595-17.
307. Silva MTJFim. Classical labeling of bacterial pathogens according to their lifestyle in the host: inconsistencies and alternatives. 2012;3:71.
308. Inaba K, Ito KJBeBA-MCR. Structure and mechanisms of the DsbB–DsbA disulfide bond generation machine. 2008;1783(4):520-9.
309. Pletnev P, Osterman I, Sergiev P, Bogdanov A, Dontsova O. Survival guide: Escherichia coli in the stationary phase. Acta Naturae (англоязычная версия). 2015;7(4 (27)).
310. Nyström T. Stationary-phase physiology. Annu Rev Microbiol. 2004;58:161-81.
311. Thompson A, Rolfe MD, Lucchini S, Schwerk P, Hinton JC, Tedin K. The bacterial signal molecule, ppGpp, mediates the environmental regulation of both the invasion and intracellular virulence gene programs of Salmonella. Journal of Biological Chemistry. 2006;281(40):30112-21.
312. Guisbert E, Yura T, Rhodius VA, Gross CA. Convergence of molecular, modeling, and systems approaches for an understanding of the Escherichia coli heat shock response. Microbiol Mol Biol Rev. 2008;72(3):545-54.
313. Gunesekere IC, Kahler CM, Powell DR, Snyder LA, Saunders NJ, Rood JI, et al. Comparison of the RpoH-dependent regulon and general stress response in Neisseria gonorrhoeae. Journal of bacteriology. 2006;188(13):4769-76.
314. Cerveny L, Straskova A, Dankova V, Hartlova A, Ceckova M, Staud F, et al. Tetratricopeptide repeat motifs in the world of bacterial pathogens: role in virulence mechanisms. Infection and immunity. 2013;81(3):629-35.
315. Bang S, Min C-K, Ha N-Y, Choi M-S, Kim I-S, Kim Y-S, et al. Inhibition of eukaryotic translation by tetratricopeptide-repeat proteins of Orientia tsutsugamushi. Journal of Microbiology. 2016;54(2):136-44.
316. Reniere ML. Reduce, induce, thrive: bacterial redox sensing during pathogenesis. Journal of bacteriology. 2018;200(17):e00128-18.
317. Gulevskaia SA, Popov VL, Ignatovich VF. [Current data on the polymorphism of Rickettsia prowazekii and burneti in cultured cells]. Zh Mikrobiol Epidemiol Immunobiol. 1975(7):68-72.
318. Steele S, Radlinski L, Taft-Benz S, Brunton J, Kawula TH. Trogocytosis-associated cell to cell spread of intracellular bacterial pathogens. Elife. 2016;5:e10625.
319. Ireton KJOb. Molecular mechanisms of cell–cell spread of intracellular bacterial pathogens. 2013;3(7):130079.
320. Sokołowska E, Błachnio-Zabielska AU. A Critical Review of Electroporation as A Plasmid Delivery System in Mouse Skeletal Muscle. International journal of molecular sciences. 2019;20(11):2776.
321. Hatamoto M, Ohashi A, Imachi H. Peptide nucleic acids (PNAs) antisense effect to bacterial growth and their application potentiality in biotechnology. Applied microbiology and biotechnology. 2010;86(2):397-402.
322. Beare PA, Howe D, Cockrell DC, Omsland A, Hansen B, Heinzen RA. Characterization of a Coxiella burnetii ftsZ mutant generated by Himar1 transposon mutagenesis. Journal of bacteriology. 2009;191(5):1369-81.
323. Baldridge GD, Burkhardt N, Herron MJ, Kurtti TJ, Munderloh UG. Analysis of fluorescent protein expression in transformants of Rickettsia monacensis, an obligate intracellular tick symbiont. Appl Environ Microbiol. 2005;71(4):2095-105.

324. Driskell LO, Yu X-j, Zhang L, Liu Y, Popov VL, Walker DH, et al. Directed mutagenesis of the Rickettsia prowazekii pld gene encoding phospholipase D. Infection and immunity. 2009;77(8):3244-8.
325. Enatsu T, Urakami H, Tamura A. Phylogenetic analysis of Orientia tsutsugamushi strains based on the sequence homologies of 56-kDa type-specific antigen genes. FEMS microbiology letters. 1999;180(2):163-9.
326. Paris D, Aukkanit N, Jenjaroen K, Blacksell S, Day N. A highly sensitive quantitative real-time PCR assay based on the groEL gene of contemporary Thai strains of Orientia tsutsugamushi. Clinical microbiology and infection. 2009;15(5):488-95.
327. Varghese GM, Janardhanan J, Mahajan SK, Tariang D, Trowbridge P, Prakash JA, et al. Molecular epidemiology and genetic diversity of Orientia tsutsugamushi from patients with scrub typhus in 3 regions of India. Emerging infectious diseases. 2015;21(1):64.
328. Leggett HC, Cornwallis CK, Buckling A, West SA. Growth rate, transmission mode and virulence in human pathogens. Philosophical Transactions of the Royal Society B: Biological Sciences. 2017;372(1719):20160094.
329. Mattick JS, Makunin IV. Non-coding RNA. Human molecular genetics. 2006;15(suppl_1):R17-R29.
330. Kwek KY, Murphy S, Furger A, Thomas B, O'Gorman W, Kimura H, et al. U1 snRNA associates with TFIIH and regulates transcriptional initiation. Nature structural biology. 2002;9(11):800-5.
331. Bernstein E, Allis CD. RNA meets chromatin. Genes & development. 2005;19(14):1635-55.
332. Allen TA, Von Kaenel S, Goodrich JA, Kugel JF. The SINE-encoded mouse B2 RNA represses mRNA transcription in response to heat shock. Nature structural & molecular biology. 2004;11(9):816-21.
333. Rikihisa Y, Lin M. Anaplasma phagocytophilum and Ehrlichia chaffeensis type IV secretion and Ank proteins. Current opinion in microbiology. 2010;13(1):59-66.
334. Evans SM, Rodino KG, Adcox HE, Carlyon JA. Orientia tsutsugamushi uses two Ank effectors to modulate NF-κB p65 nuclear transport and inhibit NF-κB transcriptional activation. PLoS pathogens. 2018;14(5):e1007023.
335. Shelite TR, Liang Y, Wang H, Mendell NL, Trent BJ, Sun J, et al. IL-33-dependent endothelial activation contributes to apoptosis and renal injury in Orientia tsutsugamushi-infected mice. PLoS neglected tropical diseases. 2016;10(3).
336. Julio SM, Heithoff DM, Mahan MJ. ssrA (tmRNA) plays a role inSalmonella enterica serovar Typhimurium pathogenesis. Journal of bacteriology. 2000;182(6):1558-63.
337. Svetlanov A, Puri N, Mena P, Koller A, Karzai AW. Francisella tularensis tmRNA system mutants are vulnerable to stress, avirulent in mice, and provide effective immune protection. Molecular microbiology. 2012;85(1):122-41.
338. Cho N-H, Seong S-Y, Choi M-S, Kim I-S. Expression of chemokine genes in human dermal microvascular endothelial cell lines infected with Orientia tsutsugamushi. Infection and immunity. 2001;69(3):1265-72.
339. Koh Y-S, Yun J-H, Seong S-Y, Choi M-S, Kim I-S. Chemokine and cytokine production during Orientia tsutsugamushi infection in mice. Microbial pathogenesis. 2004;36(1):51-7.
340. Mendell NL, Bouyer DH, Walker DH. Murine models of scrub typhus associated with host control of Orientia tsutsugamushi infection. PLoS neglected tropical diseases. 2017;11(3):e0005453.